NUREG/CR-6471, Vol. 2
PNNL-11143B

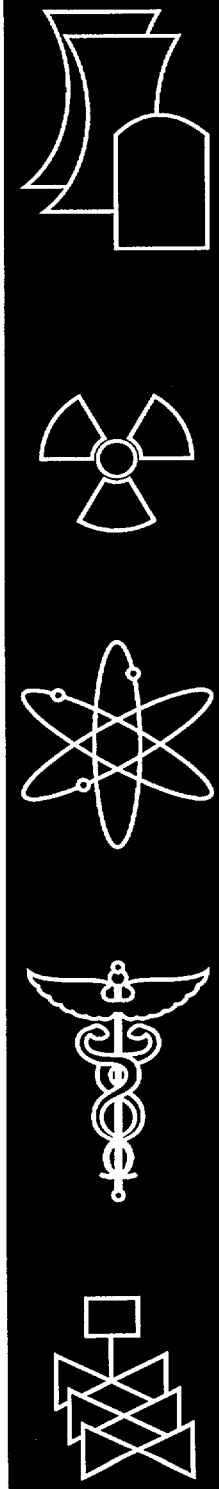

Characterization of Flaws in U.S. Reactor Pressure Vessels

Validation of Flaw Density and Distribution in the Weld Metal of the PVRUF Vessel

Pacific Northwest National Laboratory

U.S. Nuclear Regulatory Commission
Office of Nuclear Regulatory Research
Washington, DC 20555-0001

AVAILABILITY OF REFERENCE MATERIALS IN NRC PUBLICATIONS

NRC Reference Material

As of November 1999, you may electronically access NUREG-series publications and other NRC records at NRC's Public Electronic Reading Room at www.nrc.gov/NRC/ADAMS/index.html. Publicly released records include, to name a few, NUREG-series publications; *Federal Register* notices; applicant, licensee, and vendor documents and correspondence; NRC correspondence and internal memoranda; bulletins and information notices; inspection and investigative reports; licensee event reports; and Commission papers and their attachments.

NRC publications in the NUREG series, NRC regulations, and *Title 10, Energy*, in the Code of *Federal Regulations* may also be purchased from one of these two sources.

1. The Superintendent of Documents
   U.S. Government Printing Office
   P. O. Box 37082
   Washington, DC 20402–9328
   www.access.gpo.gov/su_docs
   202–512–1800
2. The National Technical Information Service
   Springfield, VA 22161–0002
   www.ntis.gov
   1–800–533–6847 or, locally, 703–805–6000

A single copy of each NRC draft report for comment is available free, to the extent of supply, upon written request as follows:

Address: Office of the Chief Information Officer,
Reproduction and Distribution
Services Section
U.S. Nuclear Regulatory Commission
Washington, DC 20555-0001
E-mail: DISTRIBUTION@nrc.gov
Facsimile: 301–415–2289

Some publications in the NUREG series that are posted at NRC's Web site address www.nrc.gov/NRC/NUREGS/indexnum.html are updated periodically and may differ from the last printed version. Although references to material found on a Web site bear the date the material was accessed, the material available on the date cited may subsequently be removed from the site.

Non-NRC Reference Material

Documents available from public and special technical libraries include all open literature items, such as books, journal articles, and transactions, *Federal Register* notices, Federal and State legislation, and congressional reports. Such documents as theses, dissertations, foreign reports and translations, and non-NRC conference proceedings may be purchased from their sponsoring organization.

Copies of industry codes and standards used in a substantive manner in the NRC regulatory process are maintained at—

The NRC Technical Library
Two White Flint North
11545 Rockville Pike
Rockville, MD 20852–2738

These standards are available in the library for reference use by the public. Codes and standards are usually copyrighted and may be purchased from the originating organization or, if they are American National Standards, from—

American National Standards Institute
11 West 42nd Street
New York, NY 10036–8002
www.ansi.org
212–642–4900

The NUREG series comprises (1) technical and administrative reports and books prepared by the staff (NUREG–XXXX) or agency contractors (NUREG/CR–XXXX), (2) proceedings of conferences (NUREG/CP–XXXX), (3) reports resulting from international agreements (NUREG/IA–XXXX), (4) brochures (NUREG/BR–XXXX), and (5) compilations of legal decisions and orders of the Commission and Atomic and Safety Licensing Boards and of Directors' decisions under Section 2.206 of NRC's regulations (NUREG–0750).

NUREG/CR-6471, Vol. 2
PNNL-11143B

Characterization of Flaws in U.S. Reactor Pressure Vessels

Validation of Flaw Density and Distribution in the Weld Metal of the PVRUF Vessel

Manuscript Completed: June 2000
Date Published: August 2000

Prepared by
G. J. Schuster, S. R. Doctor, A.F. Pardini, S.L. Crawford

Pacific Northwest National Laboratory
Richland, WA 99352

D.A. Jackson, NRC Project Manager

Prepared for
Division of Engineering Technology
Office of Nuclear Regulatory Research
U.S. Nuclear Regulatory Commission
Washington, DC 20555-0001
NRC Job Code L1099 and W6275

NUREG/CR-6471, Vol. 2 has been reproduced from the best available copy.

For sale by the U.S. Government Printing Office
Superintendent of Documents, Mail Stop: SSOP, Washington, DC 20402-9328

ISBN 0-16-050490-2

ABSTRACT

Characterization of Flaws in U.S. Reactor Pressure Vessels is a multi-volume report. Volume 2, this document, contains the results of a destructive analysis for fabrication flaws in weld metal removed from the Pressure Vessel Research User Facility (PVRUF) vessel. Confirmed flaw rates are estimated, and a comparison is made to the Marshall distribution. The first volume of this multi-volume report gives the density and distribution of flaw indications recorded from the volumetric ultrasonic inspections of the vessel made through the cladding. Volume 3 reports the distribution of flaw indications in material removed from a BWR vessel, the Shoreham vessel.

This volume provides a description of research methods developed at Pacific Northwest National Laboratory for confirming flaw rates in weld metal. The data, acquired during the research, are shown with the estimates of flaw density as a function of through-wall size. Because the largest flaws were found in repair weld metal, the report contains the size and number of repairs to the PVRUF vessel.

CONTENTS

Page

ABSTRACT iii

EXECUTIVE SUMMARY xiii

ACKNOWLEDGMENTS xv

GLOSSARY AND ABBREVIATIONS xvii

1 INTRODUCTION 1.1

2 RESEARCH METHODS APPLIED TO THE VALIDATION OF FLAW INDICATIONS IN PVRUF 2.1

2.1 Distribution of the Volume 1 Flaw Indications 2.1
2.2 Removal of Material from PVRUF 2.2
2.3 Confirmation of Weld Position and Cross Section 2.3
2.4 Indication Positioning Error and the Amount of Material Inspected 2.3
2.5 Removal and Weld-Normal Ultrasonic Testing of Weld Metal 2.4
2.5.1 Removal of Weld Metal from PVRUF Specimens 2.4
2.5.2 Ultrasonic Testing Normal to the Weld Metal 2.4
2.6 Removal and Radiographic Testing of 25-mm-Thick Plates 2.5
2.6.1 Cutting of Radiographic Specimens 2.5
2.6.2 Radiography of 25-mm Plates 2.5
2.7 Ultrasonic, Radiographic, and Metallographic Analysis of 25-mm Cubes 2.6
2.7.1 Ultrasonic Testing and Flaw Sizing in 25-mm Cubes 2.6
2.7.2 Radiography and Flaw Sizing Using 25-mm Specimens 2.6
2.7.3 Metallographic Analysis 2.6
2.8 Summary of Validation Methods 2.7

3 VALIDATION RESULTS 3.1

3.1 Flaws in Machine-Made Weld Metal and Located on the Fusion Surface of the Weld with the Base Metal 3.1
3.1.1 Weld-Normal Ultrasonic Testing of Machine-Made Weld Metal 3.2
3.1.2 Radiographic Testing of 25-mm Thick Plate 3.3
3.1.3 Metallographic Testing of Machine-Made Weld Metal 3.3
3.1.4 Summary of Validation Results for Machine-Made Weld Metal 3.3
3.2 Flaws in Back-Fill Weld Metal 3.5
3.2.1 Analysis of PVRUF Cube 5-10EB1-IIbIIc 3.6
3.3 Flaws in Repair Weld Metal 3.7
3.4 Flaws in Cladding and at the Clad-to-Base Metal Interface 3.8
3.5 Flaws in Base Metal 3.9

4 CONFIRMED FLAW FREQUENCY AND DISTRIBUTION IN PVRUF VESSEL 4.1

4.1 Confirmed Flaw Frequency and Distribution in the Near Surface Zone 4.1
4.2 Confirmed Flaw Frequency in Remainder of Vessel Wall 4.3
4.3 Cumulative Flaw Rate for PVRUF and Comparison to the Marshall Distribution 4.4
4.4 Flaw Rate for Small Flaws 4.6
4.5 Validated Flaw Length in the PVRUF Vessel 4.6

5 SIZE AND FREQUENCY OF REPAIRS TO THE PVRUF VESSEL 5.1

5.1 Repairs to Weld Metal 5.1
5.2 Repairs to Base Metal 5.2

6 CONCLUSIONS 6.1

7 RECOMMENDATIONS 7.1

8 REFERENCES 8.1

FIGURES

1.1 Photograph of the PVRUF Vessel at Oak Ridge National Laboratory 1.2

2.1 Plan View, Flaw Indication Frequency in PVRUF Block 5-1 ..... 2.8

2.2 Plan View, Indication Frequency in PVRUF Specimen 5-7 ..... 2.8

2.3 PVRUF Vessel Roll-Out Showing Plan to Remove Material 2.9

2.4 Weld Cross Section for Beltline Weld 2.10

2.5 Weld Cross Section for Intermediate-to-Upper Shell Girth Weld 2.10

2.6 PVRUF Block Prepared for Removal of Weld Metal 2.11

2.7 Weld Metal Specimens Removed from PVRUF Block 2.11

2.8 Weld Metal Specimen Prepared for Ultrasonic Inspection Normal to Weld 2.12

2.9 SAFT-UT Image from Ultrasonic Inspection Normal to Weld 2.12

2.10 PVRUF Weld Metal Specimen Cut into 25-mm-Thick Plates 2.13

2.11 Radiograph of 25-mm-Thick Plate 2.13

2.12 25-mm Cube Removed from Plate of PVRUF Material 2.14

2.13 Ultrasonic Image of Flaw Indication in Near-Surface Zone Cube 2.14

2.14 Radiograph of 25-mm-Thick Specimen 2.15

2.15 Micrograph of 25-mm Cube 2.15

3.1 Side View of Weld-Normal Ultrasonic Test Showing Weld Profile as Evidenced by Small Flaw Indications 3.10

3.2 C-scan Image of Small Flaw Indications on the Weld Fusion Surface, from Weld-Normal UT Inspection 3.11

3.3 UT Image Showing Weld Profile with Weld Flaw Indication 3.12

3.4 SAFT-UT Inspection of a Large Cluster of Weld Flaws in the Mid-Wall Portion of the Vessel Beltline Weld 3.13

3.5 Weld-Normal UT Image of Flaw Indication Characterized as Extended Lack of Fusion ... 3.14

3.6 Weld-Normal Flaw Indication Characterized as Extended Lack of Fusion 3.15

3.7 Weld-Normal Ultrasonic Testing Flaw Indication Characterized as Long Lack of Fusion . 3.16

3.8 Radiograph of 25-mm Plate 5-1AB 3.17

3.9 Radiograph of 25-mm Plate 5-1AB-3 ..... 3.17

3.10 Radiograph of 25-mm Plate 5-1AB-5 Location 1 ..... 3.18

3.11 Radiograph of 25-mm Plate 5-1AB-5 Location 2 ..... 3.18

3.12 Radiograph of 25-mm Plate 5-1AB-5 Location 3 ..... 3.19

3.13 Radiograph of 25-mm Plate 5-1AB-6 Location 1 ..... 3.19

3.14 Radiograph of 25-mm Plate 5-1AB-6 Location 2 ..... 3.20

3.15 Radiograph of 25-mm Plate 5-1AB-7 Location 1 ..... 3.20

3.16 Digitized image of Radiograph of 25-mm Plate 5-1AB-7 Location 2 ..... 3.21

3.17 Digitized Image of Radiograph of 25-mm Plate 5-1AB-9 Location 1 ..... 3.21

3.18 Digitized Image Radiograph of 25-mm Plate 5-1ab-9 Location 2 ..... 3.22

3.19 Digitized image of Radiograph of 25-mm Plate 5-1AB-11 ..... 3.22
3.20 Digitized Image of Radiograph of 25-mm Plate 5-1AB-12 Location 1 ..... 3.23
3.21 Digitized Image of Radiograph of 25-mm Plate 5-1AB-12 Location 2 ..... 3.23
3.22 Digitized Image of Radiograph of 25-mm Plate 5-1AB-12 Location 3 ..... 3.24
3.23 Digitized Image of Radiograph of 25-mm Plate 5-1AB-14 ..... 3.24
3.24 Digitized Image of Radiograph of 25-mm Plate 5-1C-2 ..... 3.25
3.25 Digitized Image of Radiograph of 25-mm Plate 5-1C-4 ..... 3.25
3.26 Digitized Image of Radiograph of 25-mm Plate 5-1C-6 ..... 3.26
3.27 Digitized Image of Radiograph of 25-mm Plate 5-1C-8 ..... 3.26
3.28 Digitized Image of Radiograph of 25-mm Plate 5-1C-10 ..... 3.27
3.29 Digitized Image of Radiograph of Plate 5-1C-11 ..... 3.27
3.30 Digitized Image of Radiograph of 25-mm Plate 5-1C-12 ..... 3.28
3.31 Digitized Image of Radiograph of 25-mm Plate 5-1C-13 Location 1 ..... 3.28
3.32 Digitized Image of Radiograph of 25-mm Plate 5-1C-13 Location 2 ..... 3.29
3.33 Digitized Image of Radiograph of 25-mm Plate 5-1C-14 ..... 3.29
3.34 Digitized Image of Radiograph of Plate 5-10B-2 ..... 3.30
3.35 Digitized Image of Radiograph of 25-mm Plate 5-10B-4 ..... 3.30
3.36 Digitized Image of Radiograph of 25-mm Plate 5-10B-5 Location 1 ..... 3.31
3.37 Digitized Image of Radiograph of 25-mm Plate 5-10B-5 Location 2 ..... 3.31
3.38 Digitized Image of Radiograph of 25-mm Plate 5-10B-7 ..... 3.32
3.39 Digitized Image of Radiograph of 25-mm Plate 5-10B-8 ..... 3.32
3.40 Digitized Image of Radiograph of 25-mm Plate 5-10B-10 ..... 3.33
3.41 Digitized Image of Radiograph of 25-mm Plate 5-12BA-1 ..... 3.33
3.42 Digitized Image of Radiograph of 25-mm Plate 5-12BA-2 ..... 3.34

3.43 Digitized Image of Radiograph of 25-mm Plate 5-12BA-3 Location 1 ..... 3.34

3.44 Digitized Image of Radiograph of 25-mm Plate 5-12BA-3 Location 2 ..... 3.35

3.45 Digitized Image of Radiograph of 25-mm Plate 5-12BA-4 ..... 3.35

3.46 Digitized Image of Radiograph of Plate 5-12BA-6 ..... 3.36

3.47 Digitized Image of Radiograph of Plate 5-12BA-8 ..... 3.36

3.48 Digitized Image of Radiograph of 25-mm Plate 5-12BA-10 ..... 3.37

3.49 Digitized Image of Radiograph of 25-mm Plate 5-12BA-11 ..... 3.37

3.50 Digitized Image of Radiograph of 25-mm Plate 5-12BA-13 ..... 3.38

3.51 Micrograph of 25-mm Cube Showing Location of Fusion Surface Flaw 3.39

3.52 Micrograph of Fusion Surface Flaw Before Maximum Extent as Polished and Etched 3.39

3.53 Micrograph of 2-mm Flaw at Maximum Extent as Machined 3.40

3.54 Micrograph of 25-mm Cube Showing a Portion of a Large Cluster of Small Weld Flaws .. 3.40

3.55 Micrograph of a Cross-Section of One Weld Flaw from the Large Cluster 3.41

3.56 Micrograph of Flaw from the Cluster Shown in Figure 3.54 ..... 3.42

3.57 Micrograph of Small Flaw Shown in Figure 3.56. ..... 3.42

3.58 Micrograph of Typical PVRUF Weld Profile Showing Back-Gouge and Clad-to-Base Metal Interface 3.43

3.59 Photograph of 14 Near-Surface Zone 25-mm Cubes 3.43

3.60 Depth Sizing Performance of SAFT-UT in the Near Surface Zone 3.44

3.61 Micrograph of Cube 5-10EB1-IIbIIc Showing Shallow Back Gouge 3.45

3.62 Radiograph of Cube 5-10EB1-IIbIIc 3.46

3.63 Micrograph of Cube 5-10EB1-IIbIIc Showing Complex Flaw Above First Tandem Arc Weld Passes 3.46

3.64 Micrograph of Lack of Side-Wall Fusion 3.47

3.65 Micrograph of Cube Showing Failed Weld Bead 3.47

3.66 Micrograph of Cube 5-10EB1-IIbIIc Showing Flaws in the First Weld Pass of the Back-Fill 3.48

3.67 Micrograph of Cube 5-10EB1-IIbIIc Showing Contamination of the First Weld Pass of the Back-Fill 3.48

3.68 Micrograph of Crack in Flawed Weld Bead, Near Surface Zone of PVRUF 3.49

3.69 Micrograph of Cracked Weld Bead 3.50

3.70 Weld-Normal UT C-scan Image of Weld Fusion Surface Showing Profile of Weld Repair's Low Acoustic Energy Signature 3.51

3.71 Radiographic Images of 17-mm Flaw Indication in a Repair to the Beltline Weld of the PVRUF Vessel 3.52

3.72 Micrograph of a Portion of the 17-mm Flaw 3.53

3.73 Micrograph Showing a Magnified View of a Portion of the 17-mm Flaw 3.53

3.74 Micrograph Showing a Magnified View of the Crack-like Portion of the 17-mm Flaw 3.54

3.75 Focused Ultrasound Result Showing Top View of Flaw in 5-12AC2. ..... 3.55

3.76 Focused Ultrasound Result Showing Side View of Flaw in 5-12AC2 ..... 3.56

3.77 Focused Ultrasound Result Showing End View of Flaw in 5-12AC2 ..... 3.57

3.78 Micrograph of Upper Portion of Weld in PVRUF Specimen 5-6Eca 3.57

3.79 Photograph of PVRUF Specimen Showing Small Slag Inclusions at the Clad-to-Base Metal Interface 3.58

3.80 Photograph of PVRUF Specimen 4-5DBAC-Z5 as Machine Cut 3.58

3.81 Digitized Image of Radiograph Showing of Base Metal Lamination Cluster 3.59

4.1 Comparison of Validated PVRUF and Marshall Cumulative Flaw Rates 4.5

4.2 Size Distribution of Small Flaws in PVRUF Vessel as Measured by Radiographic Testing of 25-mm Thick Plate 4.6

5.1 PVRUF Vessel Roll-Out Showing Weld Identification Numbers 5.4

TABLES

2.1 Amount of Material Inspected in PVRUF 2.4

3.1 List of RT Indications Found at the Location of Weld-Normal UT Indications in a Sample of PVRUF Material Sectioned into 25-mm Plates 3.4

3.2 RT Indications from the Testing of PVRUF Material Contained a Large Flaw Indication Reported in Volume 1 ..... 3.5

3.3 Validation Sizing Results for 14 Flaw Indications in Back-Gouge Weld Metal 3.7

4.1 Flaws in Weld Metal of the Inner 25 mm of the PVRUF Vessel 4.2

4.2 Flaws in Cladding and at the Clad-to-Base Metal Interface 4.3

4.3 Indications in Base Metal of the Inner 25 mm of the PVRUF Vessel 4.3

4.4 Flaws in Weld Metal Outside the Near-Surface of the PVRUF Vessel 4.4

4.5 Flaws in Base Metal Outside the Near-Surface of the PVRUF Vessel 4.4

4.6 Flaws in Repairs 4.4

5.1 Repairs to Circumferential Welds (Girth Seams) 5.5

5.2 Repairs to Axial Welds (Long Seams) 5.5

5.3 Repairs to Closure Head 5.5

5.4 Repairs to Bottom Head 5.5

5.5 Repairs to Nozzle-to-Vessel Welds 5.6

5.6 Repairs to Safe Ends 5.6

5.7 Repairs to Mating Surface 203-106 and 204-106 ..... 5.7

5.8 Repairs to Nozzle Base Metal 5.7

EXECUTIVE SUMMARY

This report describes the confirmed through-wall size distribution of fabrication flaws in the weld metal of the Pressure Vessel Research User Facility vessel, a pressurized water reactor (PWR) vessel made by Combustion Engineering. The validation data that contributed to the confirmed flaw distribution are presented in this report. This report is Volume 2 of a multi-volume set. The first volume gives the density and distribution of flaw indications recorded during previous volumetric ultrasonic inspection through the vessel's clad inner surface. Volume 3 provides the density and distribution of flaw indications in material removed from the Shoreham vessel, a boiling water reactor (BWR) plant.

This research, on material removed from the PVRUF vessel, was performed to validate the presence of flaws, the characteristics of the fabrication flaw density and distribution, and to provide confirmed flaw statistics for use in probabilistic fracture mechanics analysis. The report describes the methodology used by Pacific Northwest National Laboratory (PNNL) to produce validated flaw rates. The methodology included sectioning of the vessel, ultrasonic examinations, radiography, and metallography. The data, acquired on the flaws, are presented along with estimates of flaw rates. A comparison to the Marshall distribution is given. Because the largest flaws were found in repair weld metal, the report describes the size and number of repairs to the PVRUF vessel as found in the construction records.

Among the principal findings of this report are that the comparison of the PVRUF data with the Marshall distribution shows that repair weld metal is a significant source of flaws. Secondly, the larger flaws are a complex mixture of cracks, lack of fusion, slag, inclusions, and porosity. Flaws can repeat on successive weld passes, a phenomenon of interest to weld simulation models. The weld fusion surfaces contain an elevated concentration of vertical planar discontinuities. Finally, the flaws are mostly small as was reported in Volume 1.

The flaw indications, reported in Volume 1, are confirmed to be fabrication flaws. The majority of the flaws can be divided into two groups based on their location. In the largest group were the flaws at the clad-to-base metal interface. The sectioning of the PVRUF cladded material confirms lack of fusion, slag, and voids at the clad-to-base metal interface. In the second largest group were the flaws on the fusion surface of the structural weld with the base metal. Radiographic testing and metallographic testing confirm lack of fusion with slag for the majority of these flaws.

It is concluded in this report that validated flaw rates have been achieved for the weld metal of the PVRUF vessel. The very limited validation efforts in the base metal of the PVRUF vessel confirmed the presence of flaws detected in the prior examinations, but showed that the larger flaws are only clusters of small indications with little or no potential significance to structural integrity. Future work will focus on better characterizing flaws in the base metal of the PVRUF vessel and other vessels.

PNNL's results on the reliability of inspection through the cladding showed that vertically oriented ultrasonic echoes are not always an indication of a large flaw. In ultrasonic testing of embedded flaws, sometimes responses are received from the top and bottom (tip-diffracted signals) and not from the face of the flaw. Because of the elevated concentration of small flaws on the weld fusion surfaces and because small flaws can repeat on subsequent weld passes, ultrasonic signals along the fusion surfaces are not specific to the upper and lower tips of a large flaw.

ACKNOWLEDGMENTS

The authors acknowledge the contributions of PNNL staff members Mr. Robert Bowey for his assistance in preparing the PVRUF material for sectioning and Mr. Lawrence Priest for assistance at the PNNL Metallography Laboratory. The authors would also like to thank Ms. Kay Hass for assistance in preparing this manuscript.

The authors thank Dr. William Pennel and Wallace McAfee of Oak Ridge National Laboratory for providing the PVRUF vessel material, access to the construction records, and assistance while at their facility.

The authors also wish to thank the U.S. Nuclear Regulatory Commission, Office of Nuclear Regulatory Research for supporting this work and, in particular, the NRC program manager Ms. Deborah A. Jackson.

GLOSSARY AND ABBREVIATIONS

BWR. Boiling water reactor. A nuclear reactor in which the coolant is water, maintained at such a pressure as to allow it to boil and form steam.

Butt weld. The structural welds in reactor pressure vessels (piping, etc.). This includes a vessel's circumferential and axial welds but does not include the cladding weld metals.

Base metal. The metal that composes the plates or forged rings of a reactor pressure vessel. The plates (e.g., alloy A533B) and forged rings (e.g., A508) are assembled into the vessel by butt-welding.

Cumulative flaw rate. The density of flaws greater than a specified size.

Defect. A discontinuity or discontinuities that by nature or accumulated effect (for example, total crack length) render a part of product unable to meet minimum applicable acceptance standards or specifications. This term designates rejectability. See also discontinuity and flaw. (AWS 1984)

Discontinuity. An interruption of the typical structure of a weldment, such as a lack of homogeneity in the mechanical, metallurgical, or physical characteristics of the material or weldment. A discontinuity is not necessarily a defect. See also defect and flaw. (AWS 1984)

False call. The characterization of a blank unit of material as flawed or cracked.

Flaw. An imperfection or unintended discontinuity in a material. A void, porosity, inclusion, lack of fusion or crack that is physically distinct from the metallic microstructure.

Flaw density. The number of flaws per unit length, area, or volume.

Flaw depth size. See through-wall extent.

Flaw distribution. The number of flaws measured in separate categories.

Flaw rate. The flaw density expressed as a function of flaw through-wall extent.

Fusion line. One of two lines, on the cross-section of the weld, that form the boundary between the weld metal and the base metal.

HAZ. Heat-affected zone. A portion of the base metal (adjacent to the weld) whose microstructure is altered by heat deposited during welding.

H&D units. Hurter and Driffield units. A relation between the exposure applied to a photographic material (film) and the resulting photographic density.

Indication (of a flaw). The response or evidence of a flaw from the application of nondestructive evaluation. For ultrasonic testing, a coherent packet of (ultrasonic) energy that is characterized as originating from a flaw.

Inclusion. A foreign solid, (e.g., slag, scale, oxide, or non-metallic substance) entrapped in the base metal or weld metal.

LOF. Lack of fusion. Lack of metallic bond between weld passes or between a weld pass and the base metal.

LTOP. Low temperature over-pressurization.

LWR. Light water reactor. Either of two nuclear fission reactor designs (see ***BWR*** and ***PWR***) that heat water as a means of power production.

Laminar flaws. Planar flaws that are oriented within 10 degrees of a plane parallel to the surface of the component. See ASME (1998).

Marshall Distribution. A flaw rate in the weld metal of reactor pressure vessels. See Marshall (1982).

Midland vessel. The pressure vessel from Consumers Power Unit 2 reactor. See Booth (1989).

NDE. Nondestructive evaluation.

Near-surface zone. The first 25 mm (1.0 in.) of reactor pressure vessel material from the cladding's wetted surface.

OD. Outside diameter.

Outside the near-surface zone. The remainder of vessel wall when the near-surface zone is excluded.

PVRUF vessel. The Pressure Vessel Research Users' Facility vessel, at Oak Ridge National Laboratory, was a pressurized water reactor vessel from a canceled U.S. plant. See Pennel (1989).

Planar flaw. A flat two-dimensional flaw in a plane other than parallel to the surface of the component. In this study, it includes a crack or lack of fusion that is primarily vertical in orientation in the vessel.

POD. Probability of detection. the expected value for the fraction of flawed or cracked units of material that will be found to be flawed or cracked by an inspection system.

Porosity. A group of voids located close to each other.

PWR. Pressurized water reactor. A nuclear reactor in which the coolant is water, maintained at such a pressure as to keep it from boiling.

PTS. Pressurized thermal shock.

RPV. Reactor pressure vessel.

Ring down. An ultrasonic term that refers to the period of time, following excitation of the transmit transducer, when acoustic interference is present at the receiver.

RT. Radiographic testing.

SAFT-UT. Synthetic Aperture Focusing Technique for Ultrasonic Testing. See Doctor (1996).

Size. See ***through-wall extent.***

SMA. Shielded metal arc welding.

Through-wall extent. The maximum dimension, normal to the surface of the component, of the rectangle circumscribing the flaw.

Void. A volume of gas entrapped in the vessel material.

Volumetric flaw. A three-dimensional flaw such as a void, porosity, or inclusion. Also includes *laminar flaws.*

Weldment. An assembly whose component parts are joined by welding. (AWS 1984)

Weld metal. That portion of a weld that has been melted during welding. (AWS 1984)

Weld profile. The shape of the weld metal when sectioned across the weld.

1 INTRODUCTION

The U.S. Nuclear Regulatory Commission (NRC) has funded a multi-year program at the Pacific Northwest National Laboratory (PNNL) entitled "Assessment of the Reliability of UT and Improved Programs for Inservice Inspection." As a part of this program, NRC has directed PNNL to estimate the rate of occurrence of fabrication flaws in U.S. light-water reactor pressure vessels (RPVs). PNNL's methodology for estimating the density and size distribution of fabrication flaws in U.S. reactor pressure vessels involves the nondestructive evaluation (NDE) of vessel material from cancelled nuclear plants and the destructive validation of detected flaws.

In related work for NRC, PNNL has developed a welding model to extrapolate the flaw densities and size distributions measured by NDE (Chapman and Simonen 1998) to other vessels. Future work will gather information on vessel fabrication techniques to aid in producing generalized flaw density and size distributions for application to the entire population of U.S. reactor pressure vessels.

The objective of this research is to develop empirically based estimates of fabrication flaws in the RPVs of operating nuclear power plants for use in fracture mechanics structural integrity assessments. Structural assessments, such as those that predict vessel failure, are performed using computer codes that require, as input, accurate estimates of flaw rates. The likelihood of vessel failure is sensitive to the location, type, size, and other characteristics of the flaws. The objective of this research is to estimate these and other relevant properties of fabrication flaws in U.S. reactor pressure vessels.

Materials from four different reactor pressure vessels have been selected for study. The major vessel manufacturers and the major vessel designs have been considered in the selection. See Doctor et al. (1999). Figure 1.1 shows the PVRUF vessel, located at Oak Ridge National Laboratory, before disassembly.

NDE was performed on pressurized water reactor (PWR) vessels made by Babcock & Wilcox (Midland vessel) and Combustion Engineering (PVRUF vessel) (Schuster et al. 1998). A boiling water reactor (BWR) vessel made by Combustion Engineering (Shoreham vessel) has been examined by NDE (Schuster et al. 1999).

Volume 1 of this report (Schuster et al. 1998) describes the nondestructive evaluation of fabrication flaw indications obtained from ultrasonic, volumetric inspections made from the PVRUF vessel's inside, cladded surface. The report includes a discussion of those flaw characteristics that were predicted by fracture mechanics calculations to be most important for vessel integrity. Design and fabrication information on RPVs is presented especially on the subclass of vessels used in PWRs, along with the specifications for the PVRUF vessel. The report discusses the most significant indications found by the inspections through the cladding and documents their important features. The distributions of the indications in those categories important for vessel integrity were presented along with a methodology for fitting a parametric rate function to the distribution of indications detected in the NDE measurements. The details of the inspections of the material removed from the Midland vessel, manufactured by Babcock & Wilcox, were included as an appendix.

Volume 3 (Schuster et al. 1999) documents the results of the nondestructive examination of vessel material removed from the canceled Shoreham nuclear power station. The report gives the number and characteristics of the flaw indications detected and sized in the non-destructive examination. The Shoreham material

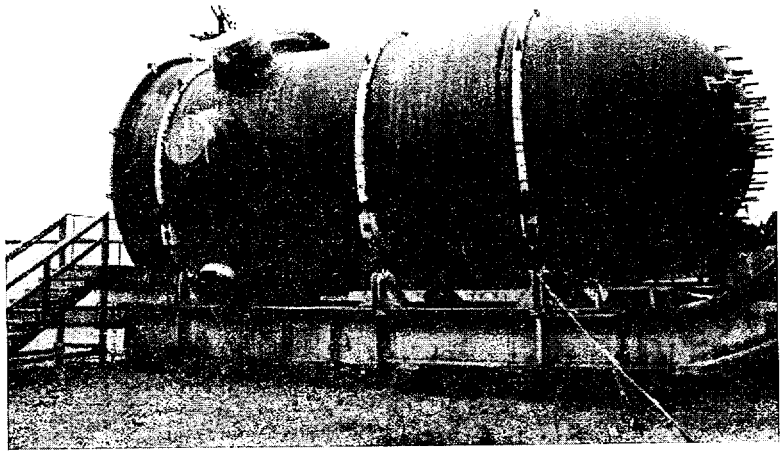

Figure 1.1 Photograph of the PVRUF Vessel at Oak Ridge National Laboratory

is described and PNNL's approach to the research is given. The performance of the SAFT-UT inspection system is reported with a complete list of inspection results.

The research reported in Volume 2 (this document) on material removed from the PVRUF vessel, was performed to validate the presence and characteristics of the fabrication flaw density and distribution. Chapter 2 of this report describes the methodology used by PNNL researchers to produce validated flaw rates: weld-normal ultrasonic testing, radiography of 25-mm thick plates, and metallography of 25-mm cubes. Chapter 3 shows the data obtained by the validation research. Chapter 4 describes the validated flaw density and distribution that was obtained from the data. Because repair welds contained the largest flaws, the repair information was extracted from the vessel construction records, and Chapter 5 lists the size and number of repairs to the vessel. Conclusions and recommendations are given in Chapters 6 and 7, respectively.

2 RESEARCH METHODS APPLIED TO THE VALIDATION OF FLAW INDICATIONS IN PVRUF

The principle objective of this work was to provide high quality flaw statistics for use in probabilistic fracture mechanics analyses, such as pressurized thermal shock (PTS) analyses. Part of achieving this objective was to validate the presence and the sizes for the larger indications reported in Schuster et al. (1998). Selective destructive confirmation was required for the purpose. In this chapter, the SAFT-UT indications found during the inspections from the clad surface and reported in Schuster et al. (1998) are referred to as "Volume 1 flaw indications."

Flaws with 6 mm or more through-wall extent are most useful for assessment of structural integrity. All Volume 1 flaw indications in the near-surface zone larger than 5 mm in through-wall size were received by PNNL. All indications greater than 7 mm in the remainder of the vessel wall were received. Using this size criterion, 30 Volume 1 flaw indications were identified for validation.

To provide high-quality flaw statistics, it was important to ensure that large flaws had not been missed by the inspection procedure documented in Volume 1. And, it was important to validate the density and distribution of the smaller flaws because they may be related to the larger ones and their presence and characteristics will affect NDE reliability.

A secondary objective of the validation was to evaluate the reliability of the inspections of the PVRUF weld metal through the cladding. One or two of the analysis rules determined the size of the largest flaw indications. The validation of these sizing rules was an efficient step in measuring the NDE reliability.

This chapter describes the analysis methods that were applied to the validation of the PVRUF flaw indications. The spatial distribution of the large and small SAFT-UT flaw indications was developed before the material was removed from the PVRUF vessel. Large specimens of material were removed from the vessel and selected specimens were sent to PNNL. The shape and size of the weld cross sections were measured in the specimens, and the volume of weld metal inspected by SAFT-UT was confirmed. The effects of positioning error were estimated. The weld metal was removed from the PVRUF specimens, and weld-normal ultrasonic testing was performed. Radiographic testing was performed on 25-mm-thick plates removed from the weld metal specimens. Ultrasonic, radiographic, and metallographic analysis was performed on 25-mm cubes removed from the 25-mm-thick plate specimens. Details of these methods are presented in the following sections.

2.1 Distribution of the Volume 1 Flaw Indications

The validation of flaw indications reported in Volume 1 (Schuster et al. 1998) required the removal of material from the PVRUF vessel. Before this was done, the distribution of both the large and the small flaw indications was needed to establish how the material should be removed and which specimens were needed at PNNL. The large flaws were needed to confirm their presence and size and to have validated flaw density and size distributions. The small flaws were used to establish the sensitivity of the database to noise sources and to confirm that they really were small flaws.

The indication database showed that most of the indications were small, that is, on the order of 2 mm (0.08 in.) or smaller through-wall. The data showed that 97% of the indications were less than 2 mm (0.08 in.) in size in the near-surface

zone, that is, within 25 mm (1.0 in.) of the inner surface of the PVRUF vessel. For the remainder of the vessel wall, the data showed that 80% were smaller than 4 mm (0.16 in.) in size. The rate of false detections in the database, from all noise sources, was expected to be low because the detection rules were based on the high correlation of SAFT-UT indications with flaws validated by destructive tests of material removed from the Midland vessel.

The first evidence that the small flaw indications were discontinuities in the weld was the ratio of indication density in weld metal to that in the base metal. The calculation of the flaw indication density for the near-surface weld metal and base metal showed a greater estimated density of flaws in the weld metal. This ratio was 4 to 1 when only the planar flaws greater than or equal to 2 mm (0.08 in.) were considered. The destructive validation of the SAFT-UT indications provided valuable metallographic data on the nature of flaws in the two distinct populations.

Comparisons of the indication densities for the weld metal, heat-affected zone, and base metal in the portion of the vessel outside the near surface zone showed a greater estimated density of flaws in the heat-affected zone and weld metal. For planar indications greater than or equal to 4 mm (0.08 in.), the density ratio was 8 to 1 for the heat-affected zone compared to the base metal. PNNL expected that the density ratios of weld to base metal flaws would increase after estimates of echo location errors become known through this flaw validation work. It was expected that these errors were systematically causing flaws near the fusion line to be incorrectly positioned in the base metal.

Figure 2.1 shows the plan view of the indication density for Block 5-1, one of the approximately 1800-kg (4000-lb) PVRUF specimens. Block 5-1 is typical of other PVRUF material in that the indication density is greatest on the weld fusion line. First, these data show that the small flaws are neither random nor associated with the couplant pooling on the cladding but rather must be ascribed to acoustic discontinuities on the fusion line of the weld with the base metal. Second, these data show that the effects of position errors are greater than anticipated from a more uniform flaw indication distribution through the weld metal. Furthermore, it is valid to assume that a number of flaw indications on the fusion line were assigned mistakenly to the base metal because of position uncertainty. An analysis of indication positioning error is given in Section 2.4.

Figure 2.2 shows the plan view of indication density for Block 5-7. This material contained a significant density of indications in the base metal. Data confirmed the presence of mid-wall inclusions in the base metal of this specimen. These indications were not associated with one of the axial welds present in this material.

2.2 Removal of Material from PVRUF

After the distribution of both the large and the small flaw indications was generated, it was possible to establish how the material should be removed from the PVRUF vessel. The size of the specimens was chosen to permit the original SAFT-UT measurements to be repeated and to limit the weight of the specimens to an amount that was manageable in the PNNL NDE laboratories.

Figure 2.3 shows a vessel roll-out drawing with the specimens identified relative to the weld metals. Material selected for validation of Volume 1 flaw indications was located on the weld metals that were inspected. Dimensions for one of the typical PNNL specimens was 127 cm long, 61 cm wide, and 22.9 cm thick with the weld centered in the width. The locations of the cut lines were chosen to avoid the large flaw indications and significant clusters of small indications. Twelve specimens were sent to PNNL. The specimen labeled 4-7 PNNL was not

removed from the vessel; in this case, the larger indications were removed in separate small specimens.

2.3 Confirmation of Weld Position and Cross Section

In the PVRUF vessel, the location of a weld was indicated by punch marks placed on the inside surface of the vessel by the manufacturer. The welds were known to be single-Vee welds, and their cross sections were indicated on the engineering drawings of the vessel. These weld cross sections were used to estimate the amount of weld metal inspected in PVRUF by SAFT-UT.

After the PVRUF specimens were received at PNNL, it was possible to confirm the weld cross section and the volume of weld metal inspected. Figure 2.4 shows the weld cross section for a specimen from the beltline weld of the PVRUF vessel. This photograph was taken after the weld specimen was polished and acid-etched. The weld is shown to be single Vee in design. The top of Figure 2.4 shows the cladding layer as a dark band that is somewhat thicker over the weld than over the base metal. The cross-sectional area of the weld metal within the near-surface zone (25 mm from the wetted [inside] clad surface) is 4.9 cm^2. The cross-sectional area of the weld outside the near-surface zone is 73 cm^2.

Figure 2.5 shows the weld cross section for the circumferential weld (girth seam) between the upper and intermediate shell courses. The vessel makes a thickness transition at this weld. The upper shell course, which contains the nozzle penetrations, is thicker and shown to the right of the weld in Figure 2.5. The cross-sectional area of the weld metal within the near-surface zone (25 mm from the wetted clad surface) is 7.7 cm^2. The cross-sectional area of the weld outside the near-surface zone is 81 cm^2.

2.4 Indication Positioning Error and the Amount of Material Inspected

As a part of the validation of the PVRUF flaw density and distribution estimates, it is important to confirm the location of the flaws in the material. Accurate information on the location of flaws is useful to the modeling efforts attempting to describe the mechanisms that produce them.

Error in locating an ultrasonic discontinuity arises from uncertainty in the material properties; e.g., the ultrasonic wave speed can vary by several percent. Changes in wave speed cause changes in the refracted angles in the material and the time of flight or distance to the flaw. All of the SAFT-UT inspections were made through the stainless steel cladding, and the inhomogeneous nature of the cladding, combined with the surface roughness of the cladding, causes beam-steering.

Previously, PNNL had confirmed and published the concentration of fabrication flaw indications on the weld fusion line (Schuster et al. 1997). Uncorrected data revealed the significance of the fusion line in the plan views of flaw frequency. Metallographic results, presented in Chapter 3, confirm vertical planar flaws adjacent to the base metal but slightly inside the weld metal.

The 2500 indications were reanalyzed based on proximity to the fusion surface to determine the density ratio of weld flaws to base metal flaws. For all indications, PNNL researchers found this ratio to be 8 to 1. For planar indications greater than 4 mm in through-wall extent, the ratio of weld-to-base metal indications density is 14 to 1.

Future work will address the density and distribution of flaws in base metal, especially those of interest to structural integrity assessment. See Chapter 7, Recommendations.

Table 2.1 shows the amount of material inspected by SAFT-UT in the PVRUF vessel using the confirmed weld cross-sectional areas.

Table 2.1 Amount of Material Inspected in PVRUF	
Near-Surface Zone	
Clad	0.027 m^3
Clad-to-Base Metal Interface	4.6 m^2 (surface area)
Weld and HAZ	0.014 m^3
Base Metal	0.075 m^3
Outside the Near-Surface Zone	
Weld and HAZ	0.18 m^3
Base Metal	0.90 m^3 for angle beam 0.28 m^3 for normal beam

2.5 Removal and Weld-Normal Ultrasonic Testing of Weld Metal

The weld metal was removed from all 12 large PVRUF specimens. An ultrasonic inspection surface was machined onto one of the cut faces of the weld metal specimens in preparation for testing normal to the weld metal. All of the removed weld specimens were examined by weld-normal ultrasonic inspection using the SAFT-UT system. This was the first step in a sequence of methods that also included cutting of radiographic specimens, radiography and flaw sizing, and finally metallographic analysis. These methods were developed on a relatively flaw-free piece of PVRUF material and on a relatively small flaw. They were then successfully applied to the larger indications selected for destructive testing.

Figure 2.6 shows one of the 12 large PVRUF specimens as it was prepared for removal of the weld metal. The black cut lines in Figure 2.6 were placed to avoid large indications and clusters of small indications. Two specimens containing the entire weld metal were removed from each block, as shown in Figure 2.7.

2.5.1 Removal of Weld Metal from PVRUF Specimens

The large-scale cutting of PVRUF material was performed with a band saw. This work involves cutting the 4000-lb blocks into as many as six to nine pieces. All 12 blocks were marked for cutting in such a way as to avoid destroying significant flaws and clusters of flaws. The cuts are made to provide a scanning surface parallel to the weld metal and approximately 75 mm distant (from the weld center line). Specimens that contain weld metal are typically 61 cm long, 15.2 cm wide, and 22.9 cm thick with the weld centered in the width. The coordinates of all pieces are stamped into the clad surface metal to preserve the orientation of all material with respect to the vessel.

Figure 2.7 shows two weld specimens removed from the PVRUF material. These specimens weigh about 227.3 kg each and are easily moved and positioned in the laboratory. Furthermore, this size specimen is easily cut into 25-mm-thick plates for radiographic testing.

2.5.2 Ultrasonic Testing Normal to the Weld Metal

The weld metal was re-inspected, for all specimens, by ultrasonic testing normal to the weld metal. This inspection mode was chosen because it is very sensitive to discontinuities that have through-wall extent. These data showed a concentration of small flaws on the fusion line (weld metal to base metal) as predicted by the scatter diagrams of indications detected in the original data.

Normal beam ultrasonic measurements were made using the SAFT-UT system and a curved track. The curved scanner track allows the

scanner to record the material coordinates of the indications. These material coordinates were used to reconfirm detection of the significant flaws from the original measurements. The curved track also permitted a consistent inspection of the inner and outer portions of the material.

Figure 2.8 shows the weld-normal SAFT-UT inspections under way on a weld specimen. The weld cross section is faintly visible in Figure 2.8 on the end of the specimen. These weld-normal inspections were useful for a number of research needs. They helped to ensure that no large flaws were missed in the original inspections, the new data also confirmed the detection of a specific flaw and provided a more accurate location for a flaw so that radiographic specimens could be prepared.

Figure 2.9 shows a typical example of weld-normal ultrasonic data. The clad surface of the specimen is to the right in Figure 2.9. The single Vee weld profile is evidenced by the ultrasonic signals from the small flaws on the fusion lines.

2.6 Removal and Radiographic Testing of 25-mm-Thick Plates

Approximately 40 indications received radiographic testing in 25-mm- (1.0-in.-) thick plates that were removed from the weld metal specimens. Radiography was performed on the plates and indications were selected for removal from the plates. The indications were centered in 25-mm (1.0-in.) cubes, and radiography was used to locate the flaws in the cubes. Metallography was used to document the nature and size of the flaws in the cubes.

2.6.1 Cutting of Radiographic Specimens

PVRUF weld material was cut into 25-mm-thick plates for radiographic testing. Large and small flaws were located in the plates, and the purposes of the radiographs were to precisely locate the large flaws in the material, to confirm the presence of small flaws, and to provide data on the sizes of the imaged flaws.

Figure 2.10 shows some of the 25-mm-thick plates removed from the weld metal specimens. The thinner plates in Figure 2.10 contained fabrication flaws and received radiographic testing.

2.6.2 Radiography of 25-mm Plates

PNNL researchers investigated the use of radiography as a means of both characterizing the flaws for controlling the metallographic process and of validating the size and character of a larger-sized sample of indications than possible with metallography alone. Small, nonvolumetric flaws can be difficult for the metallographic process to find. The radiographic data confirmed the presence of discontinuities on the fusion line as measured by the weld-normal ultrasonic testing.

Radiography of the PVRUF 1-in.-thick plates and cubes was done to Westinghouse Hanford's General Radiographic Examination Procedure (NDT-RT-4000, Rev. 3) with a Philips 450 KV x-ray machine. Required sensitivity was 2T (thickness) with a density requirement between 1.8 to 4.0 H&D units. The nominal voltage setting was 350 KV at 2.5 mA, however varied based on plate thickness. The film was single-loaded Fuji type 25. Image quality was based on conventional ASME penetrameters.

Figure 2.11 shows a typical radiograph of a 25-mm plate containing some flaws. The flaw was located by the weld-normal ultrasonic testing and the arrow markers indicate the location of the flaw as predicted by the ultrasound. The presence of a flaw is confirmed in the location predicted.

2.7 Ultrasonic, Radiographic, and Metallographic Analysis of 25-mm Cubes

Flaws were removed from the 25-mm plates by using the radiography to center the flaw in a cube of material. A 25-mm cube is a convenient size for the metallographic steps of grinding, polishing, and etching. This is also a convenient size for ultrasonic and radiographic testing. Figure 2.12 shows a 25-mm cube removed from a plate.

2.7.1 Ultrasonic Testing and Flaw Sizing in 25-mm Cubes

Ultrasonic testing was performed on the near-surface zone cubes to inspect for under-clad cracks. The flaws had been located in the plates using weld-normal ultrasound, but the proximity to the clad surface introduced errors into the characterization and sizing of the flaws. Fourteen near-surface zone cubes were removed from the plates of PVRUF material, and Figure 2.13 shows an example of ultrasonic testing results on a near-surface zone cube.

2.7.2 Radiography and Flaw Sizing Using 25-mm Specimens

Radiographic testing was performed on the 25-mm cubes to provide a necessary guide for the metallography and to provide accurate measurements of flaw size. The PNNL metallographic process requires guidance because the process is non-reversible and time-consuming. Blank material must be removed quickly, and flawed material must be removed in appropriate steps. Specification of a metallographic procedure was helpful in limiting the effort required to analyze the flaw.

Another problem is that the metallography may miss the largest portion of the flaw. The radiography can be used to control the metallographic step sizes for this purpose. In metallography, it is common to remove 2 mm of metal between the polishing and etching steps. The validation of fabrication flaws requires the metallographer to remove material in smaller steps near the maximum extent of the flaw. As a consequence of this, it was important to have the radiographs and to give accurate positions for the starts of the indications and to specify a sequence of steps for removal of material. The specification was used as guidance only and the metallographer made adjustments as the flaw was revealed.

Figure 2.14 shows the radiographic results for a 25-mm cube. The removed cube of material contains a portion of the weld fusion line. The radiography showed two linear indications in the cube. The indications in the radiographs were small lack of fusion in the weld near the side-wall.

2.7.3 Metallographic Analysis

The purpose of the metallography was to validate the flaw densities and distributions estimated from the previous SAFT-UT inspections. Most of the blank material was removed in the first step of machining the 25-mm cube. Only two or three steps of blank material were left in front of the flaw. The step is defined to be the amount of flawed material to be removed between micrographs. The step size was chosen based on the size of the flaw and is typically 10% or less of flaw length (perpendicular to the machining surface). Because some of the flaws were small, the step size could be as little as 0.25 mm.

Photographs were taken at every step, using 3x magnification to record the location of the flaw with respect to the edges of the cube and using 50x or 100x magnification to record the micrographic features of the flaw. Polishing and etching were performed to show the microstructure of the surrounding material—i.e. weld, HAZ, and base metal—and to expose the details of the ends of the flaw. The polishing step was performed infrequently, usually near the maximum extent of the flaw, because 16 hours

were needed to provide an adequate surface finish for the etchant to reveal the microstructure.

Figure 2.15 shows a micrograph of the complete face of a 25-mm cube. A 2-mm flaw is revealed as a lack of fusion just inside the weld metal (there is weld metal on both sides of the flaw).

2.8 Summary of Validation Methods

The analysis methods applied to the validation of the PVRUF flaw density and distributions required the removal of material from the PVRUF vessel. The spatial distribution of the large and small SAFT-UT flaw indications were developed before the material was removed. The shape and size of the weld cross sections were measured and the volume of weld metal inspected by SAFT-UT was confirmed using PVRUF specimens received at PNNL. The effects of positioning error were estimated and used to generate new flaw density and distribution estimates. The weld metal was removed from the PVRUF specimens and weld-normal ultrasonic testing was performed. Radiographic testing was conducted on 25-mm-thick plates removed from the weld metal specimens. Ultrasonic, radiographic, and metallographic analyses were performed on selected 25-mm cubes removed from the plate specimens.

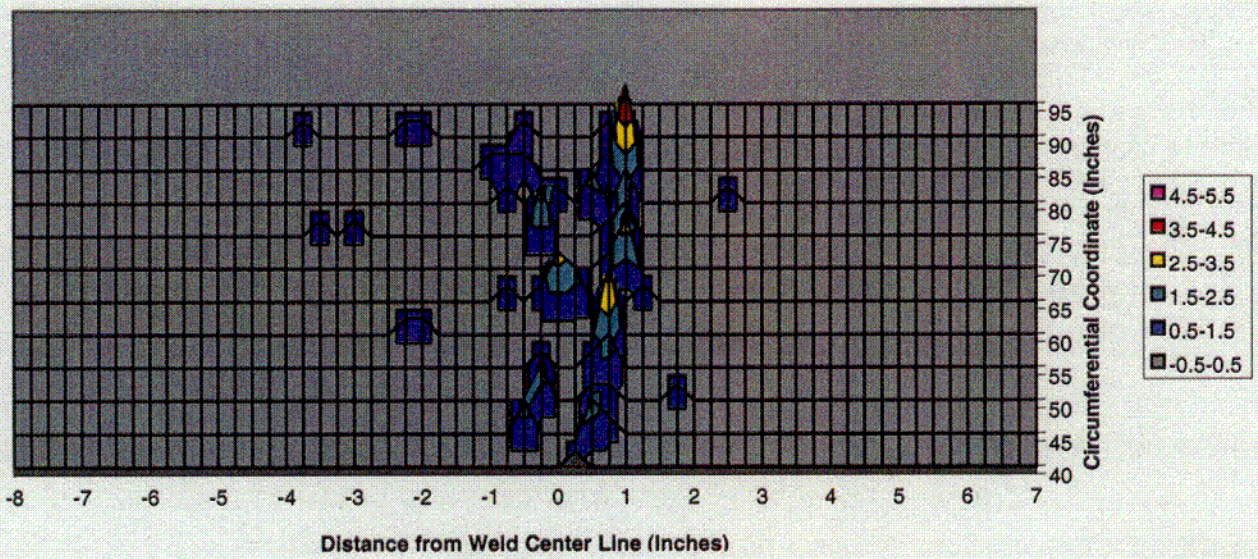

Figure 2.1 Plan View, Flaw Indication Frequency in PVRUF Block 5-1

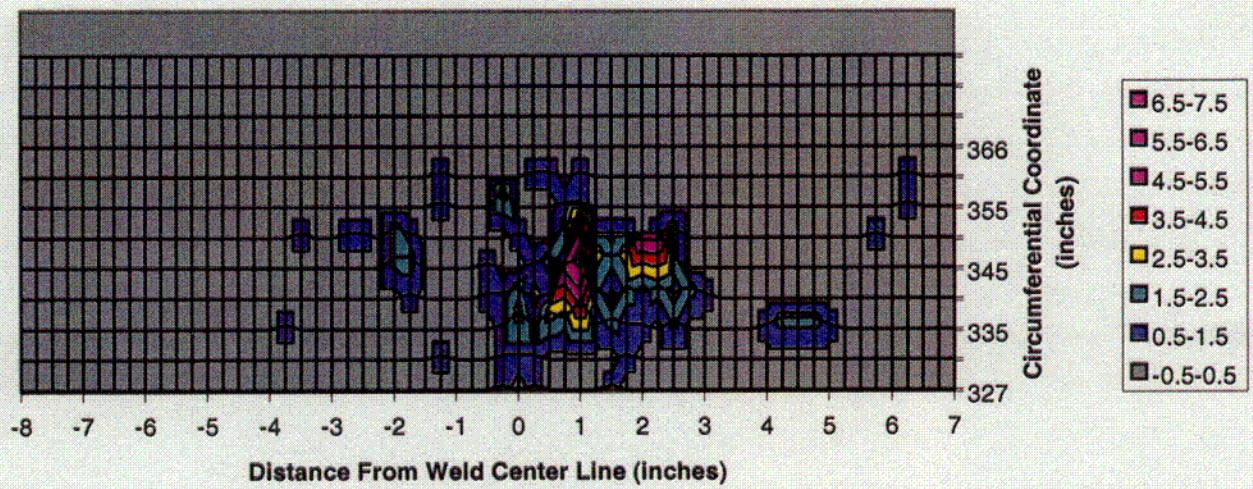

Figure 2.2 Plan View, Indication Frequency in PVRUF Specimen 5-7

C01

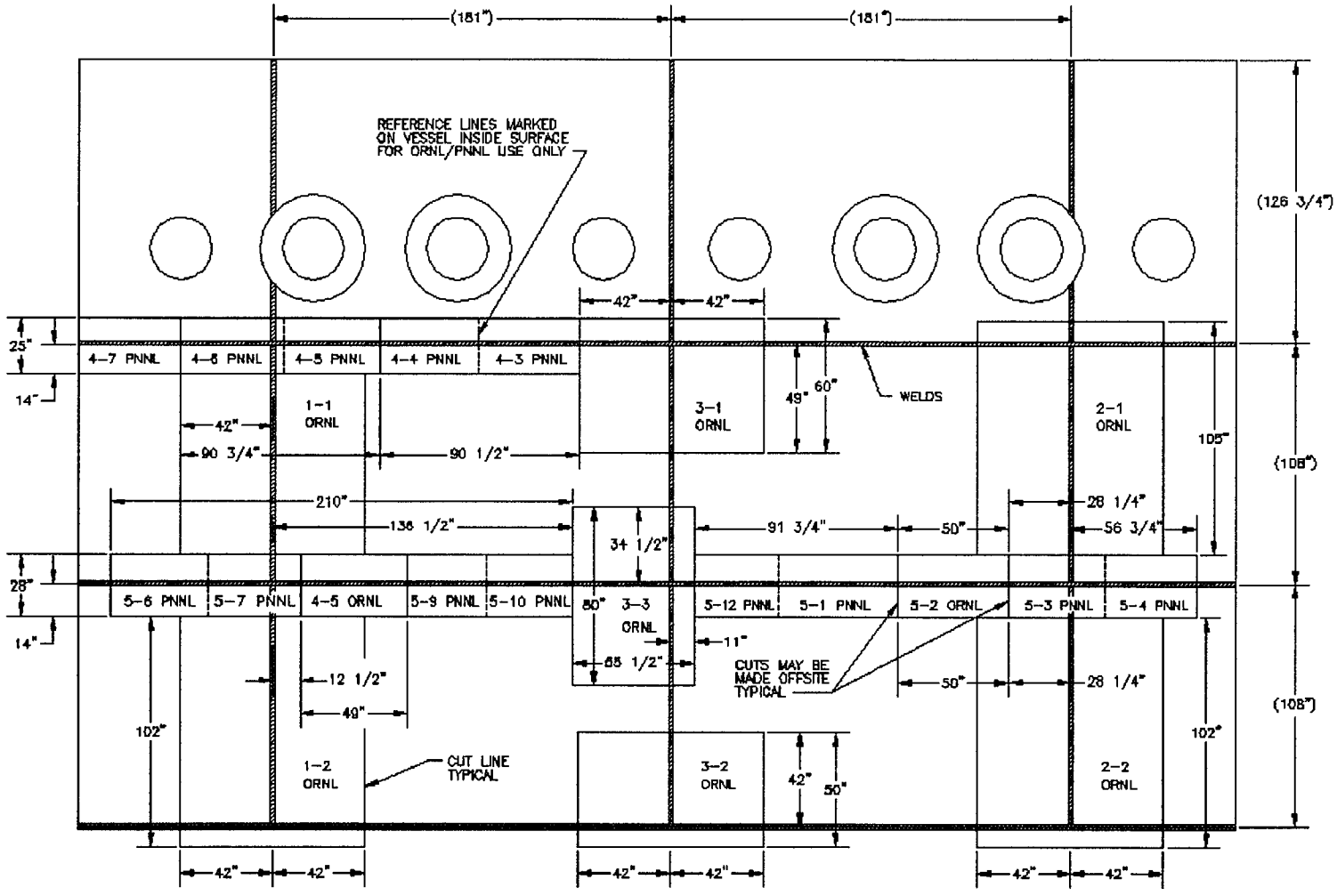

Figure 2.3 PVRUF Vessel Roll-Out Showing Plan to Remove Material

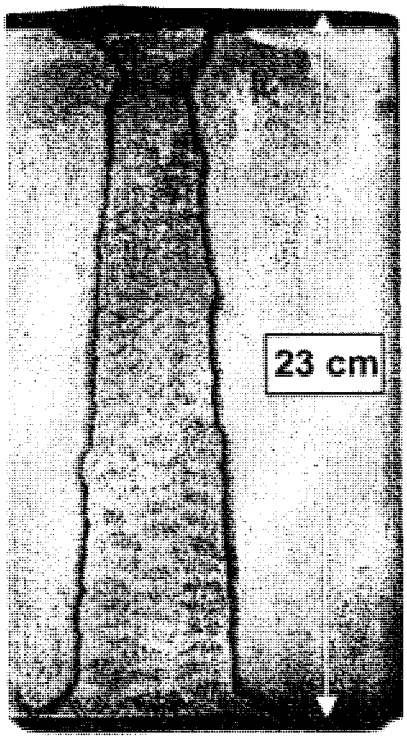

Figure 2.4 Weld Cross Section for Beltline (Lower-to-Intermediate Shell) Weld

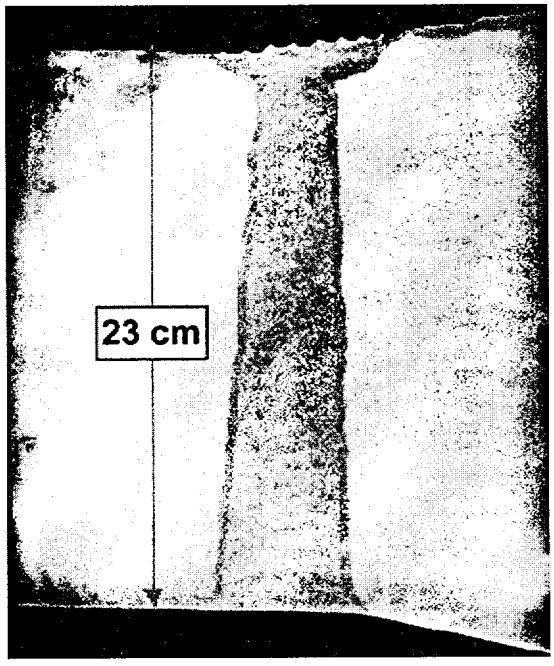

Figure 2.5 Weld Cross Section for Intermediate-to-Upper Shell Girth Weld

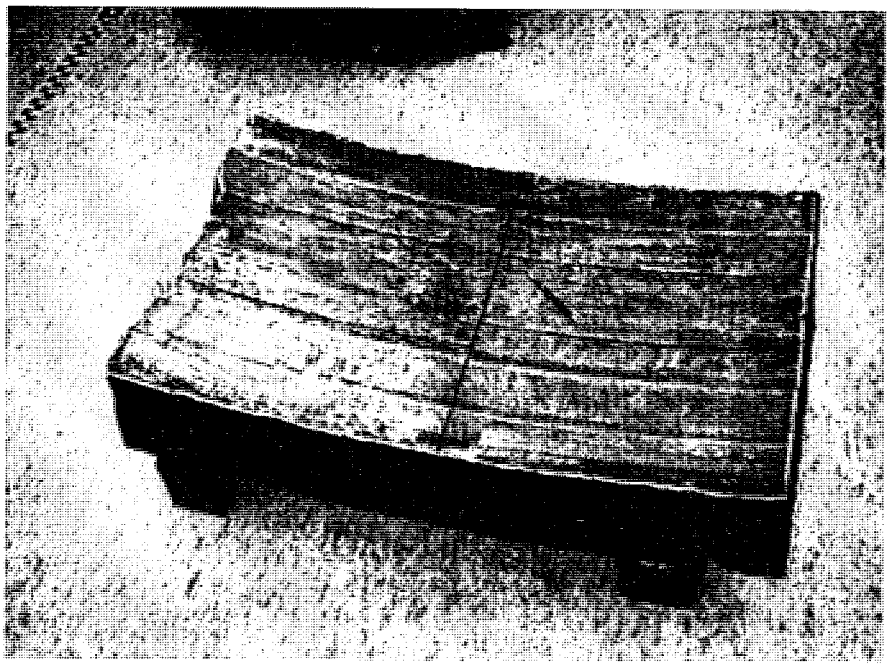

Figure 2.6 PVRUF Block Prepared for Removal of Weld Metal

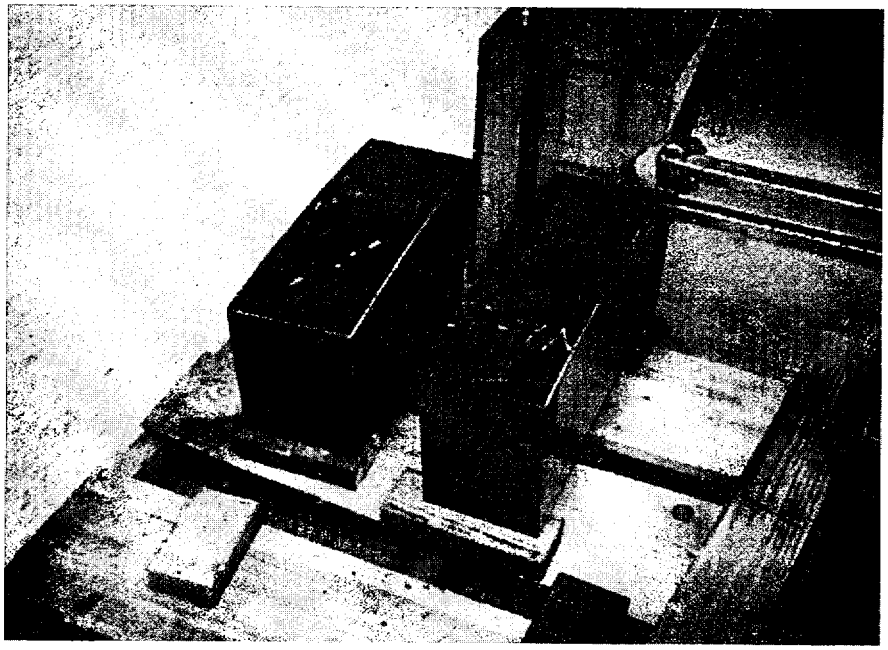

Figure 2.7 Weld Metal Specimens Removed from PVRUF Block

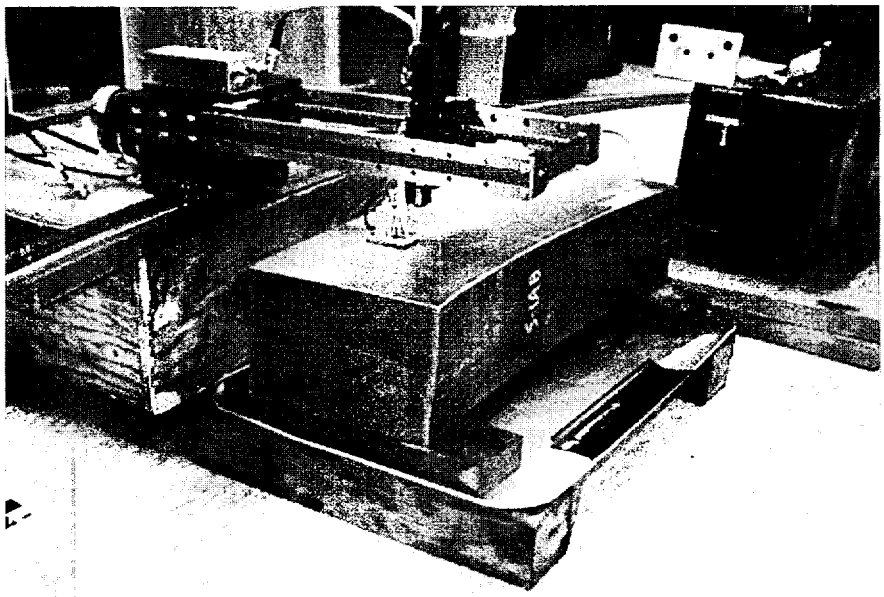

Figure 2.8 Weld Metal Specimen Prepared for Ultrasonic Inspection Normal to Weld

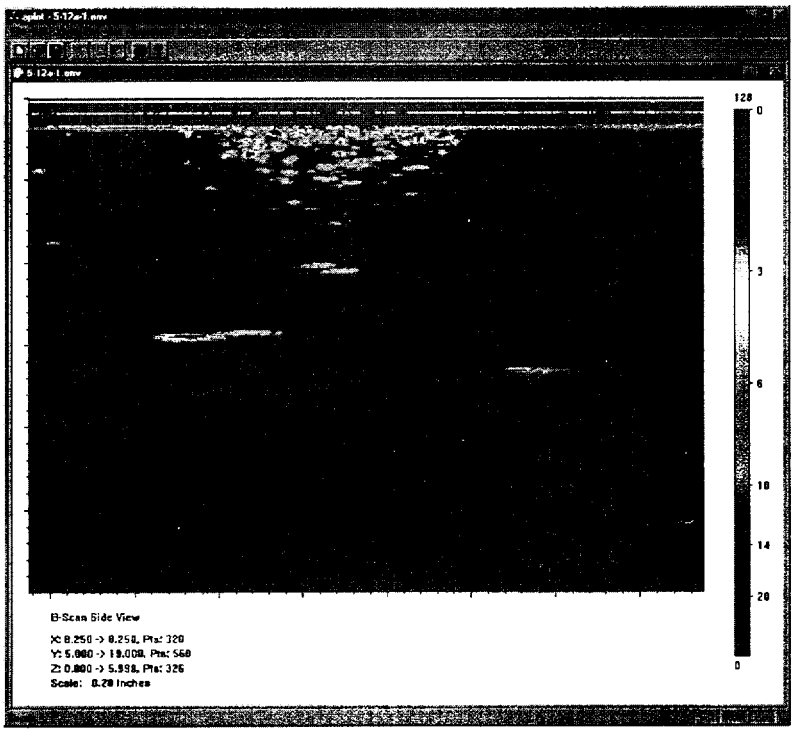

Figure 2.9 SAFT-UT Image from Ultrasonic Inspection Normal to Weld

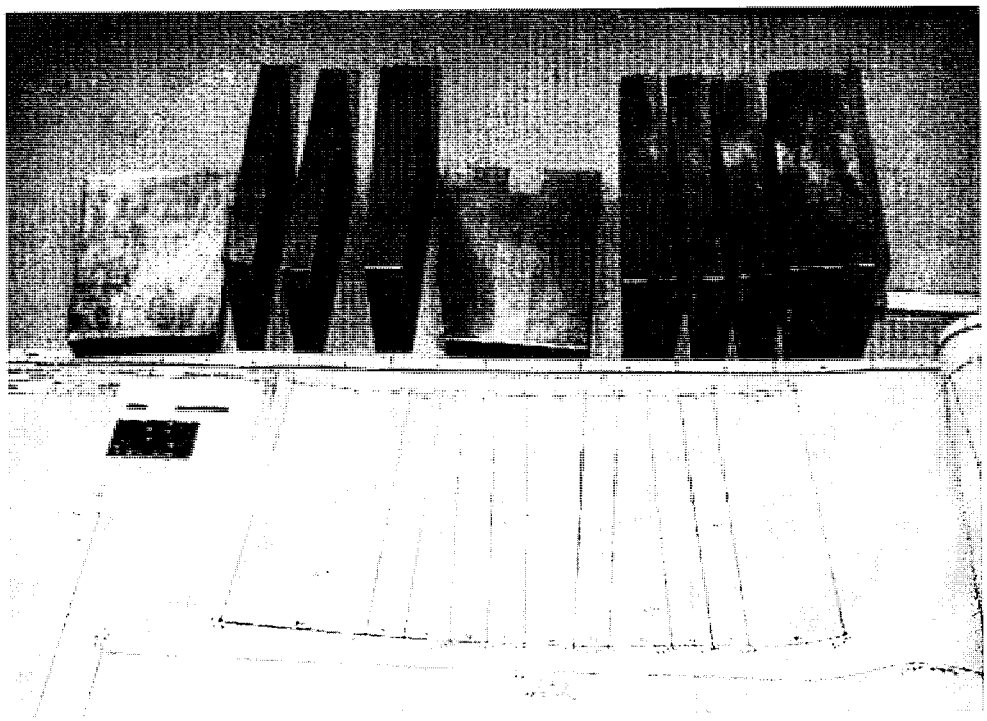

Figure 2.10 PVRUF Weld Metal Specimen Cut into 25-mm-Thick Plates

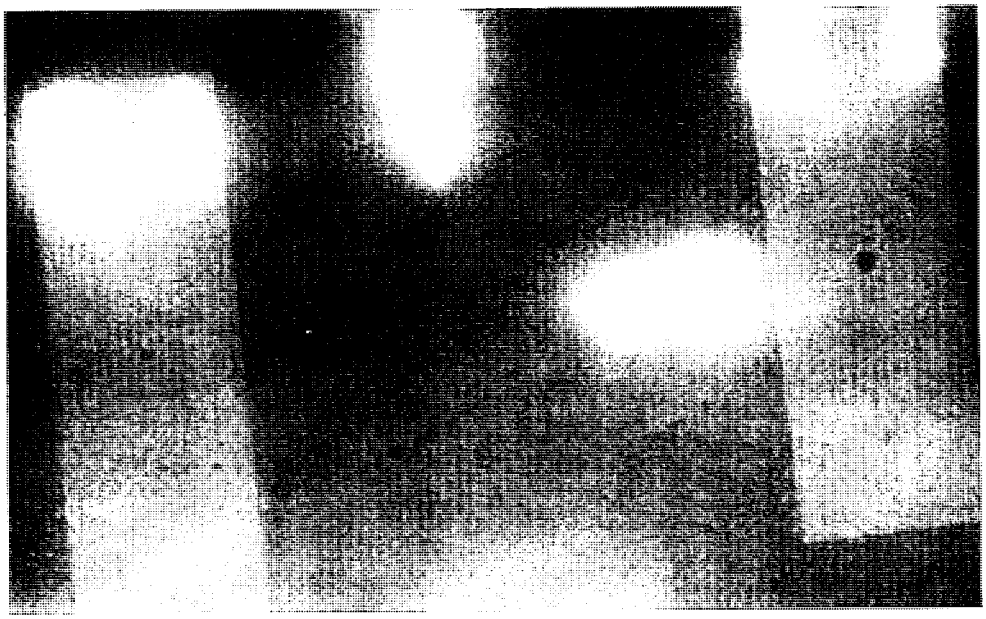

Figure 2.11 Radiograph of 25-mm-Thick Plate

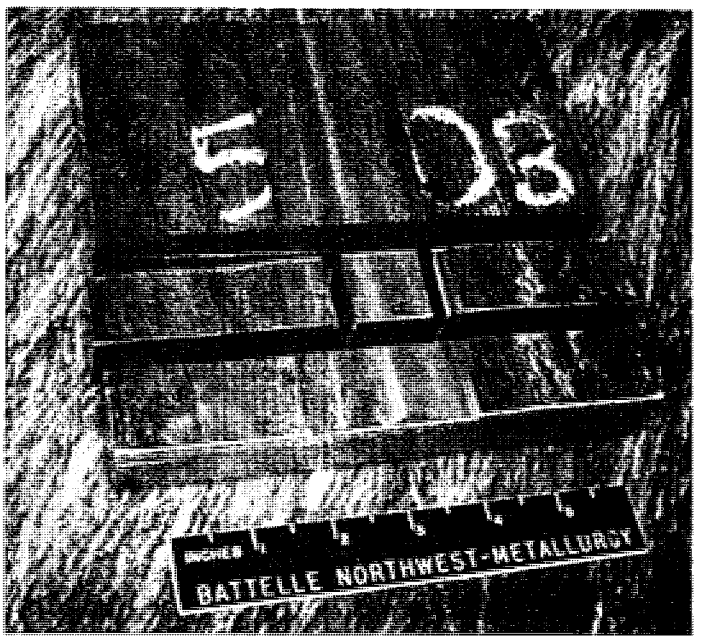

Figure 2.12 25-mm Cube Removed from Plate of PVRUF Material

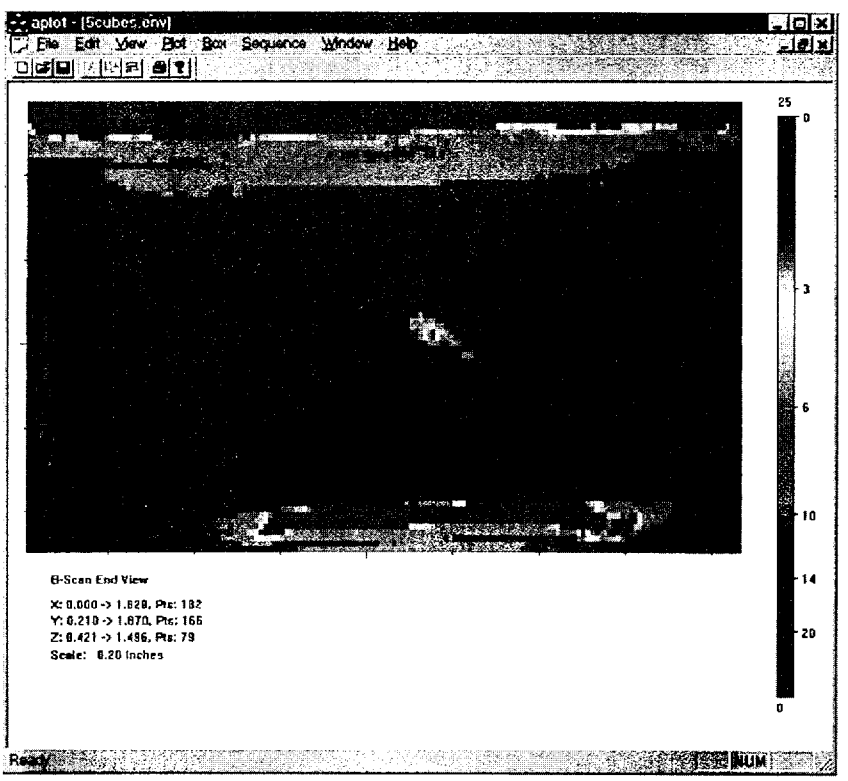

Figure 2.13 Ultrasonic Image of Flaw Indication in Near-Surface Zone Cube

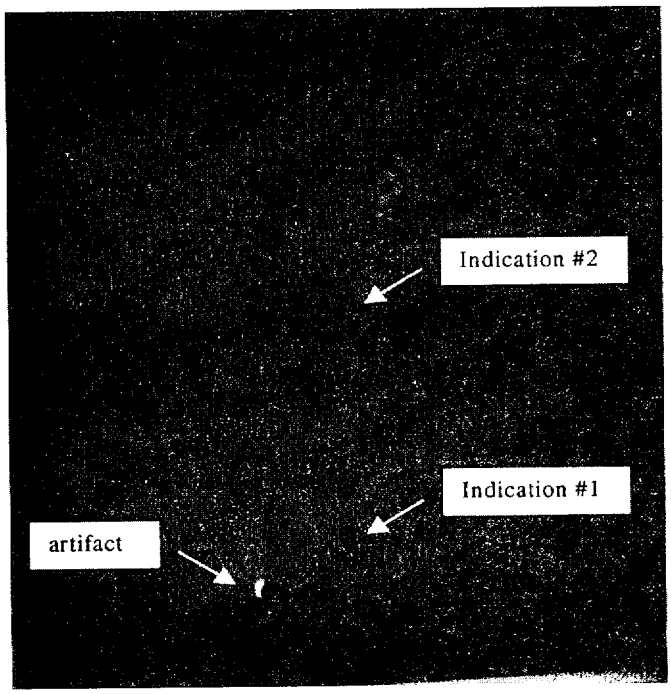

Figure 2.14 Radiograph of 25-mm-Thick Specimen

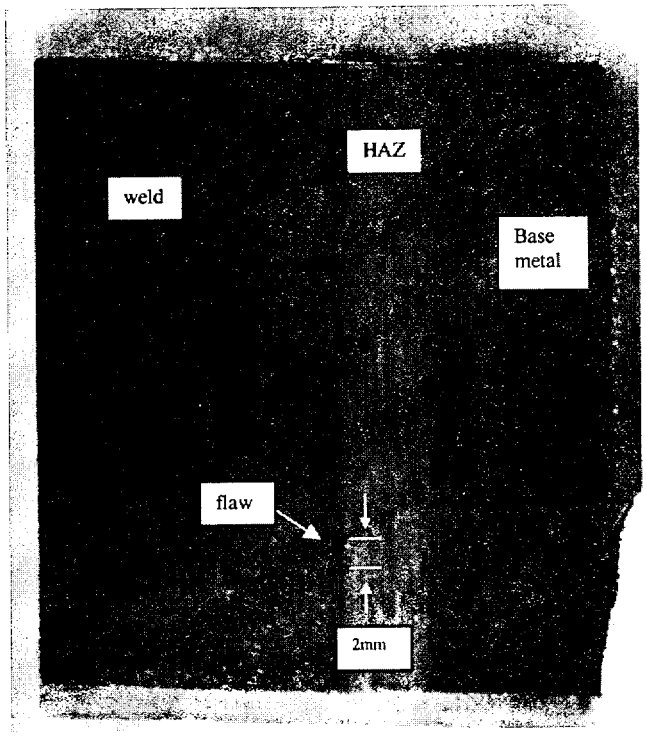

Figure 2.15 Micrograph of 25-mm Cube. Micrograph shows 2-mm flaw (dark), weld metal, HAZ, and base metal.

3 VALIDATION RESULTS

The results of the validation research are organized according to type of material or weld type in which flaws were found. References are made to flaw types as enumerated in Chapman (1998).

The PVRUF material is divided into five types as follows:

- machine-made weld metal—Most of the weld metal was deposited using tandem submerged metal arc welding from outside the vessel.
- back-fill weld metal—A back-gouge to sound metal was made from inside the vessel and back-filled with shielded metal arc welding (girth welds only).
- repair weld metal—Repairs were made and documented according to procedure.
- cladding—Cladding was applied to vessel's inside surface.
- base-metal—The majority of the PVRUF vessel material is base metal, A533B, bent plate.

A discussion of flaw types of interest to structural integrity assessment of RPVs is given in Chapman (1998). Briefly, they are

- shrinkage cracks associated with individual weld passes
- heat-affected zone cracks from either delayed hydrogen cracking or stress relief cracking
- lack of fusion on the weld fusion surface with the base metal or between the weld passes
- slag on the weld fusion surface or between the weld passes.

In addition to describing the results of PNNL's validation testing of the PVRUF material, it is important to show and explain the origin of the flaw indications reported in Schuster (1998). In this chapter, the SAFT-UT indications found during inspections from the clad surface and reported in NUREG/CR-6471, Volume 1 are referred to as "Volume 1 flaw indications."

3.1 Flaws in Machine-Made Weld Metal and Located on the Fusion Surface of the Weld with the Base Metal

The results of laboratory testing for fabrication flaws associated with the machine-made weld metal are presented in this section. This specific portion of the vessel is limited to the material within the tandem submerged metal arc weld passes made from outside the vessel. This excludes the back-fill weld passes, made from inside the vessel, and any flaws found in the first machine-made weld pass made from outside the vessel. Flaws found in this region are reported in Section 3.2.

Results of the weld-normal testing of the machine-made weld metal are presented first. All of the PVRUF weld metal sent to PNNL was inspected using weld-normal ultrasonic testing.

Results from radiographic testing (RT) of a sample of the PVRUF material are reported next. Digitized images of the radiographic film were made, and the figures show the images of the RT indications found.

Results of metallographic tests on two flaw indications within material described in this section are then reported. A test was made of a small flaw indication on the fusion surface of the machine-made weld metal with the base-metal plate. A second flaw indication found within the

weld was sectioned metallographically, and the micrographs are shown.

After analyzing all of the validation data, it was concluded that resources would be more effectively used in meeting programmatic goals by performing further destructive tests on flaws in other locations of PVRUF material. Thus, no further destructive tests were performed on flaws in this portion of the PVRUF material. Efforts were shifted to repair flaws and flaws in the inner 25 mm of the vessel.

3.1.1 Weld-Normal Ultrasonic Testing of Machine-Made Weld Metal

The weld-normal ultrasonic testing of PVRUF material confirmed an elevated concentration of flaw indications on the fusion surfaces of the structural weld with the base metal plate. Figure 3.1 shows the weld profile of the PVRUF vessel's beltline weld as it lies on its side during weld-normal testing with the transducer insonifying from the surface at the top of Figure 3.1. The weld back-gouge is on the right side. The weld profile is made evident by the ultrasonic energy returned from the numerous small flaws on the fusion surface.

Flaw indications in the machine-made weld metal were confirmed to be small. Figure 3.2 shows the top view of a weld-normal ultrasonic inspection. The major portion of the flaw indications produce circular shapes whose image sizes are determined more by the SAFT-UT system resolution (3 mm using a 5-MHz, 6-mm diameter transducer) than by the size and shape of the small flaws. The cladding is on the right side of Figure 3.2, and the vessel OD is on the left side. The weld-normal flaw indications are not randomly distributed in that some weld passes, as shown by a long line of indications in Figure 3.2, contain more small flaw indications than other weld passes.

A minor number of flaw indications was found between the weld beads of the machine-made weld metal. Figure 3.3 is similar to Figure 3.1 except that in this case a flaw indication is evident within the weld instead of along the fusion surface.

The validation work confirmed that consecutive weld passes can produce a cluster of vertically oriented small flaws. Figure 3.4 shows the results of weld-normal testing of the internal welding flaw indication shown in Figure 3.3. In this case, the cladding (not shown) is on the left side of the figure. The distance between the flaw rows of indications is 10 mm. The weld bead size is also 10 mm, and these data show that consecutive weld passes can contain flaw indications at the same circumferential location.

Weld-normal indications were up to 7 mm in size. Figures 3.5, 3.6, and 3.7 show extended and long lack of fusion indications up to 7 mm in through-wall extent. Some of the larger Volume 1 flaw indications were shown to be two or more small indications. For example, *planar indication #1 in the heat-affected zone* (Schuster 1998, p. A.126) was sized as 34 mm using a rule statement that assumes (correctly) that a large, smooth flaw will return acoustic energy from its upper and lower tips but not from the body of the flaw. The 34-mm flaw indication, when tested by weld-normal UT, was shown to be multiple small flaws. The weld-normal UT showed two rows of small indications in a pattern similar that of Figure 3.2.

The larger Volume 1 indications that did not correlate well with the weld normal indications are discussed in Section 3.1.2.

3.1.2 Radiographic Testing of 25-mm Thick Plate

Four PVRUF weld metal specimens, 5-1AB, 5-1C, 5-10B, and 5-12BA, were sectioned into 25-mm- thick plates to validate and further characterize the weld-normal flaw indications. Table 3.1 gives the results of the radiographic testing and a reference to a figure for each RT flaw indication found. Figures 3.8 through 3.50 show images of digitized radiographs containing the RT flaw indications. The vessel through-wall direction is oriented vertically in these images with the cladding at the top of all these figures.

The results of the radiographic testing showed that RT flaw indications were located at the positions predicted by the weld-normal UT. This result confirms that the fusion surfaces of the machine-made weld metal with the base-metal contain an elevated concentration of flaw indications. Furthermore, the RT flaw indications are shown to be mostly (70%) vertical linear indications, with the rest being rounded indications.

The radiographic testing results given in Table 3.1 can be used to estimate a size distribution for small flaws. A flaw density estimate can be obtained by calculating the weld volume from the weld cross section and the number of 25-mm plates in the test. Use of these RT results in calculations of flaw density and distribution is discussed in Chapter 4.

Some of the larger Volume 1 flaw indications were not detected easily in the weld-normal ultrasonic testing. To further characterize these Volume 1 flaw indications, PVRUF specimen P5D containing Volume 1 flaw *planar #2 in the weld* was sectioned into 25-mm plates. The results of the radiographic testing of these plates are given in Table 3.2. As shown in Table 3.2, rounded RT flaw indications were found in the material containing the Volume 1 flaw indication. The percentage of rounded indications is 60% in this material, significantly higher than the 30% found in material analyzed in Table 3.1. No horizontal inter-run lack of fusion was found in this material.

3.1.3 Metallographic Testing of Machine-Made Weld Metal

A 25-mm plate was sectioned, and RT flaw indications were removed in 25-mm cubes. The cube was tested by PNNL's metallographers, and Figure 3.51 shows a micrograph of this cube with the flaw that was found. The flaw is located slightly within the weld. Figure 3.52 shows a micrograph of the flaw as polished and etched. The flaw is characterized as a lack of fusion. Figure 3.53 shows a micrograph of the fusion surface flaw at maximum extent as machined by the grinder.

The flaw indication cluster (shown in Figures 3.3 and 3.4) found between the machine-made weld passes was removed into cube form for metallographic testing. Figure 3.54 shows a micrograph of a cluster of inter-bead flaws. The flaws are small and occurred in consecutive weld passes. Figure 3.55 shows a micrograph of one of the flaws from the inter-bead cluster. The flaw is shown to be lack of fusion with slag. Figure 3.56 shows a micrograph of one of the flaws from the cluster. The flaw is shown to be inter-run slag. Figure 3.57 shows a micrograph of the same flaw shown in Figure 3.56. The inter-run slag characterization has changed to inter-run slag with tail.

3.1.4 Summary of Validation Results for Machine-Made Weld Metal

The flaw validation research shows that the fusion surfaces of the structural welds with the base-metal plate contain an elevated concentration of small flaws that are mostly vertical planar lack of fusion with slag. Some small flaws occur between the weld beads, and consecutive weld passes can contain flaws at the same

Table 3.1 List of RT Indications Found at the Location of Weld-Normal UT Indications in a Sample of PVRUF Material Sectioned into 25-mm Plates

Plate Specimen	Number of UT Indications	Number of RT Indications	Figure(s)	RT Through-Wall Size (mm)
5-1AB-2	1	2	3.8	1.3 and 1.0
5-1AB-3	1	1	3.9	1.5
5-1AB-5	3	3	3.10, 11, 12	1.8, 1.0, and 1.2
5-1AB-6	2	2	3.13, 14	3.0 and 2.0
5-1AB-7	2	2	3.15, 16	2.0 and 1.0
5-1AB-9	2	1	3.17, 18	2.0
5-1AB-11	1	2	3.19	3.0 and 1.0
5-1AB-12	3	2	3.20, 21, 22	1.5 and 1.5
5-1AB-14	1	1	3.23	4.5
5-1C-2	1	1	3.24	1.1
5-1C-4	1	1	3.25	1.5
5-1C-6	1	1	3.26	1.5
5-1C-8	1	2	3.27	0.5 and 1.5
5-1C-10	1	1	3.28	1.5
5-1C-11	1	1	3.29	3.0
5-1C-12	1	1	3.30	1.5
5-1C-13	2	2	3.31, 32	1.0 and 4.0
5-1C-14	1	1	3.33	1.3
5-10B-2	1	1	3.35	3.5
5-10B-4	1	1	3.36	2.0
5-10B-5	2	2	3.37, 38	1.1 and 2.2
5-10B-7	1	1	3.39	1.5
5-10B-8	1	1	3.40	1.5
5-10B-10	1	1	3.41	1.0
5-12BA-1	1	2	3.50	1.5 and 1.5
5-12BA-2	1	1	3.51	1.0
5-12BA-3	0	1	3.52, 53	3.0
5-12BA-4	1	1	3.54	2.0
5-12BA-6	1	1	3.55	3.5
5-12BA-8	1	1	3.56	2.2
5-12BA-10	1	0	3.57	
5-12BA-11	1	1	3.58	1.75
5-12BA-13	1	1	3.59	2.5

Table 3.2 RT Indications from the Testing of PVRUF Material Containing a Large Flaw Indication Reported in Volume 1			
Plate	**RT Indication Shape**	**Location**	**RT Through-Wall Size (mm)**
P5DBB	Rounded	Fusion line	< 1.0
P5DBC	Rounded	Weld	< 1.0
P5DBD	Linear	Fusion line	1.8
P5DBE	Rounded	Fusion line	< 1.0
	Rounded	Fusion line	< 1.0
	Rounded	Fusion line	< 1.0
	Rounded	Fusion line	< 1.0
	Rounded	Fusion line	< 1.0
	Rounded	Base metal	< 1.0
	Rounded	Base metal	< 1.0
	Linear	Fusion line	1.8
	Linear	Fusion line	1.3
	Linear	Fusion line	2.8
P5DBF	Rounded	Fusion line	< 1.0
	Linear	Fusion line	1.3
	Linear	Fusion line	< 1.0

circumferential location forming a cluster of vertically oriented small flaws.

No cases of horizontal inter-run lack of fusion were found. Nor did researchers find any heat-affected-zone cracking. Characteristics of *inter-run slag* and *inter-run slag with a tail* were found in the same flaw.

Volume 1 flaw indications, when located in machine-made weld metal, were confirmed to be mostly small flaws. The larger Volume 1 indications, sized using the isolated tip rule, may be characterized best as porosity and rounded inclusions rather than planar lack of fusion at the fusion surface.

3.2 Flaws in Back-Fill Weld Metal

The girth welds in the PVRUF vessel were made using a tandem submerged metal arc welding machine located outside the vessel. The first weld pass, however, was a single arc pass, and the welding procedure specified that an air-arc back gouge be made from inside the vessel to remove weld metal to sound metal. Back-fill weld metal was applied using shielded metal arc welding.

Figure 3.58 shows a micrograph of the back-fill weld metal. The top of Figure 3.58 shows a portion (most) of the cladding. The scalloped clad to structural metal (weld and base metal) interface can be seen in the figure. The back-fill weld passes are shown to be made from inside the vessel. The transition to machine-made weld metal is shown to take place over a range of 7 mm of depth.

Seven near-surface Volume 1 indications were estimated to be greater than 5 mm in through-wall extent. Five were in the weld and two were in the base metal. These were selected for validation. The two base metal flaws were analyzed separately and are discussed in Section 3.4.

All of the back-gouge weld metal in the PVRUF material received by PNNL was inspected using weld-normal ultrasonic testing. Weld-normal testing results showed that the five Volume 1 weld flaws could be located and removed into cube form. Nine additional back-gouge weld flaws were selected from the weld-normal inspections for removal into cube form. Figure 3.59 shows a photograph of the 14 cubes arranged with images from the ultrasonic validation results on a laboratory table.

Table 3.3 gives the results of the validation of flaw indications in the back-fill weld metal of PVRUF. UT focused probe results show measurable size, somewhat smaller, for the Volume 1 indications. The nine additional weld-normal flaws were less than 3 mm in size. RT results generally confirmed UT sizes. Figure 3.60 shows the depth sizing performance of the SAFT-UT inspections reported in Volume 1 compared to the confirmed sizes obtained in the validation work. It should be noted that the sizing rules used in Volume 1 were chosen to size as accurately as possible, but to make sure that any errors would result in no undersizing. The data in Figure 3.60 shows that the selected sizing rules were successful in meeting the planned objectives. The root mean square sizing error is calculated to be 2.2 mm.

3.2.1 Analysis of PVRUF Cube 5-10EB1-IIbIIc

A 25-mm cube of PVRUF material (5-10EB1-IIbIIc) contained a complex flawed region in the near-surface zone of the vessel. The flawed region extends from the top of the first weld pass of the back-fill to the top of the first tandem submerged arc (SMA) weld pass.

Figure 3.61 shows a micrograph of Cube 5-10EB1-IIbIIc. The back gouge is somewhat shallower in this cube than that shown in Figure 3.58, and the first machine-made weld pass was not completely removed. Figure 3.62 shows a digitized image of a radiograph of Cube 5-10EB1-IIbIIc. The vessel through-wall direction is into the image. The vessel elevation is oriented horizontally in the image.

Figure 3.63 shows a micrograph of the cube exposing a complex flaw associated with the first tandem arc weld passes. This figure shows a lack of fusion with slag on the weld side wall and a horizontal inter-run lack of fusion/contamination above the first tandem weld passes. Figure 3.64 shows a micrograph of a magnified portion of the lack of side-wall fusion with slag.

Figure 3.65 shows a micrograph of the cube exposing a complex flaw associated with the first manually applied weld pass of the back-fill made from inside the vessel. The figure shows that the weld pass contains a crack, slag, and contamination. Figure 3.66 shows a micrograph of a magnified view of the failed weld-pass. The figure shows a horizontal inter-run lack of fusion with slag above the first weld pass of the back-fill. The second flaw in the figure is the crack with a horizontal lack of fusion with the underlying base metal.

Figure 3.67 shows a micrograph of the weld-pass exposing a horizontal lack of fusion and contamination in the bottom portion of the weld-pass. The etchant stained the entire weld pass in this figure. Figure 3.68 shows a micrograph of the

Table 3.3 Validation Sizing Results for 14 Flaw Indications in Back-Gouge Weld Metal				
Cube	Volume 1 Size (mm)	UT Validation Size (mm)	RT Size (mm)	Metallography Size (mm)
5-7DB1-IIbIIc	8	4	4	1
5-1AB14-IbIc	6	5	1	
5-10EB-IIbIIc	6	(not inspected)	3	4
(Same as Above)	7	6	5	5
5-10EA1-IIIbIIIc	3	2.5	(not inspected)	(not inspected)
5-4B1-IIbIIc	1.5	2	1.3	(not inspected)
5-10EA1-IVbIVc	1.5	1.5	(not inspected)	(not inspected)
5-10EC1-IIbIIc	(not detected)	3	2.5	(not inspected)
5-4B1-IIdIIe	(not detected)	2.5	2	(not inspected)
5-7H1-IbIc	(not detected)	2.5	(not inspected)	(not inspected)
5-7H1-IIbIIc	(not detected)	2.5	(not inspected)	(not inspected)
5-10EC1-IIdIIe	(not detected)	2.5	2.5	(not inspected)
5-10B5-IbIc	(not detected)	2.5	2.5	(not inspected)
5-1C4-IbIc	(not detected)	1.5	1.3	(not inspected)

crack in the failed weld-pass. The crack is shown to be broken into three segments. Figure 3.69 shows a micrograph of the crack in the failed weld-pass. The crack is shown to be multifaceted.

The flawed region in the cube extends from the top of the first weld pass of the back-fill to the top of the first tandem arc weld pass. This 8-mm flawed region is estimated to contain two separate flaws, 4 and 5 mm in through-wall size. Two flaws are entered into the size distribution table in Chapter 4 as separate 4- and 5-mm flaws.

3.3 Flaws in Repair Weld Metal

Six repairs were made to the beltline weld as described in Chapter 5. The PVRUF material received by PNNL contained two of the documented repairs. One repair, 12 in. long and 6.5 in. deep, was found in the validation testing. The second repair, made from inside the vessel, was not found by PNNL inspections.

Figure 3.70 shows the repair profile as measured in the weld-normal ultrasonic testing. The top view (C-scan) image is gated to include the ultrasonic energy received from only the repaired fusion surface. Because the small flaws in the machine-made weld metal have been removed, the repair is located by the lack of ultrasonic echo. This repair was made to the fusion surface of the structural weld, as evidenced by the repair centerline being on the structural weld fusion surface.

A 17-mm flaw was found in the documented OD repair to the PVRUF beltline weld. The 17-mm repair flaw can be seen in Figure 3.70 at a circumferential (ordinate) location of 10.5 in. (Image Y axis) and a depth (abscissa) location of 3.0 in. (image X axis) in the image. The flaw is near the top of the 6-in.- (150-mm)-deep repair.

Figure 3.71 shows the results of radiographic testing on the two cubes that contained the 17-mm flaw: 5-12AC6 and 5-12AC5. The through-wall extent of the flaw is arranged vertically in the figure with the direction of the clad surface toward the top of this figure. The flaw at the top formed on the fusion surface of the repair weld metal and the non-repair material, and then changed to a horizontal orientation between the repair weld passes at the bottom of the flaw.

The micrographs of the cubes 5-12AC5 and 5-12AC6 show the composition characteristics of the 17-mm flaw. Figure 3.72 shows a micrograph of a portion of the 17-mm repair flaw as polished and etched. The composition is taken to be slag, porosity, and contamination. Figure 3.73 shows a micrograph of a portion of the 17-mm flaw. A crack-like feature is evident in the figure. Figure 3.74 shows a micrograph of a magnified portion of the 17-mm flaw as polished and etched. The figures show slag in a small inter-bead region with crack-like features.

In summary, as shown by the micrograph, the flaw portion on the fusion surface of the weld with the base metal was complex and connected. The complex composition was made up of cracks, lack of fusion, slag, and porosity.

A second flaw was confirmed to be 12 mm in through-wall extent. This flaw was in the same documented repair as the 17-mm flaw described above. The second repair flaw had the same general shape, namely, a lack of fusion with slag between the repair weld metal. The non-repair material changing to a horizontal lack of fusion between the repair weld beads. The second largest repair flaw is located at a depth of 6.0 in. (150 mm) (from the vessel inside surface) and on the same end of the repair as the 17-mm flaw.

This second repair flaw (in Cube 5-12AC2) was inspected with radiography and with a 10-MHz ultrasonic immersion probe. Figure 3.75 shows the top view image of an ultrasonic inspection of Cube 5-12AC2. This view is the projection with the vessel through-wall into the page. The flaw is shown to be on the fusion surface of the repair with the non-repair metal. Figure 3.76 shows the side view image of the second largest flaw in the repair to the beltline weld. Figure 3.77 shows the end view image of the second largest flaw in the repair to the beltline weld. Further work on this flaw is in progress using computed tomography to hopefully provide additional information to better characterize this complex flaw.

A second reported repair, made from inside the vessel, was not found when the metallography was performed at the documented location of the repair. Figure 3.78 shows a micrograph of the upper portion of PVRUF specimen 5-6ECA. A weld repair, made from inside the vessel, was documented to be located in this material. The figure shows no evidence of a repair.

3.4 Flaws in Cladding and at the Clad-to-Base Metal Interface

The results of the validation showed that the approximately 1500 clad flaw indications reported in Volume 1 are lack of fusion with slag at the clad-to-base metal interface. The majority of the 2500 Volume 1 flaw indications were in this category. Of these flaws, most were located at the inside diameter change between the nozzle and intermediate shell courses. Figure 3.79 shows some of these flaws.

Figure 3.80 shows the largest flaw found in the validation of the cladding flaws. This flaw was found at the location of Volume 1 flaw *planar #1 in the near surface base metal.* The flaw is 4-mm through-wall and appears to be contained entirely

within the cladding. A micro-polish and etch was not performed. The image in the figure shows the PVRUF specimen as machine cut.

3.5 Flaws in Base Metal

Some of the Volume 1 base metal flaws were subsequently established not to be actually in base metal. They were, for example, in repair weld metal. A separate study of the density and distribution of flaws in RPV base metal is under way and will be documented in a separate NUREG/CR report using base metal from PVRUF, Shoreham, River Bent Unit 2, and Hope Creek Unit 2.

Figure 3.81 shows the results of a radiographic test of a Volume 1 base-metal flaw indication. The RT flaw indication is characterized as a mid-wall lamination cluster. The through-wall extent of the cluster is 8 mm. This mid-wall lamination cluster is shown in the distribution table for the base metal in Chapter 4.

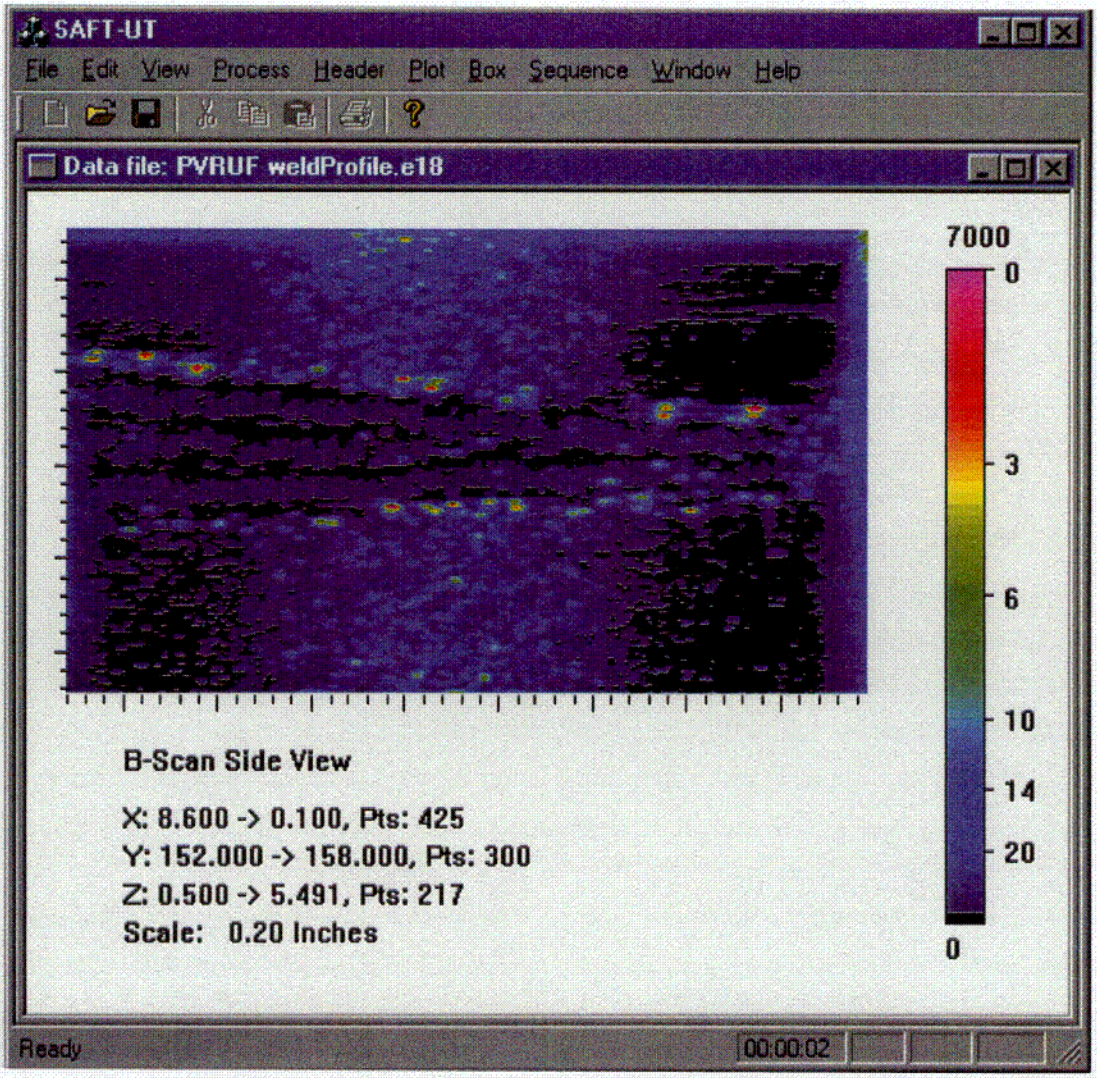

Figure 3.1 Side View of Weld-Normal Ultrasonic Test Showing Weld Profile as Evidenced by Small Flaw Indications

C02

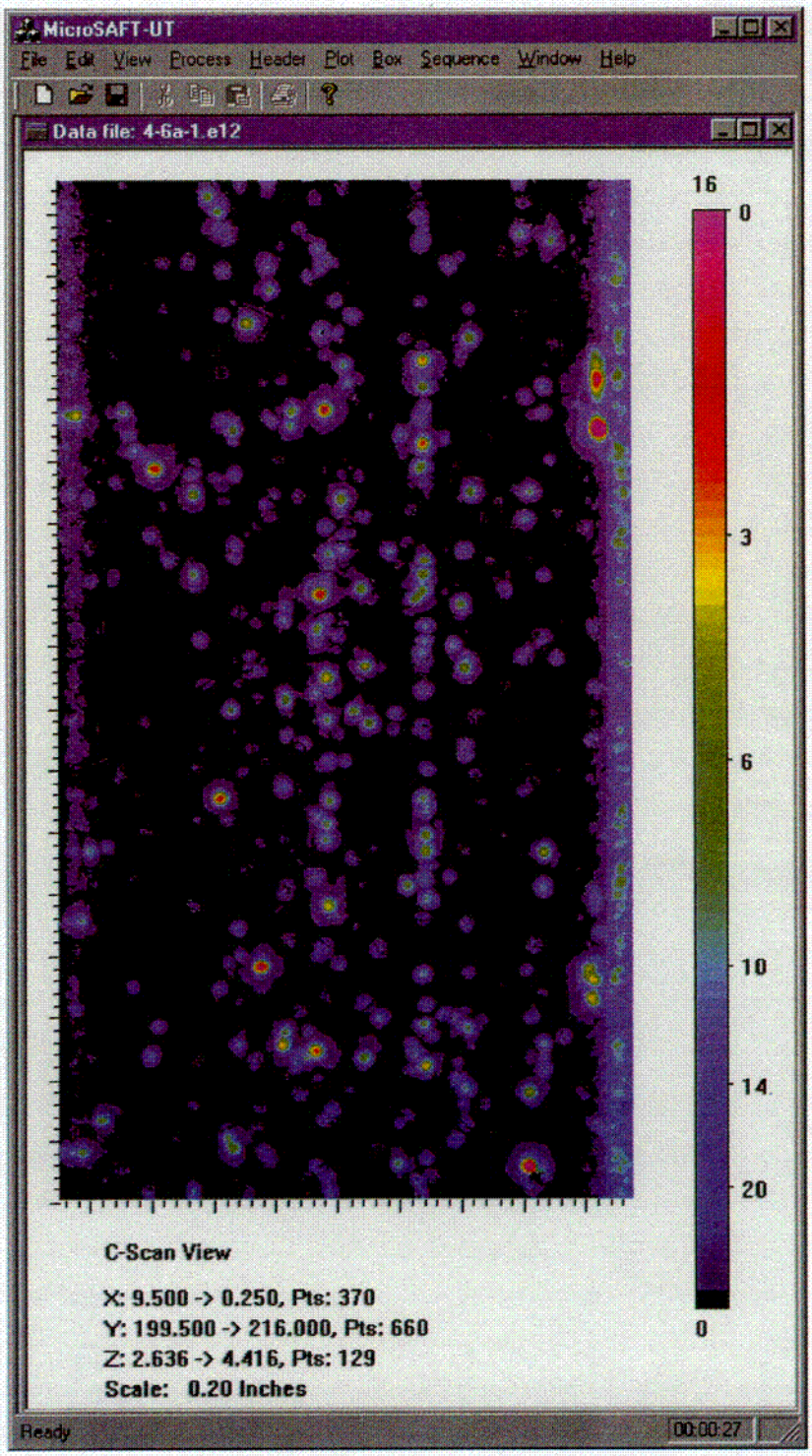

Figure 3.2 C-scan (top view) Image of Small Flaw Indications on the Weld Fusion Surface, from Weld-Normal UT Inspection

C03

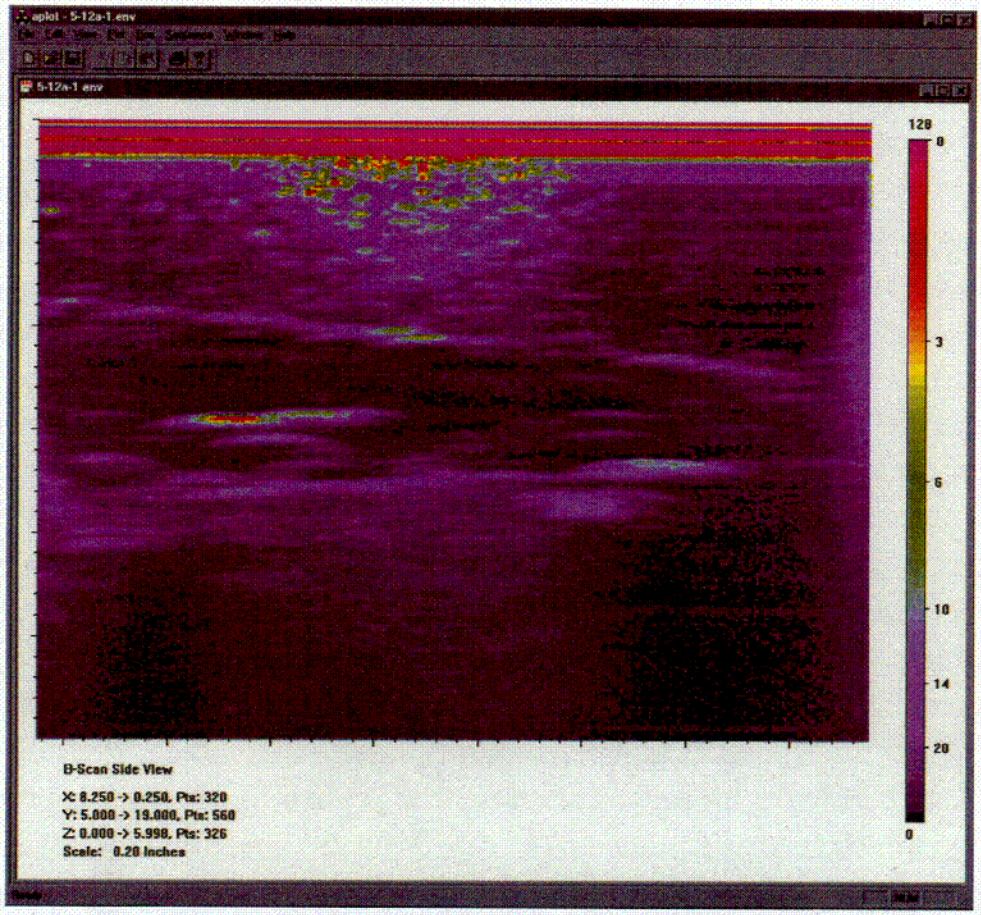

Figure 3.3 UT Image Showing Weld Profile with Weld Flaw Indication

C04

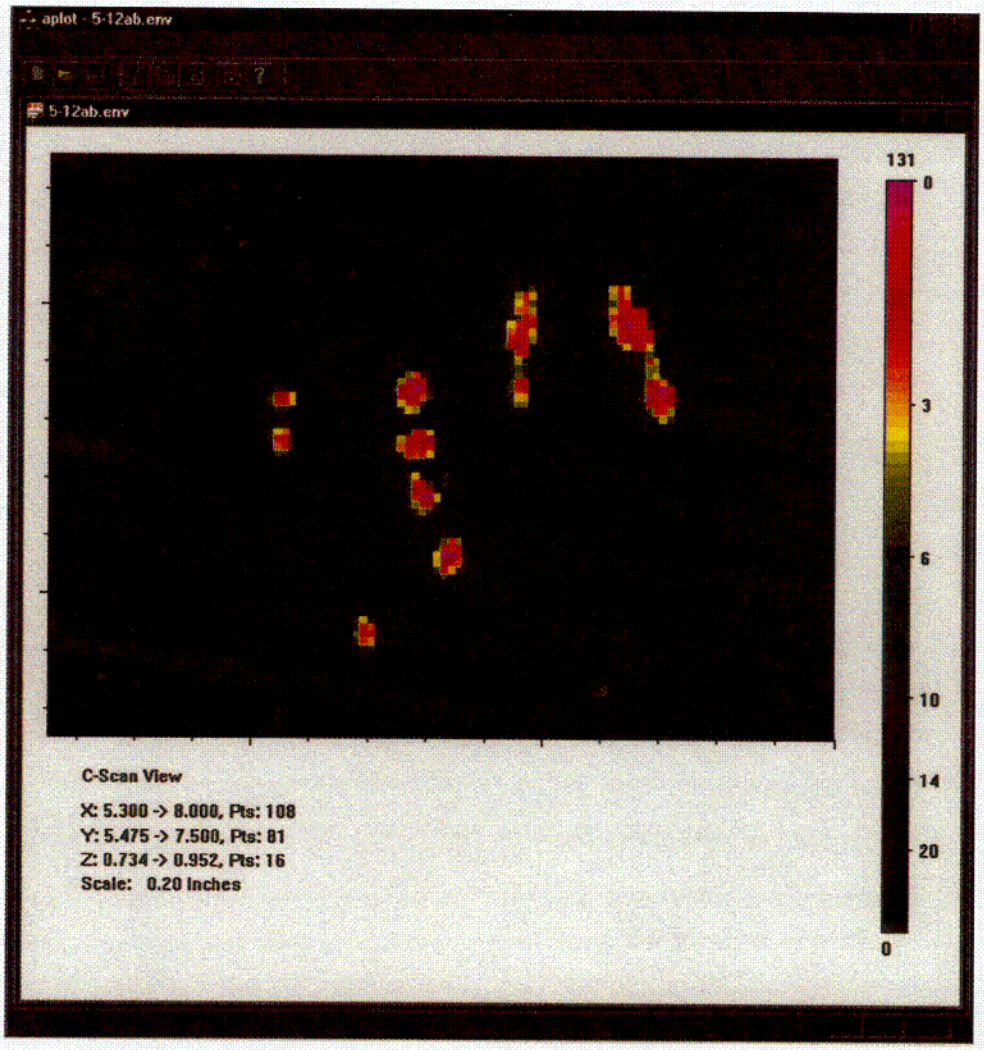

Figure 3.4 SAFT-UT Inspection of a Large Cluster of Weld Flaws in the Mid-Wall Portion of the Vessel Beltline Weld. The through-wall direction, vessel "Z", is on the abscissa and labeled as X: 5.475 -> 8.000 inches in the image. The distance along the beltline weld, vessel "Y", is on the ordinate and labeled as Y: 5.475 -> 7.500 inches.

C05

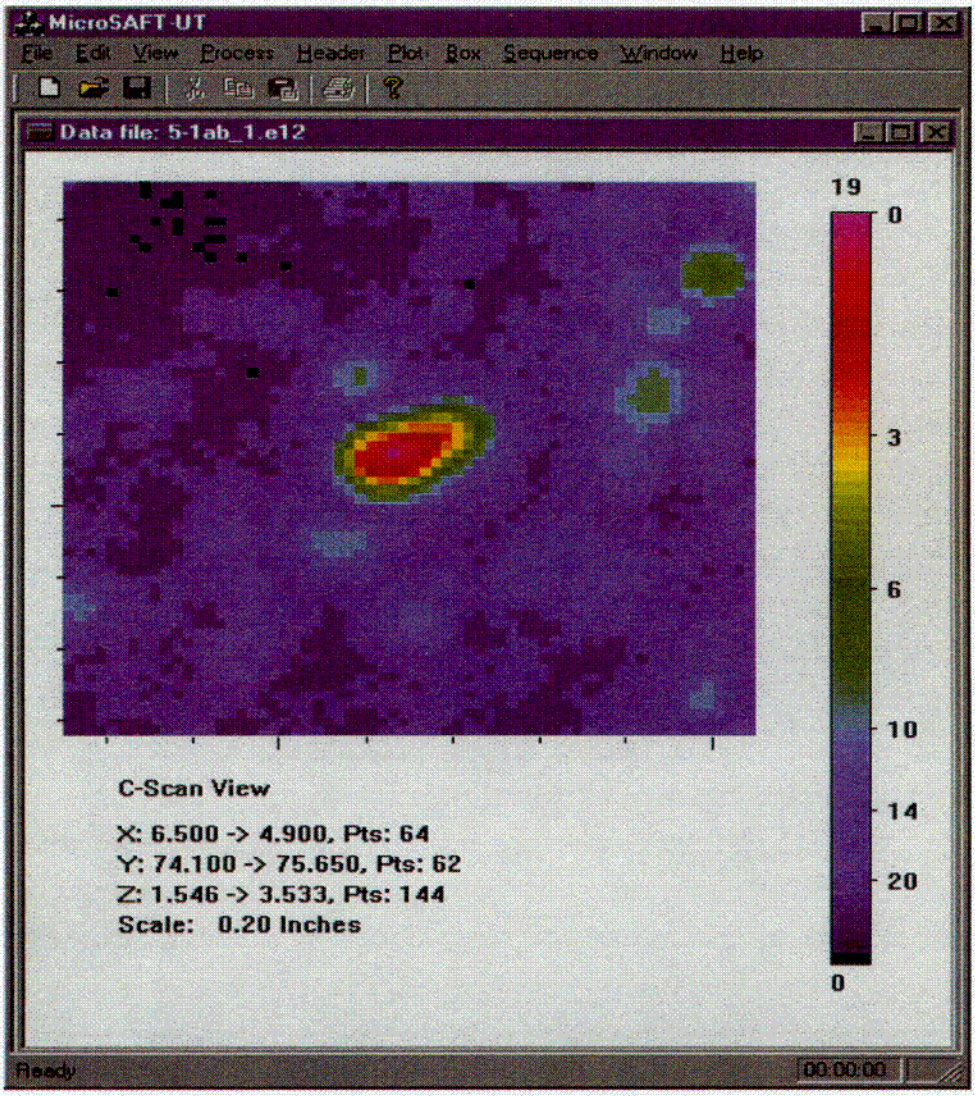

Figure 3.5 Weld-Normal UT Image of Flaw Indication Characterized as Extended Lack of Fusion. Clad is to the right in the figure.

C06

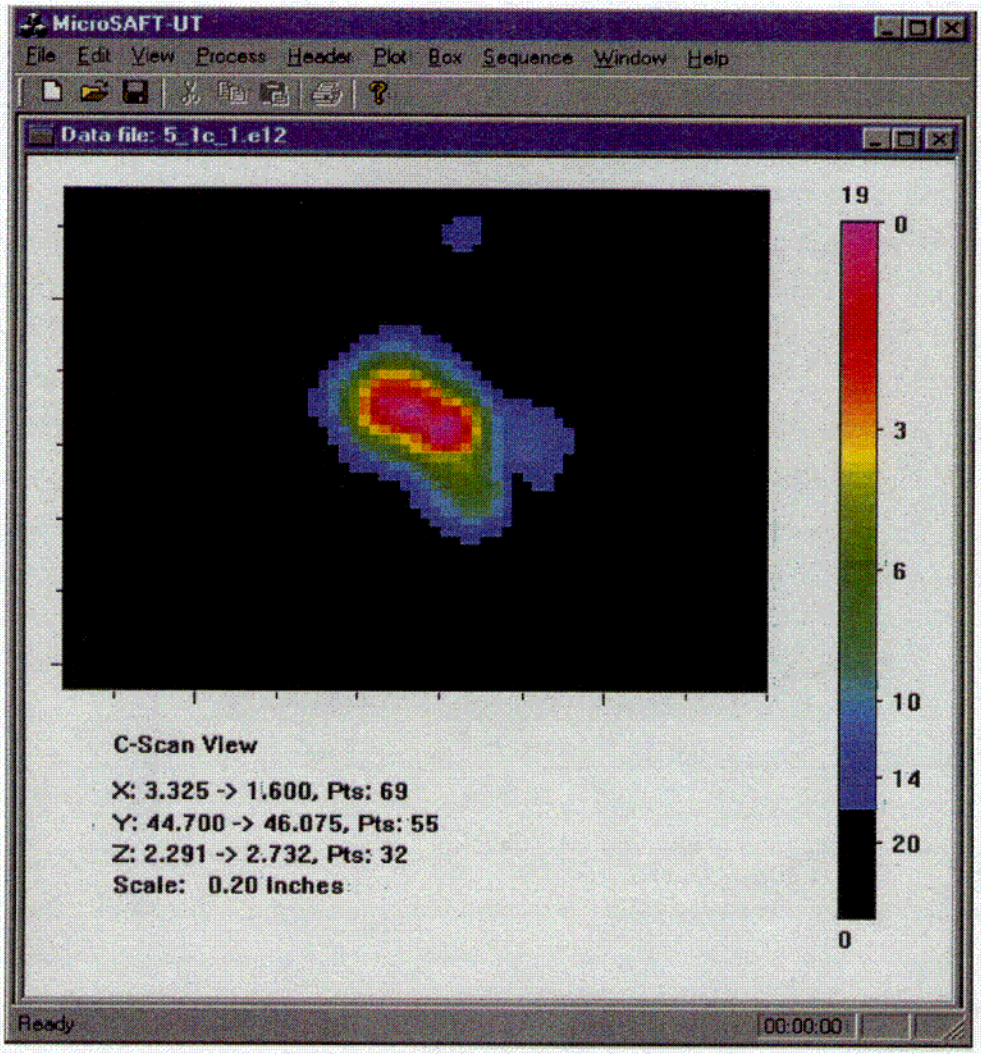

Figure 3.6 Weld-Normal Flaw Indication Characterized as Extended Lack of Fusion. Clad is to the right in the figure.

C07

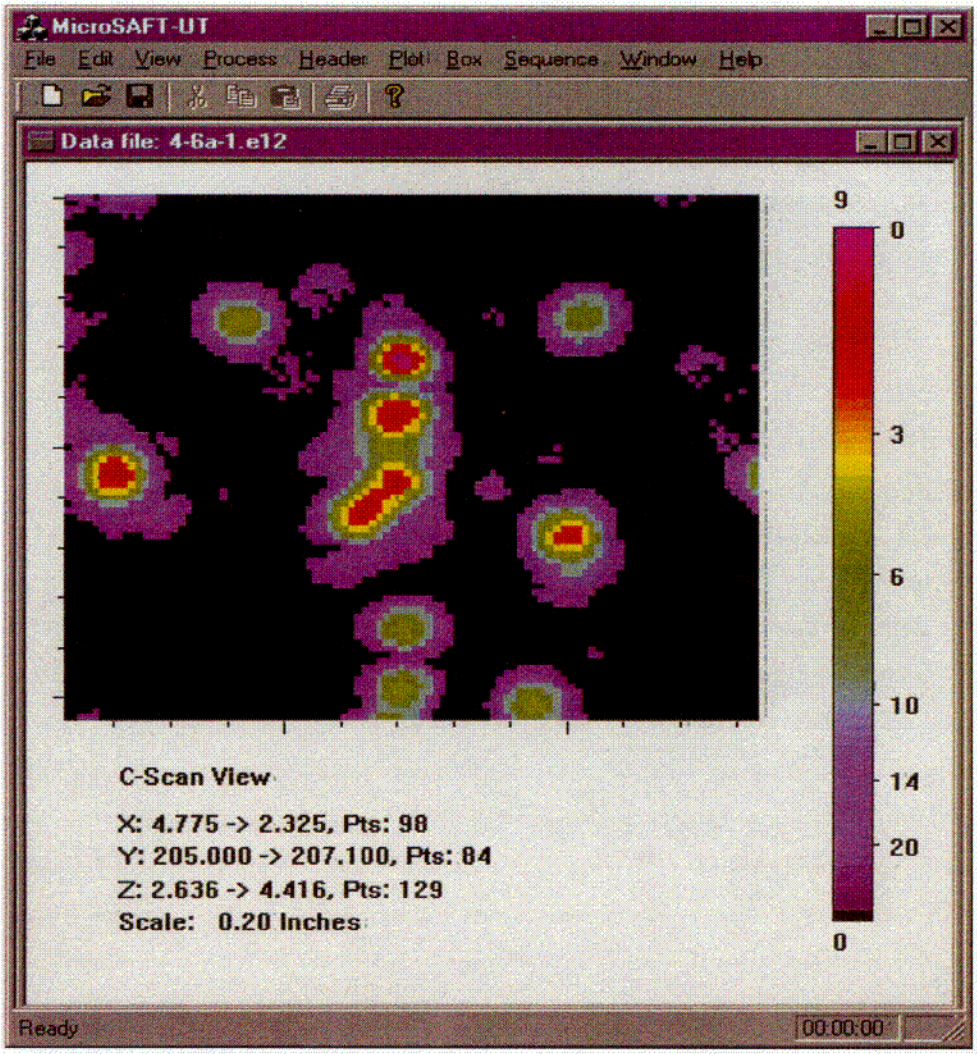

Figure 3.7 Weld-Normal Ultrasonic Testing Flaw Indication Characterized as Long Lack of Fusion. Clad is to the right in the figure.

C08

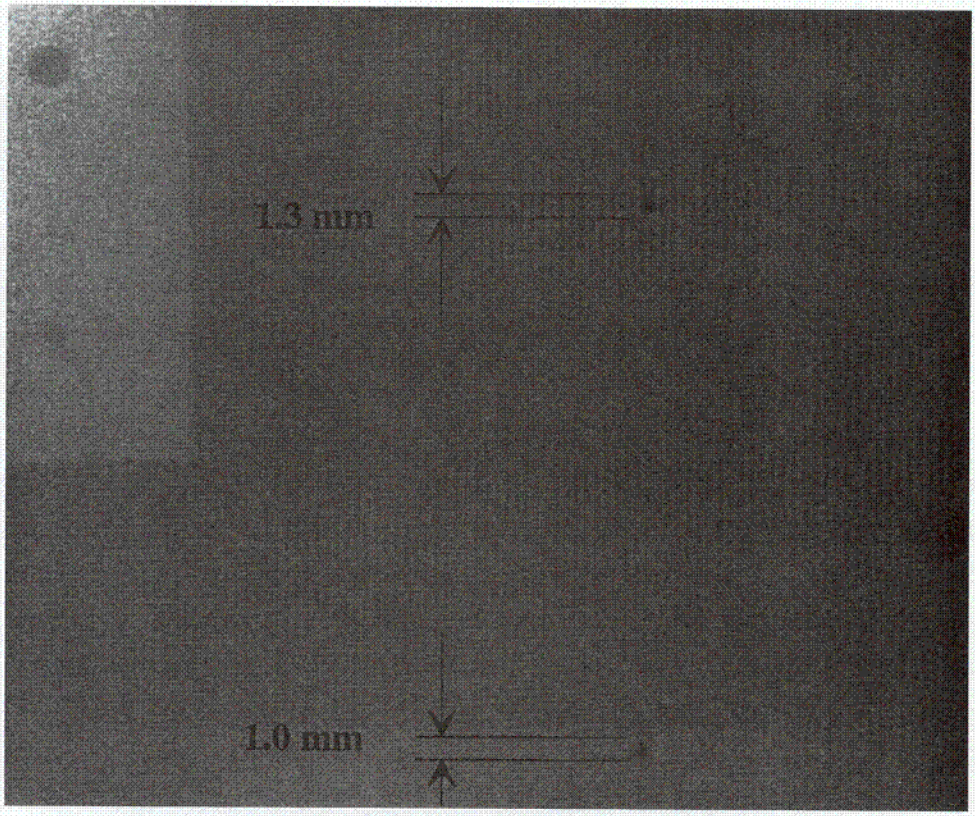

Figure 3.8 Radiograph of 25-mm Plate 5-1AB-2

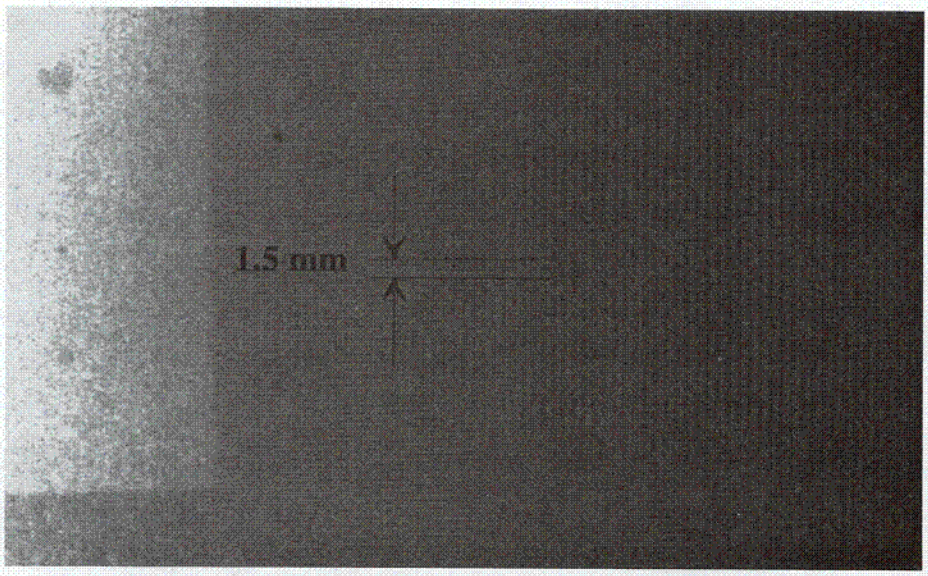

Figure 3.9 Radiograph of 25-mm Plate 5-1AB-3

C09

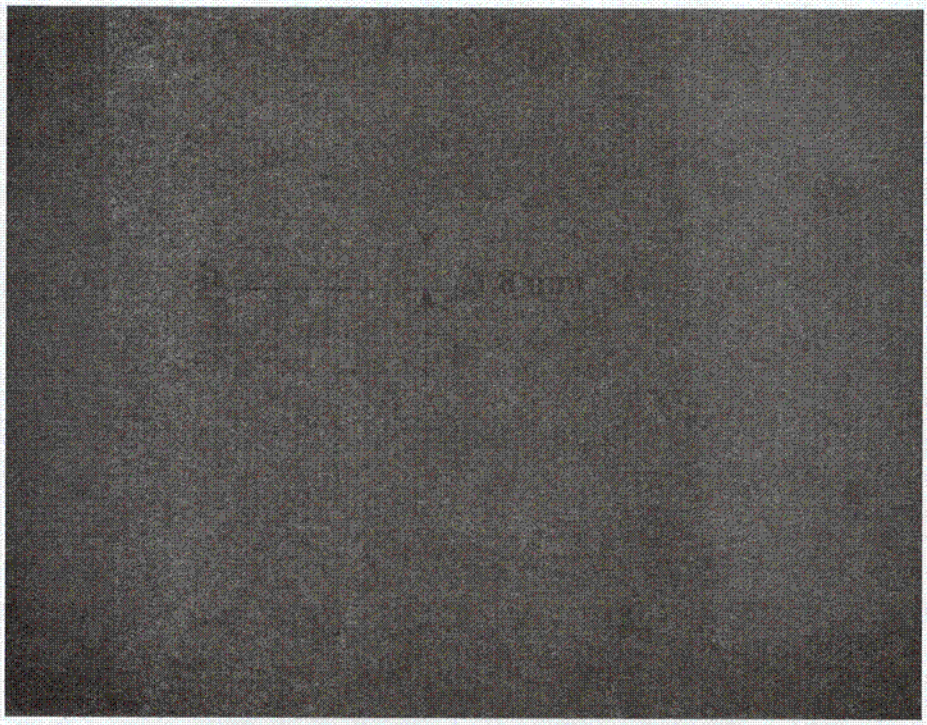

Figure 3.10 Radiograph of 25-mm Plate 5-1AB-5 Location 1

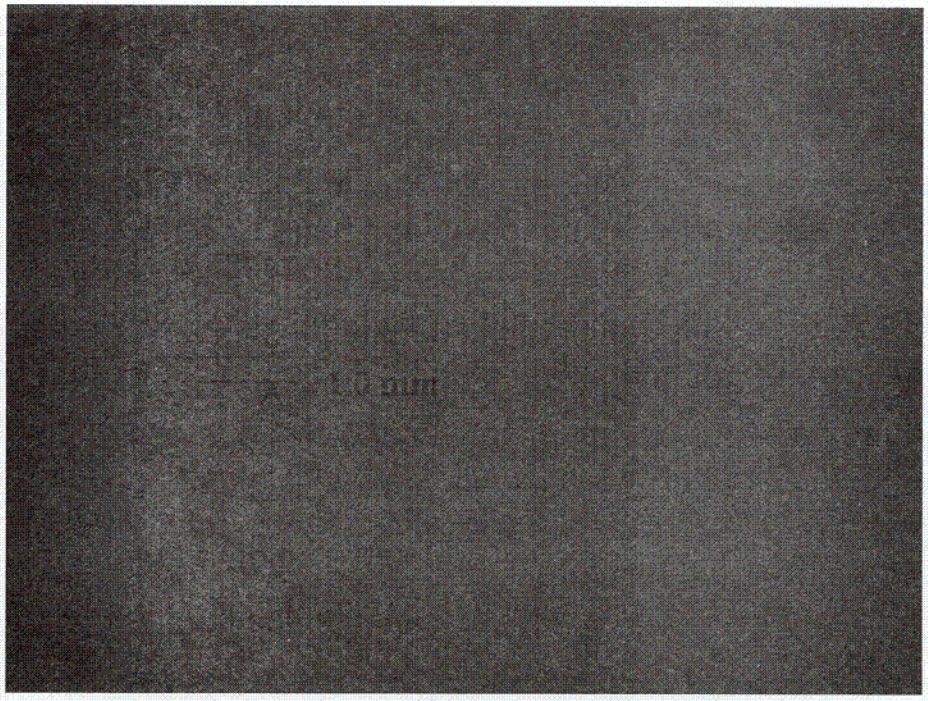

Figure 3.11 Radiograph of 25-mm Plate 5-1AB-5 Location 2

C10

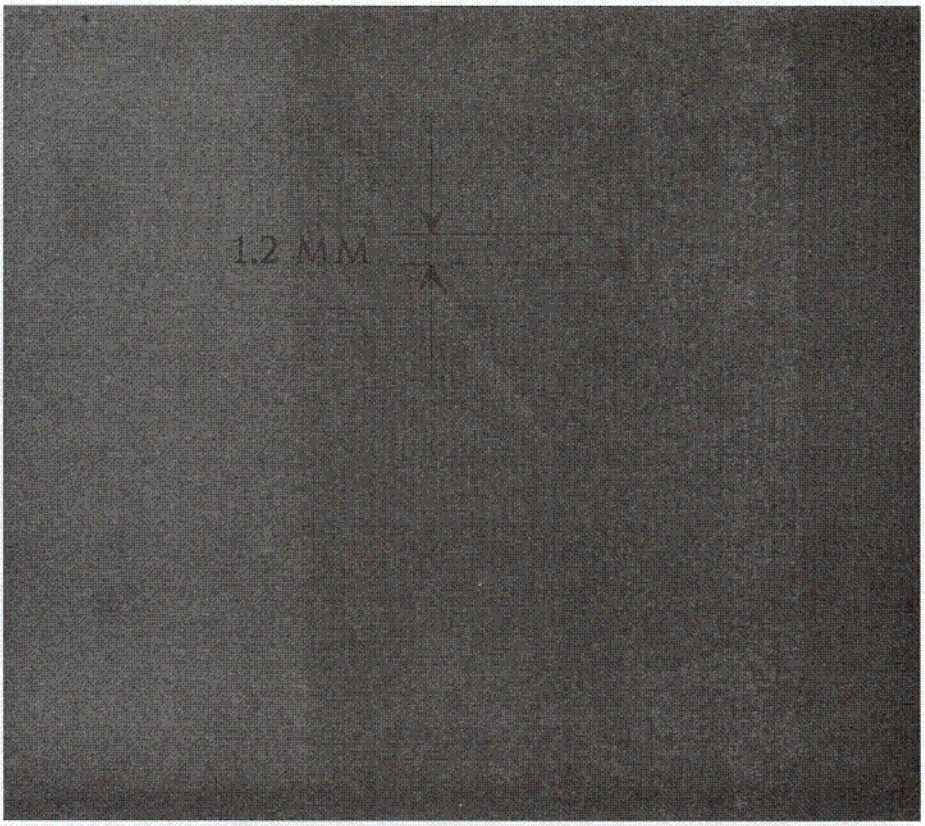

Figure 3.12 Radiograph of 25-mm Plate 5-1AB-5 Location 3

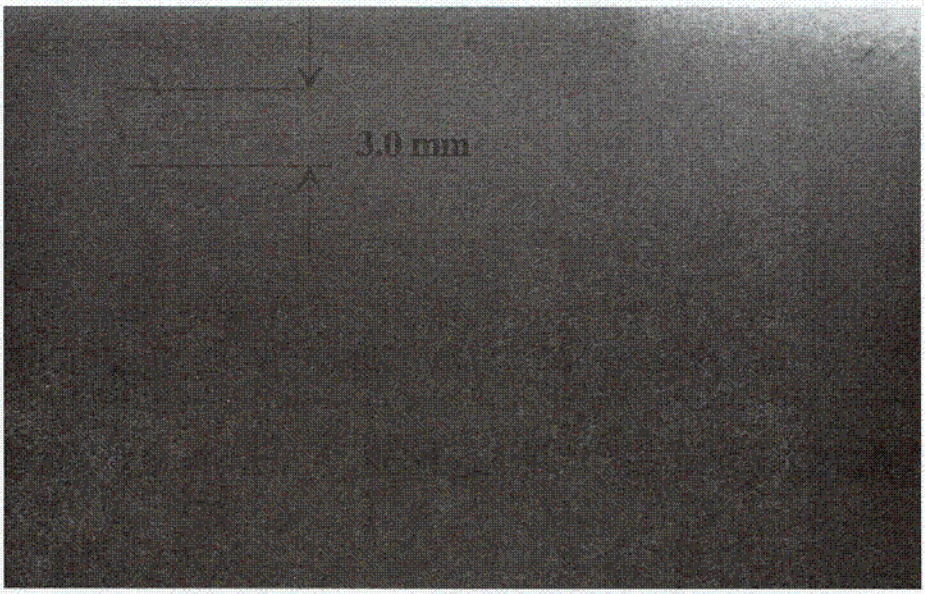

Figure 3.13 Radiograph of 25-mm Plate 5-1AB-6 Location 1

C11

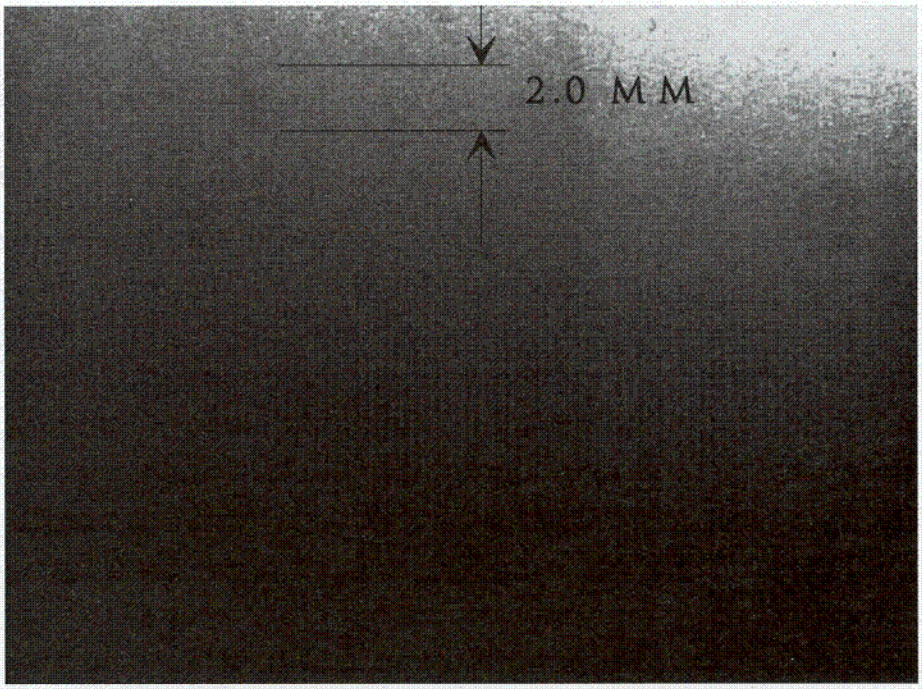

Figure 3.14 Radiograph of 25-mm Plate 5-1AB-6 Location 2

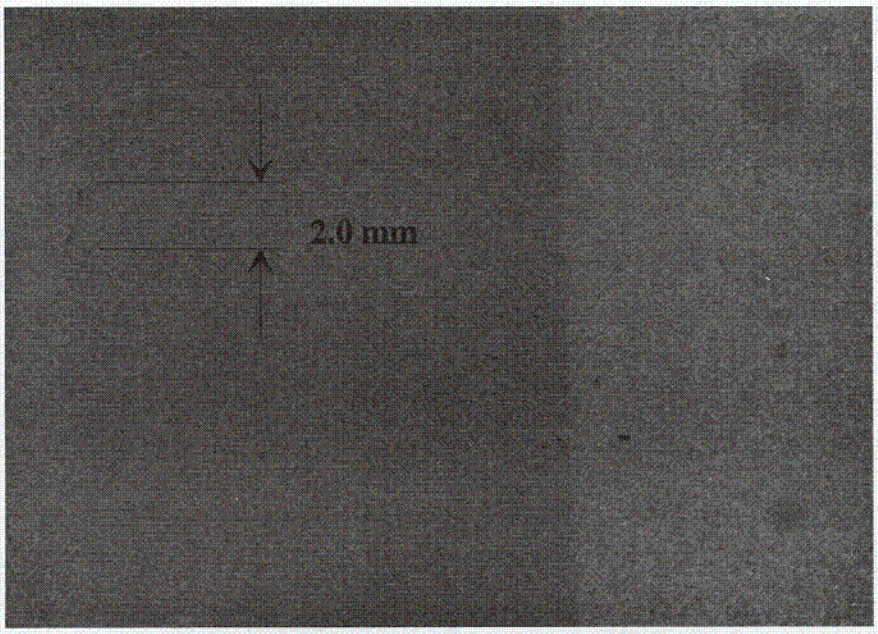

Figure 3.15 Radiograph of 25-mm Plate 5-1AB-7 Location 1

C12

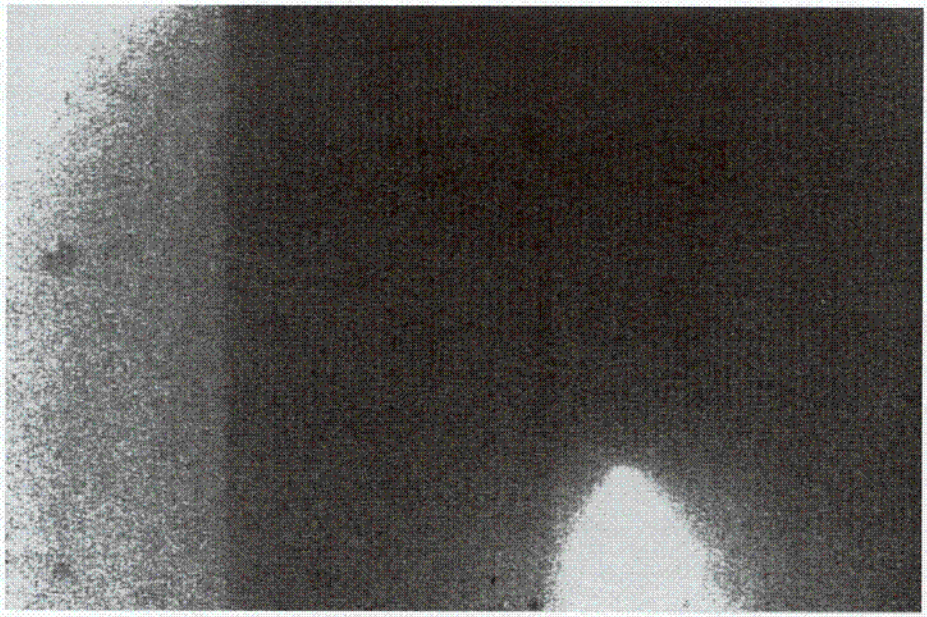

Figure 3.16 Digitized Image of Radiograph of 25-mm Plate 5-1AB-7 Location 2. RT indication did not reproduce in digitized image but is evident in original radiograph.

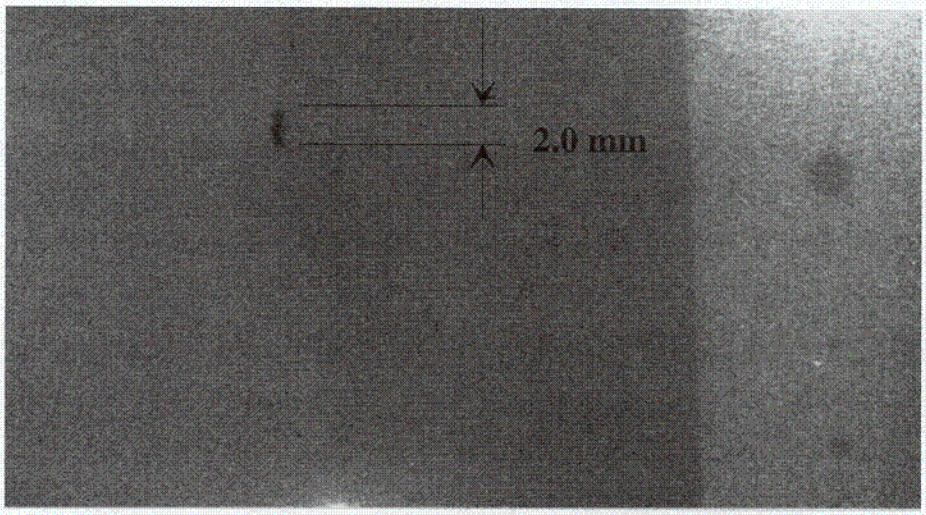

Figure 3.17 Digitized Image of Radiograph of 25-mm Plate 5-1AB-9 Location 1

C13

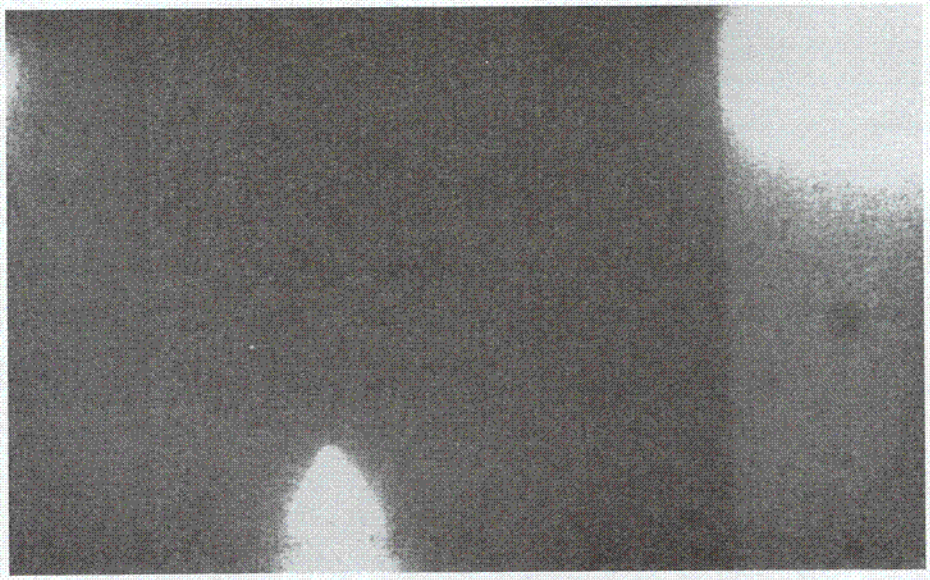

Figure 3.18 Digitized Image Radiograph of 25-mm Plate 5-1ab-9 Location 2. No RT indication was found at this location.

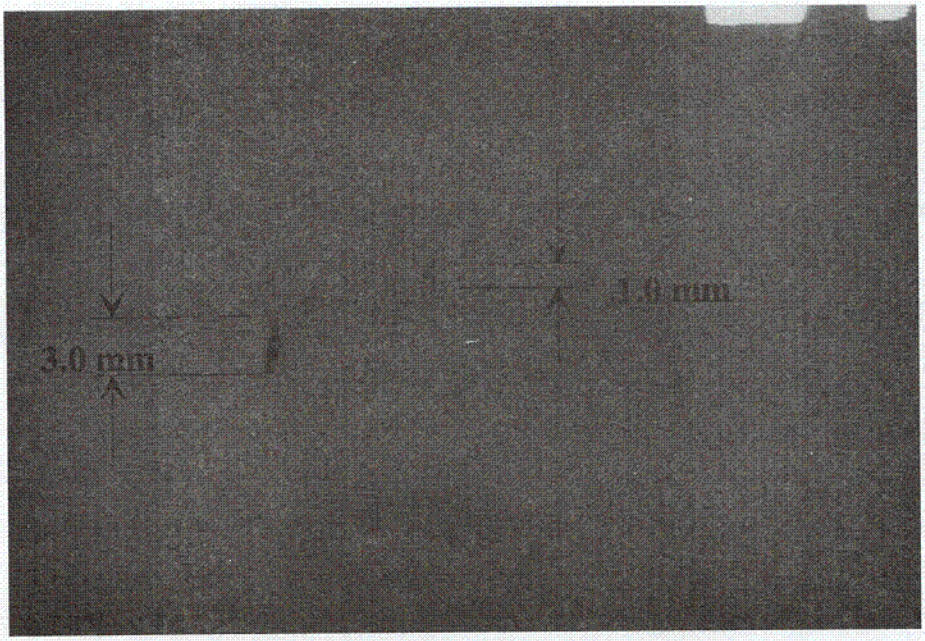

Figure 3.19 Digitized image of Radiograph of 25-mm Plate 5-1AB-11

C14

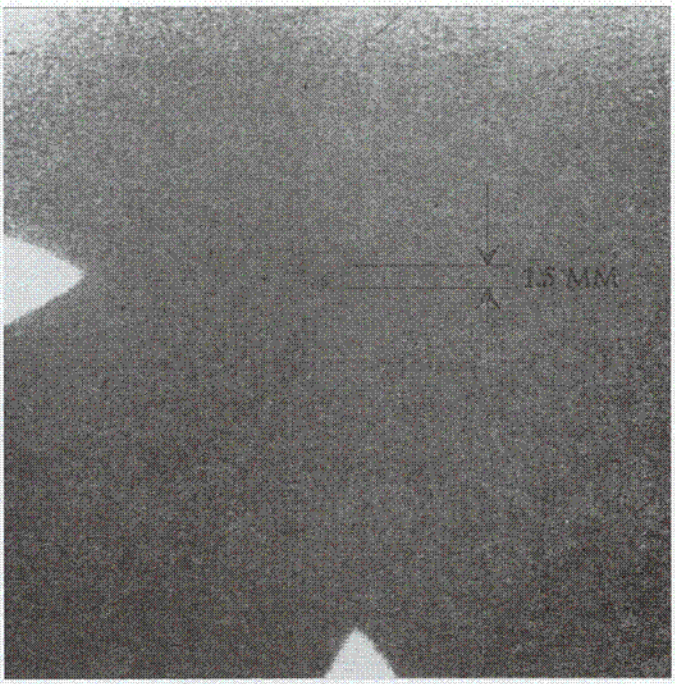

Figure 3.20 Digitized Image of Radiograph of 25-mm Plate 5-1AB-12 Location 1

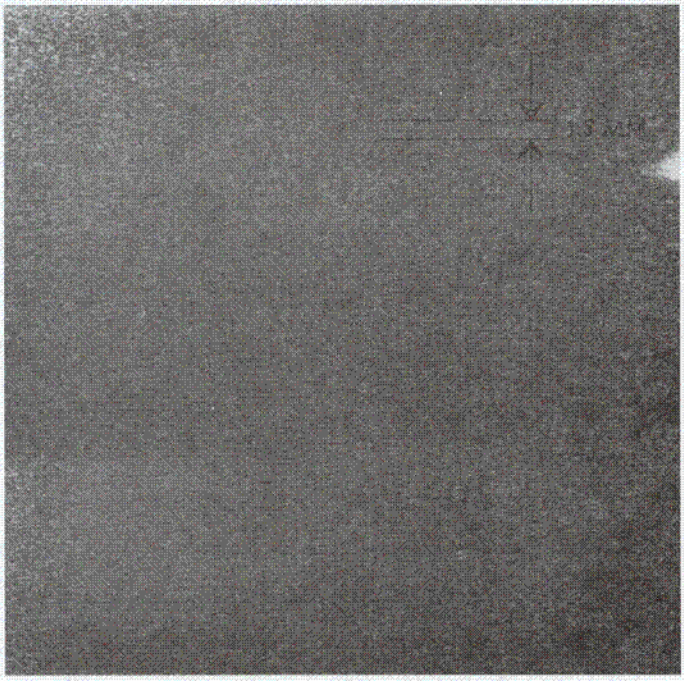

Figure 3.21 Digitized Image of Radiograph of 25-mm Plate 5-1AB-12 Location 2

C15

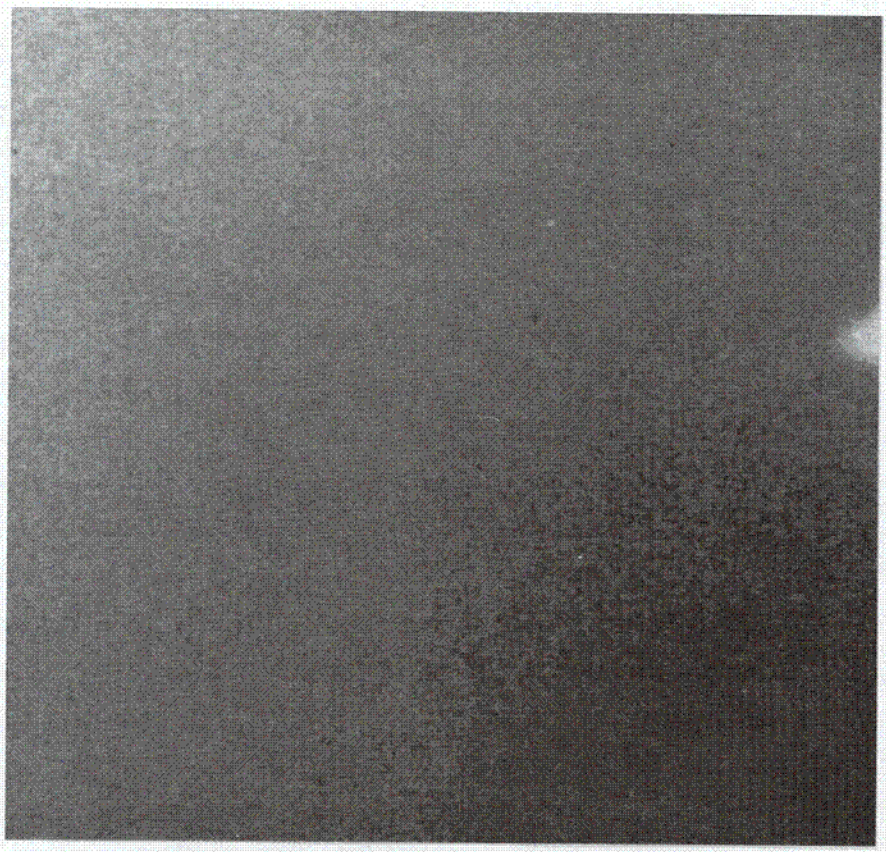

Figure 3.22 Digitized Image of Radiograph of 25-mm Plate 5-1AB-12 Location 3. No RT indication was detected in this radiograph.

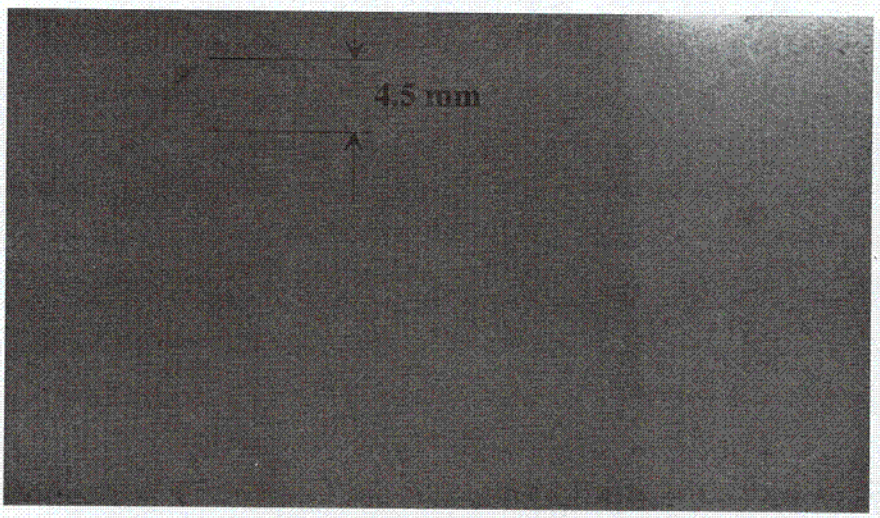

Figure 3.23 Digitized Image of Radiograph of 25-mm Plate 5-1AB-14

C16

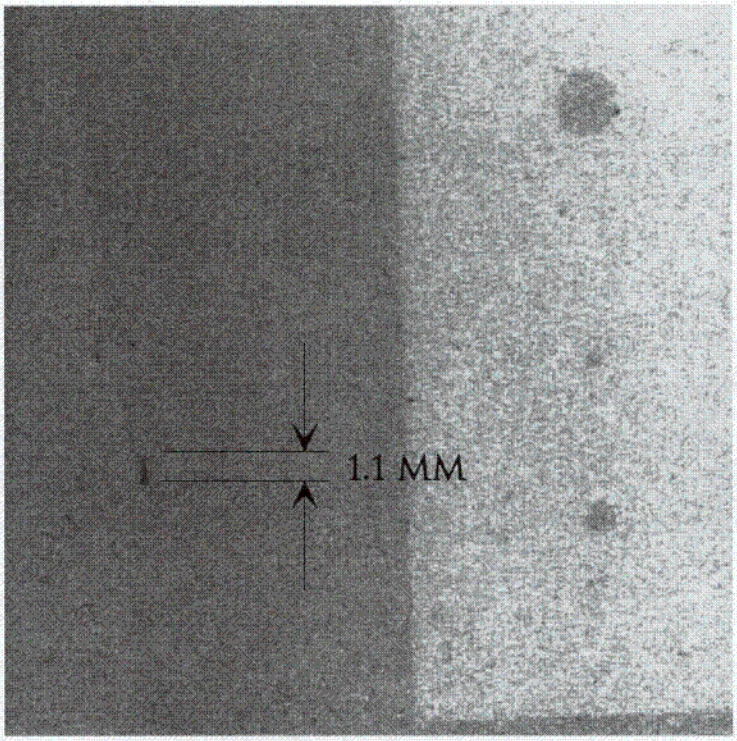

Figure 3.24 Digitized Image of Radiograph of 25-mm Plate 5-1C-2

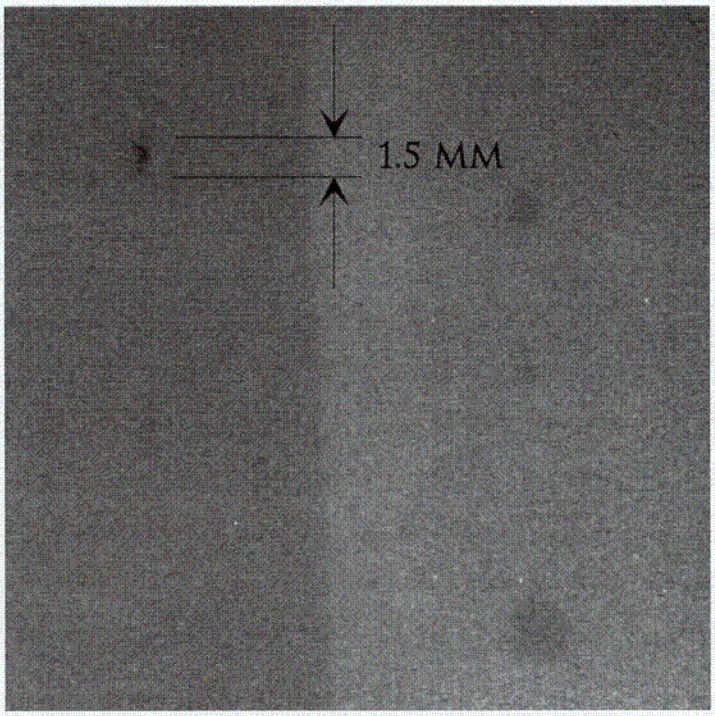

Figure 3.25 Digitized Image of Radiograph of 25-mm Plate 5-1C-4

C17

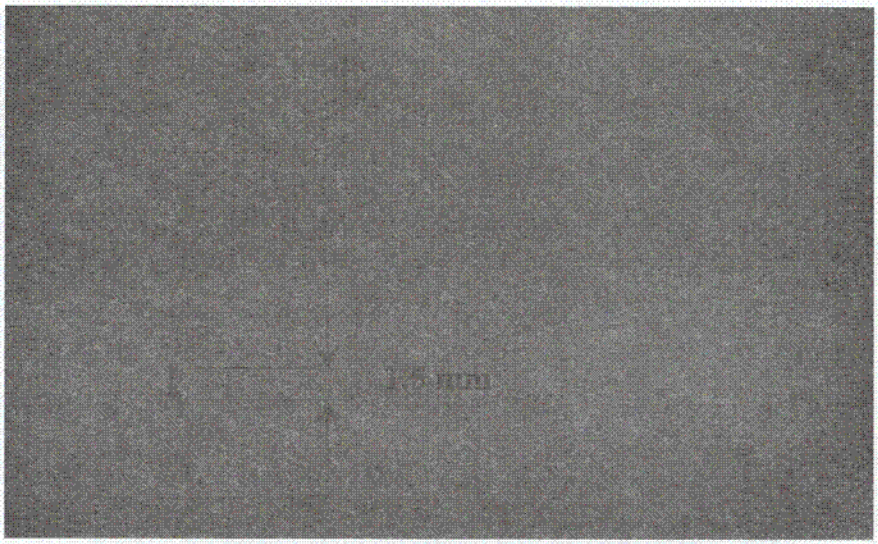

Figure 3.26 Digitized Image of Radiograph of 25-mm Plate 5-1C-6

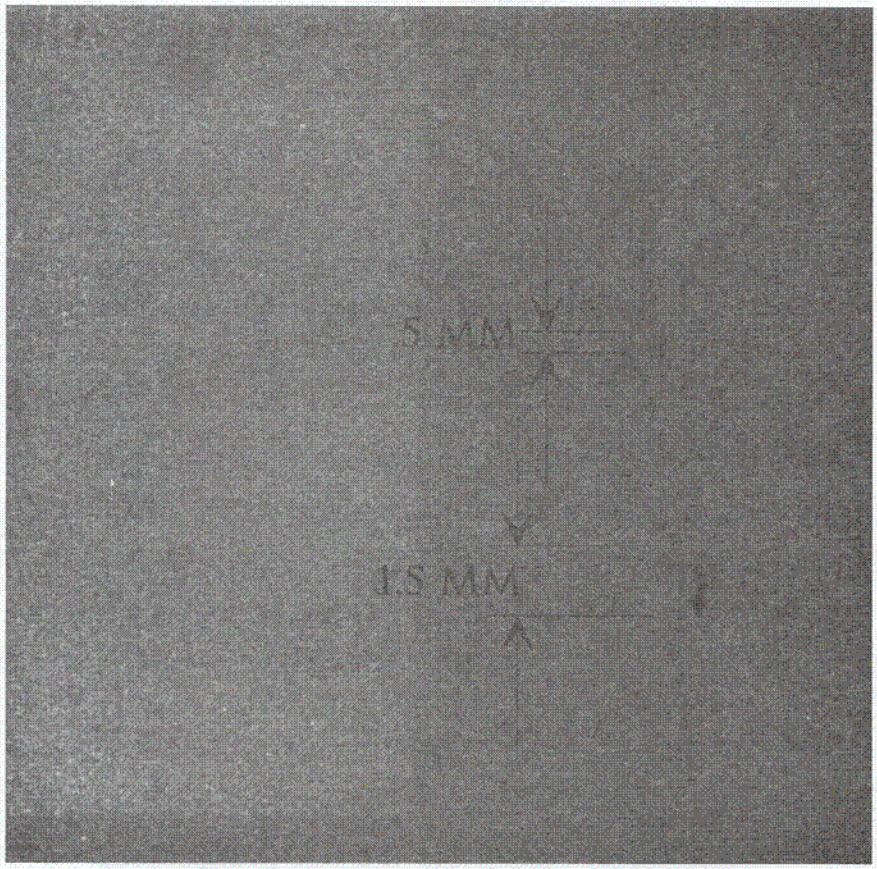

Figure 3.27 Digitized Image of Radiograph of 25-mm Plate 5-1C-8

C18

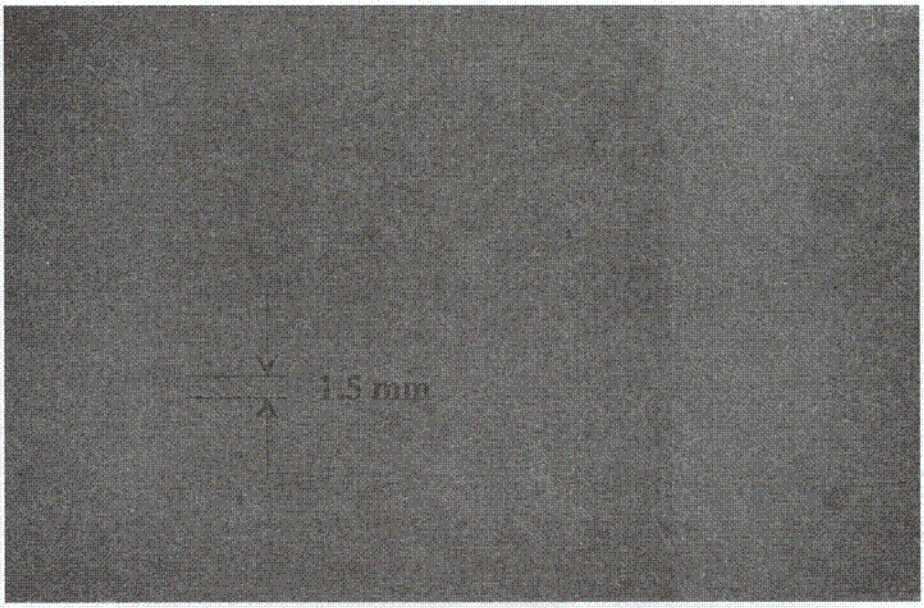

Figure 3.28 Digitized Image of Radiograph of 25-mm Plate 5-1C-10

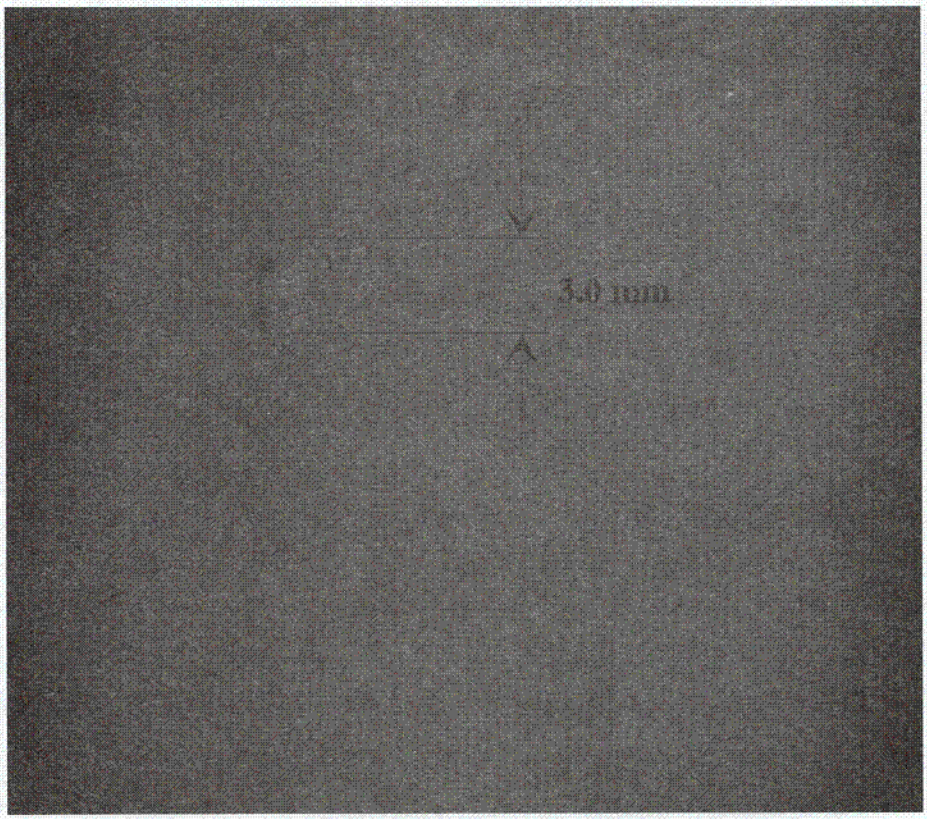

Figure 3.29 Digitized Image of Radiograph of Plate 5-1C-11

C19

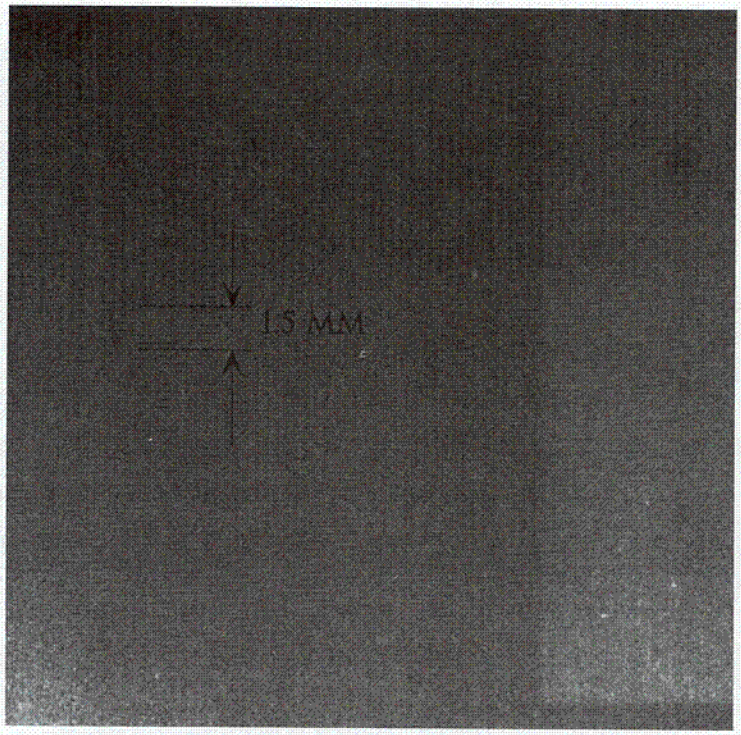

Figure 3.30 Digitized Image of Radiograph of 25-mm Plate 5-1C-12

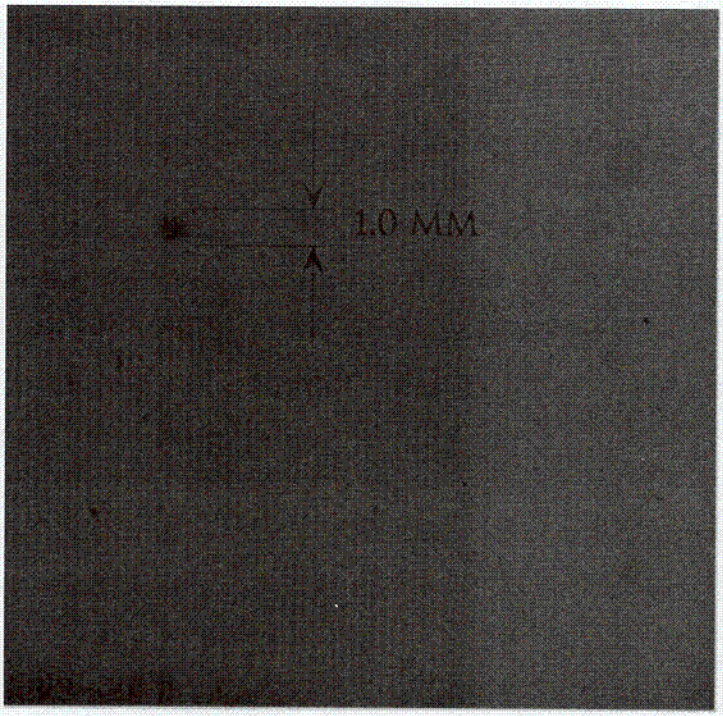

Figure 3.31 Digitized Image of Radiograph of 25-mm Plate 5-1C-13 Location 1

C20

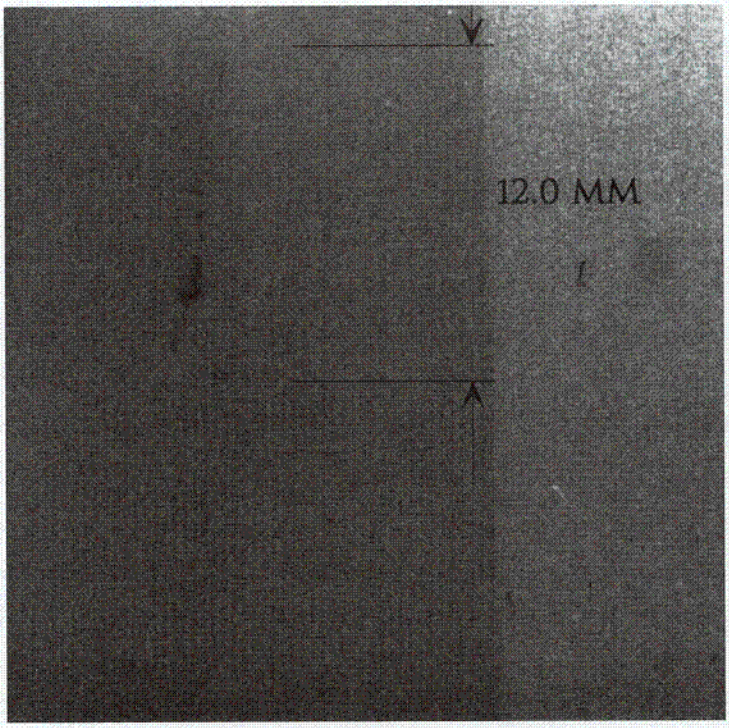

Figure 3.32 Digitized Image of Radiograph of 25-mm Plate 5-1C-13 Location 2

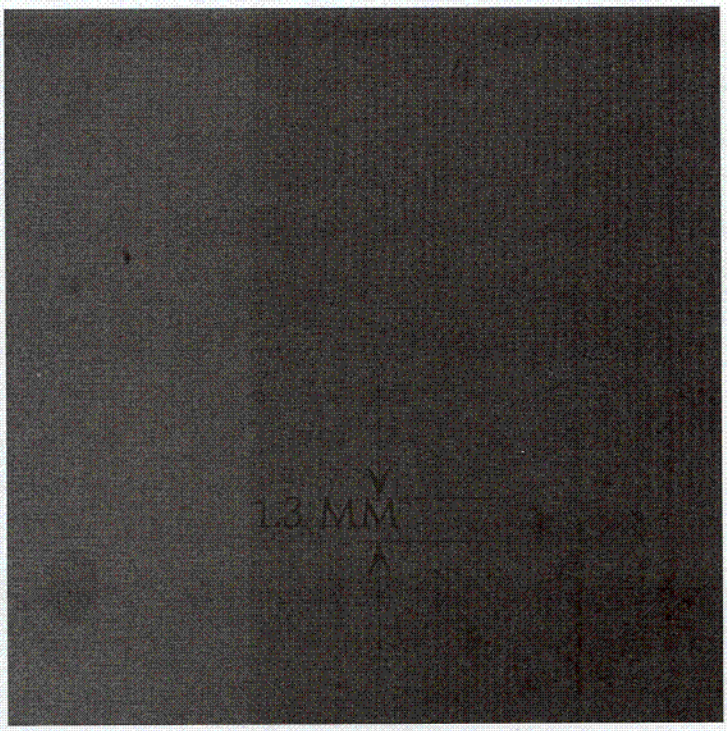

Figure 3.33 Digitized Image of Radiograph of 25-mm Plate 5-1C-14

C21

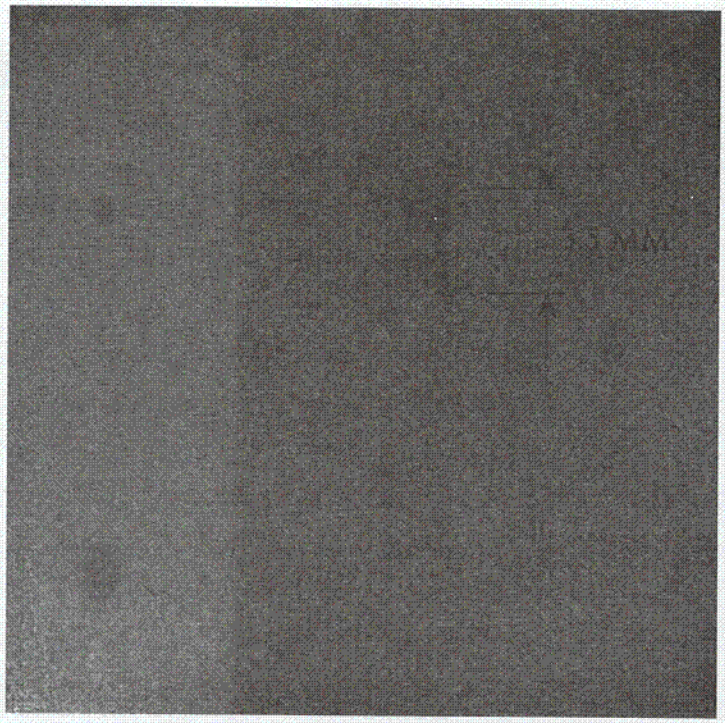

Figure 3.34 Digitized Image of Radiograph of Plate 5-10B-2

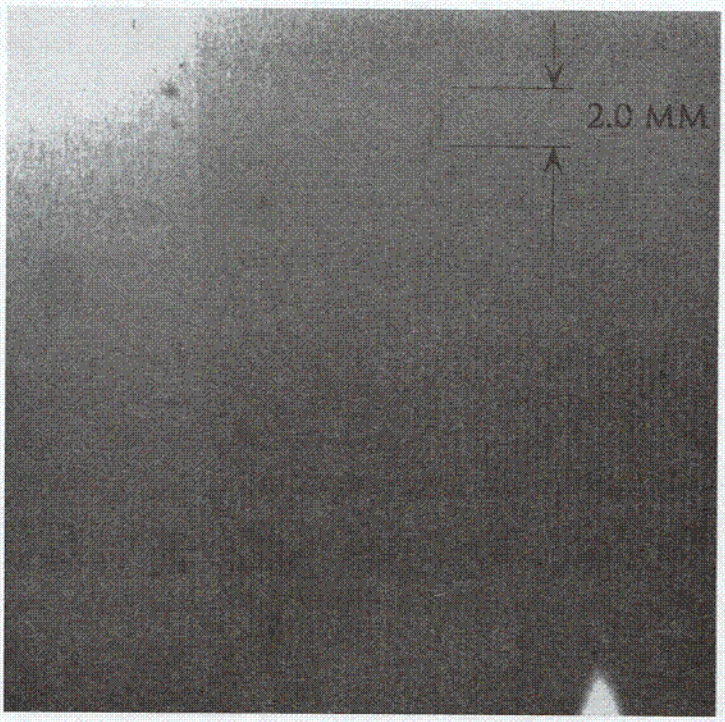

Figure 3.35 Digitized Image of Radiograph of 25-mm Plate 5-10B-4

C22

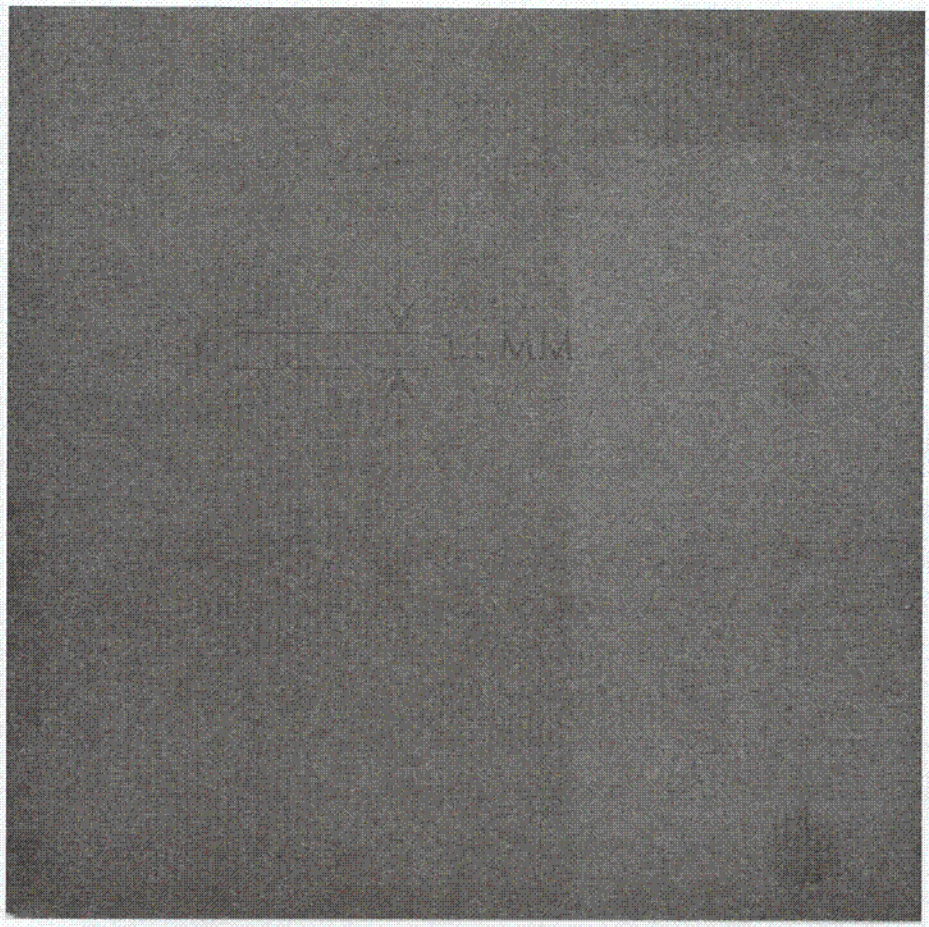

Figure 3.36 Digitized Image of Radiograph of 25-mm Plate 5-10B-5 Location 1

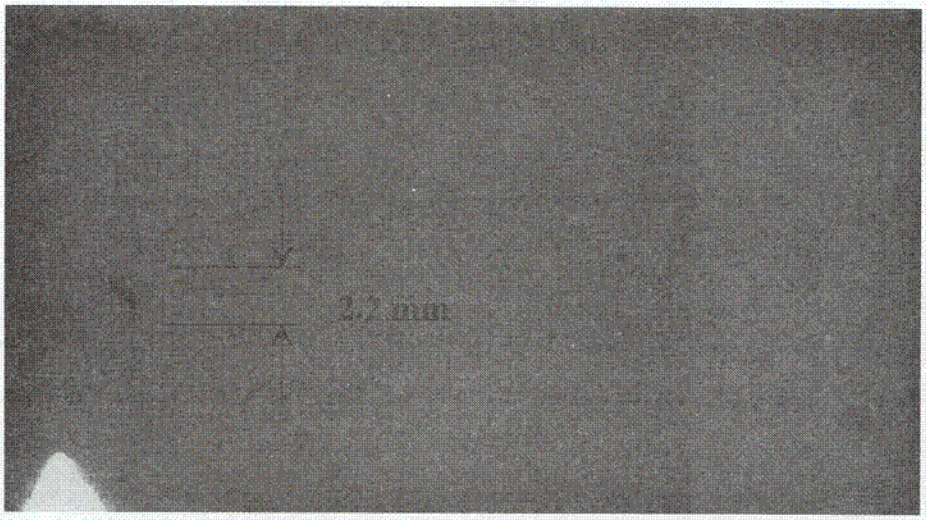

Figure 3.37 Digitized Image of Radiograph of 25-mm Plate 5-10B-5 Location 2

C23

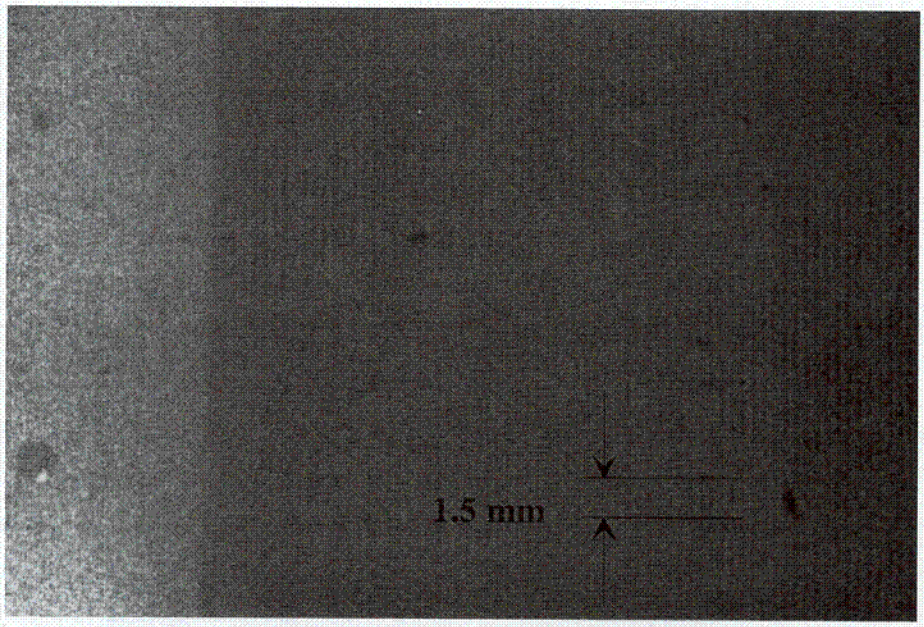

Figure 3.38 Digitized Image of Radiograph of 25-mm Plate 5-10B-7

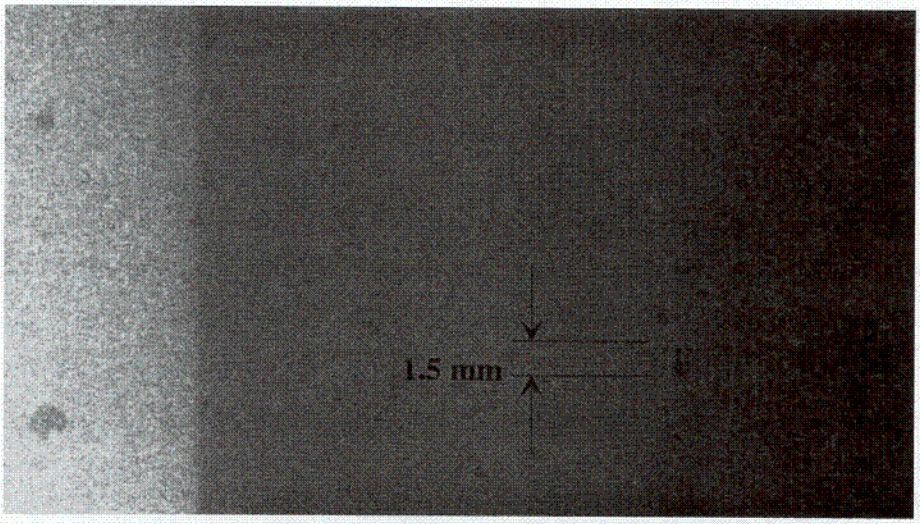

Figure 3.39 Digitized Image of Radiograph of 25-mm Plate 5-10B-8

C24

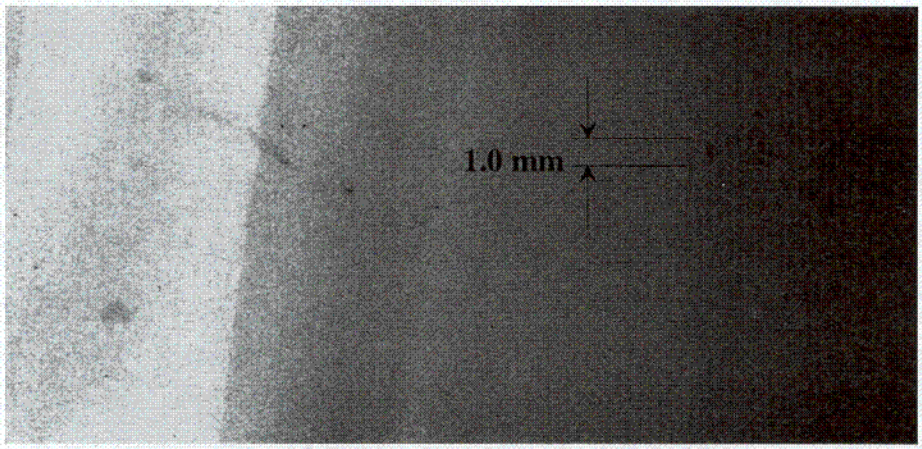

Figure 3.40 Digitized Image of Radiograph of 25-mm Plate 5-10B-10

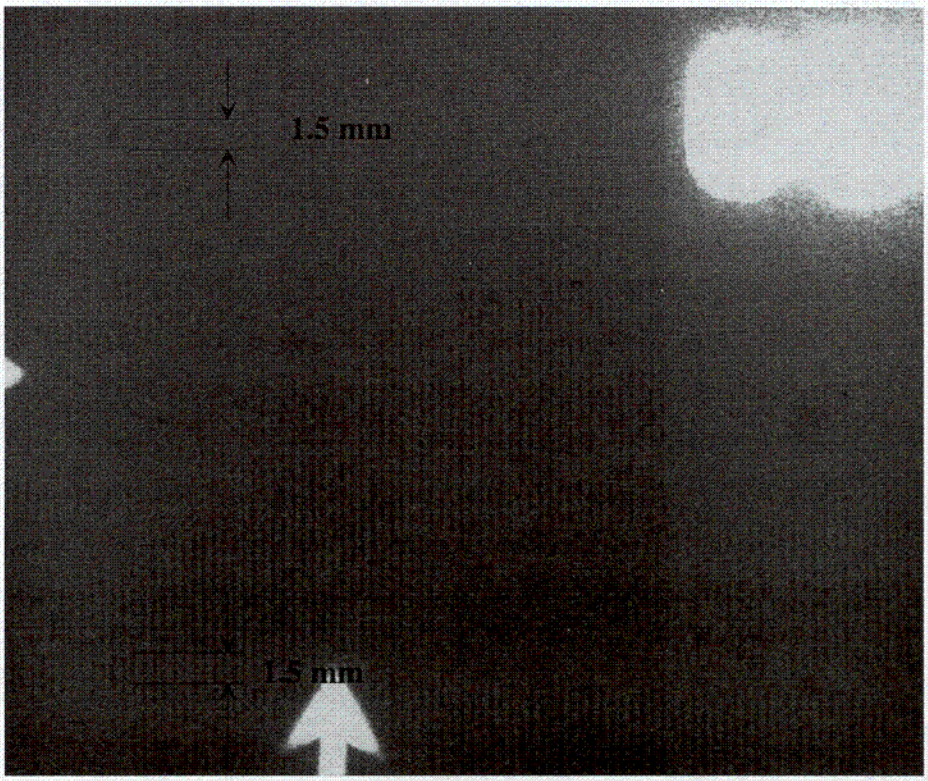

Figure 3.41 Digitized Image of Radiograph of 25-mm Plate 5-12BA-1

C25

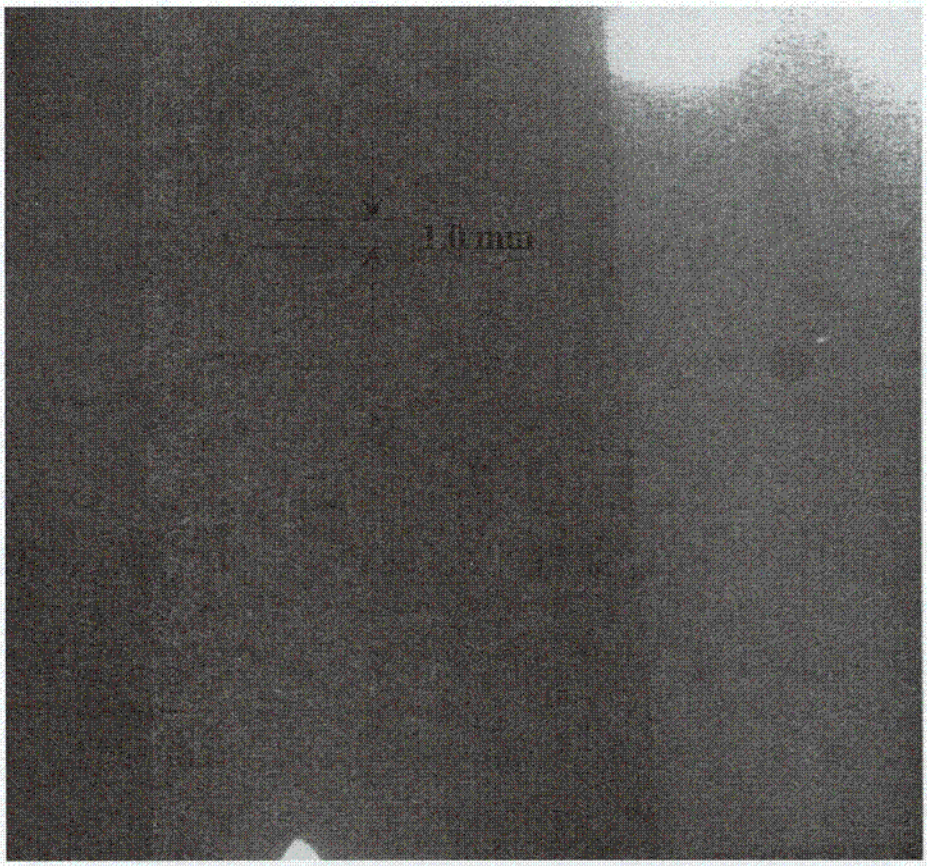

Figure 3.42 Digitized Image of Radiograph of 25-mm Plate 5-12BA-2

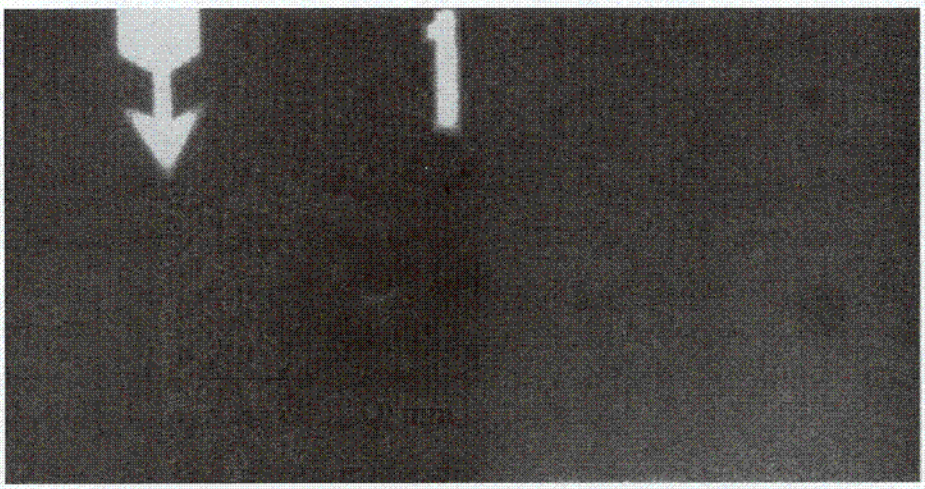

Figure 3.43 Digitized Image of Radiograph of 25-mm Plate 5-12BA-3 Location 1

C26

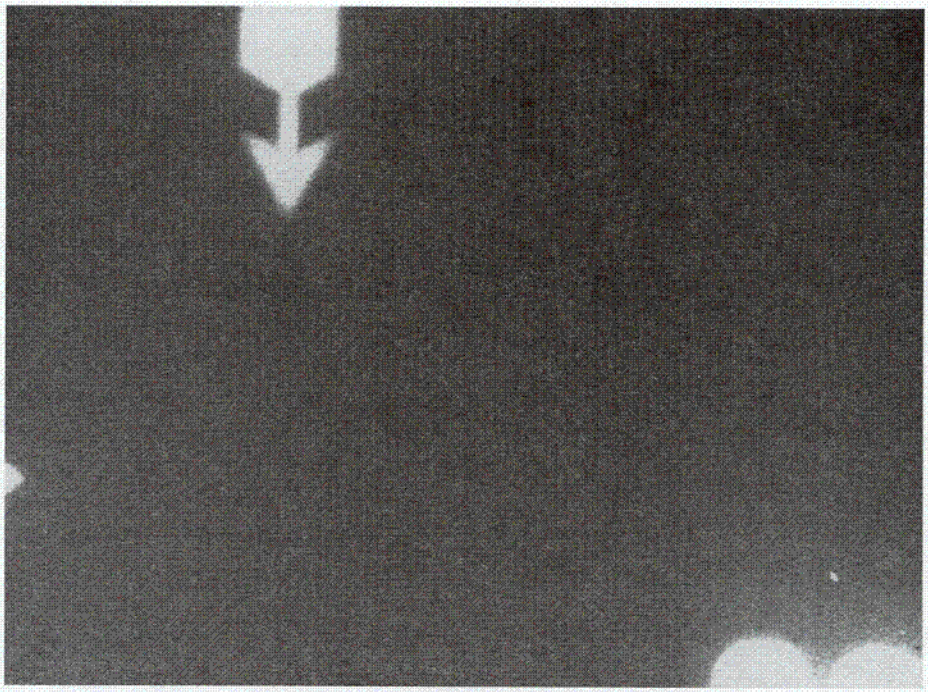

Figure 3.44 Digitized Image of Radiograph of 25-mm Plate 5-12BA-3 Location 2. No RT indication was detectable at this location.

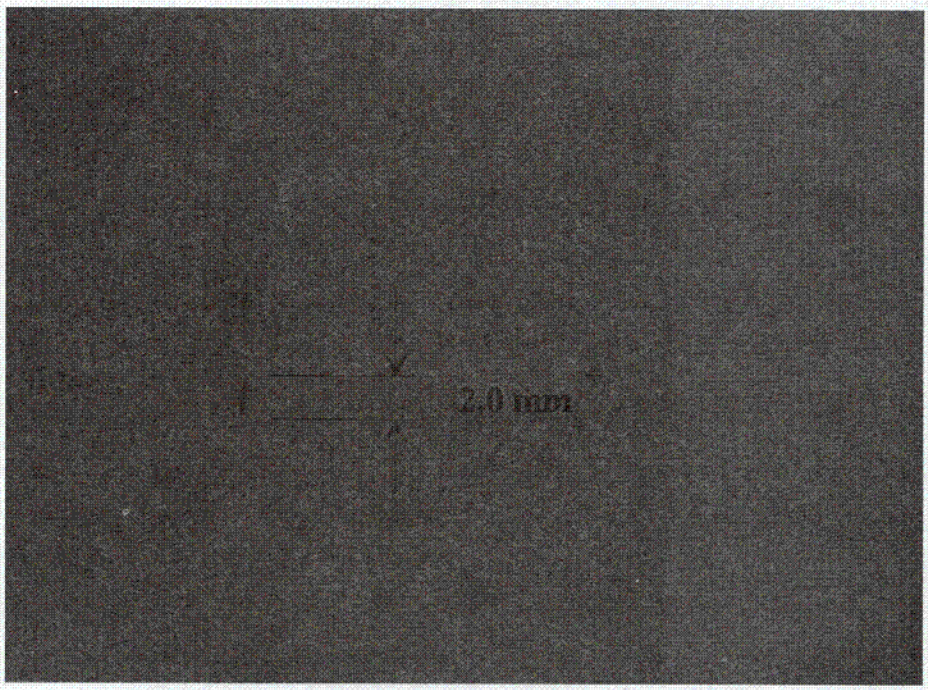

Figure 3.45 Digitized Image of Radiograph of 25-mm Plate 5-12BA-4

C27

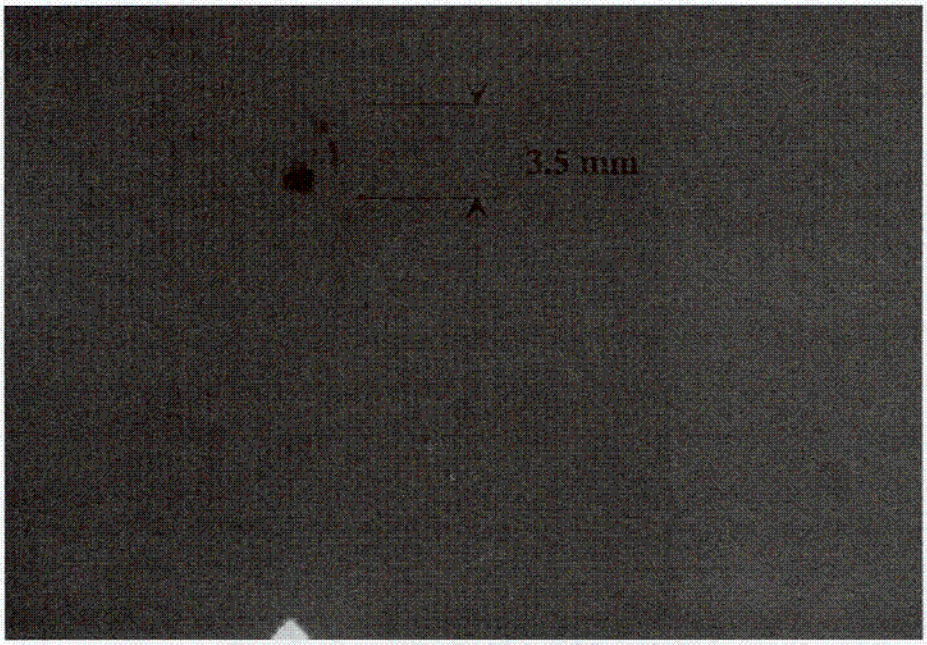

Figure 3.46 Digitized Image of Radiograph of Plate 5-12BA-6

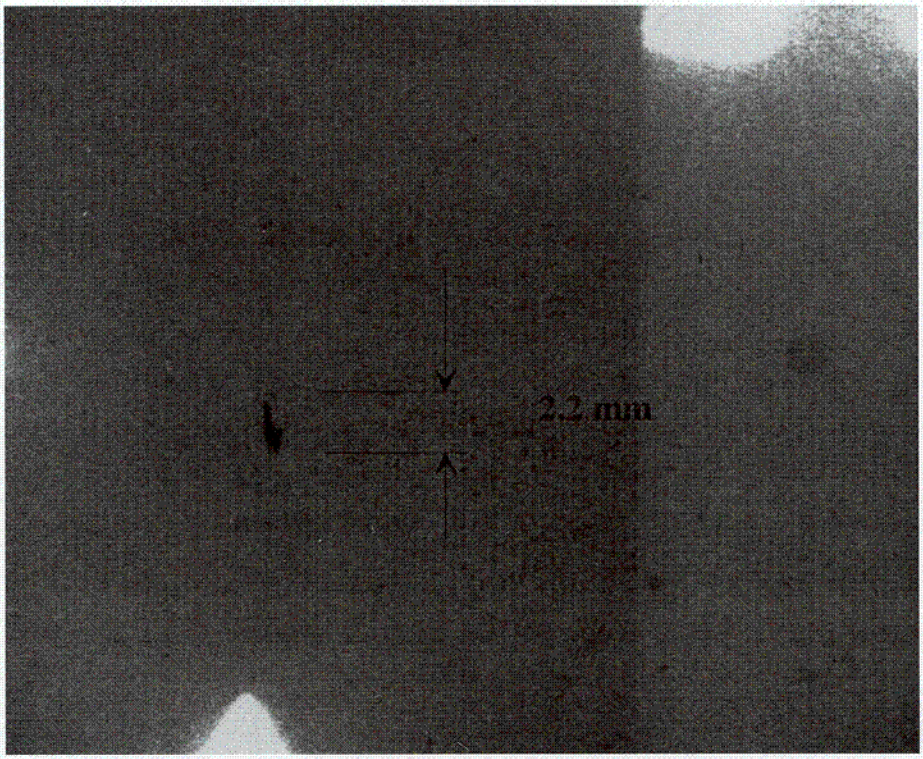

Figure 3.47 Digitized Image of Radiograph of Plate 5-12BA-8

C28

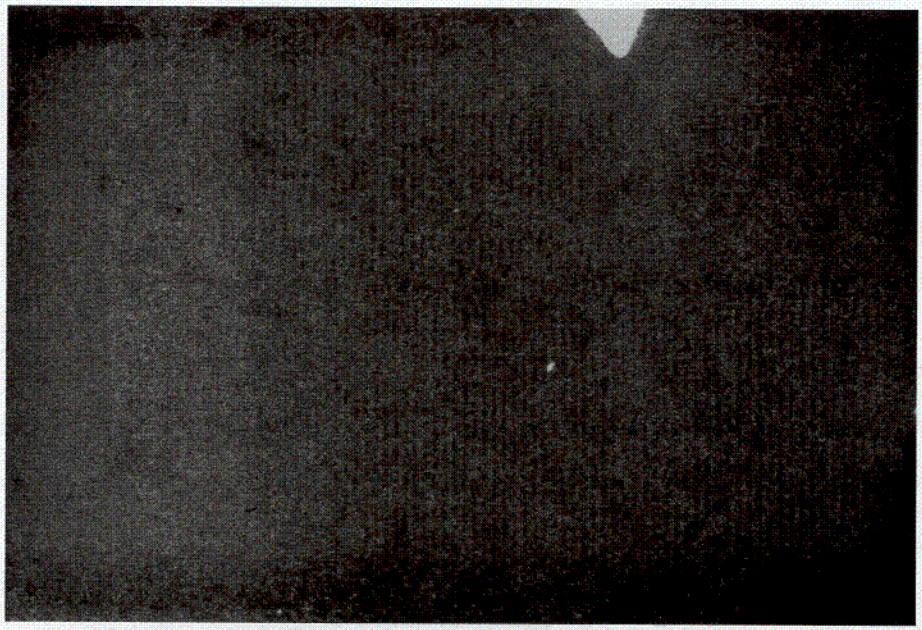

Figure 3.48 Digitized Image of Radiograph of 25-mm Plate 5-12BA-10. No RT indication was detectable at this location.

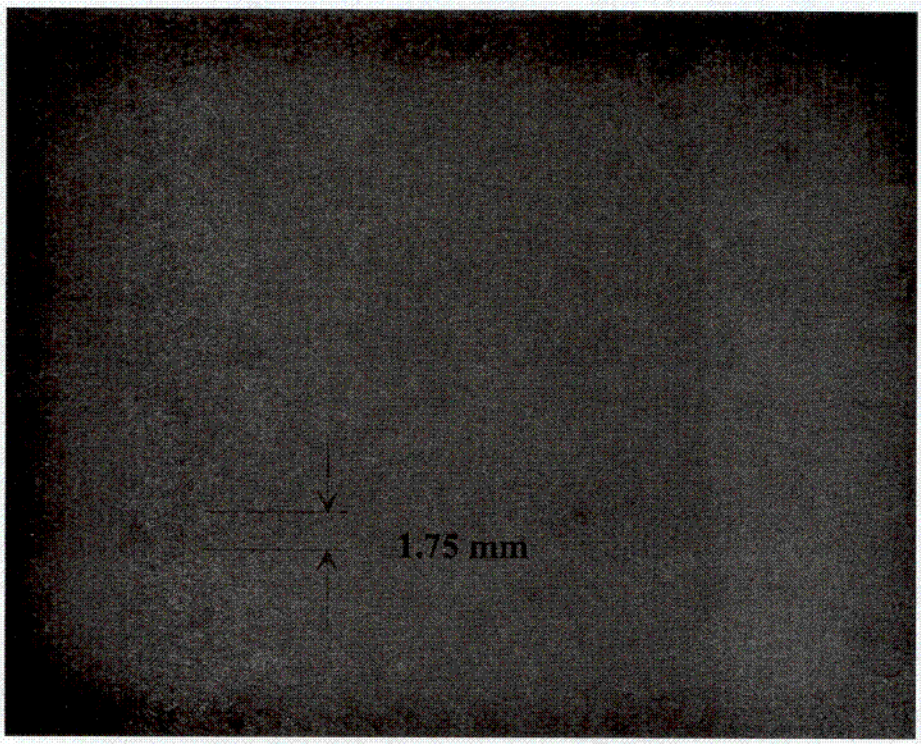

Figure 3.49 Digitized Image of Radiograph of 25-mm Plate 5-12BA-11

C29

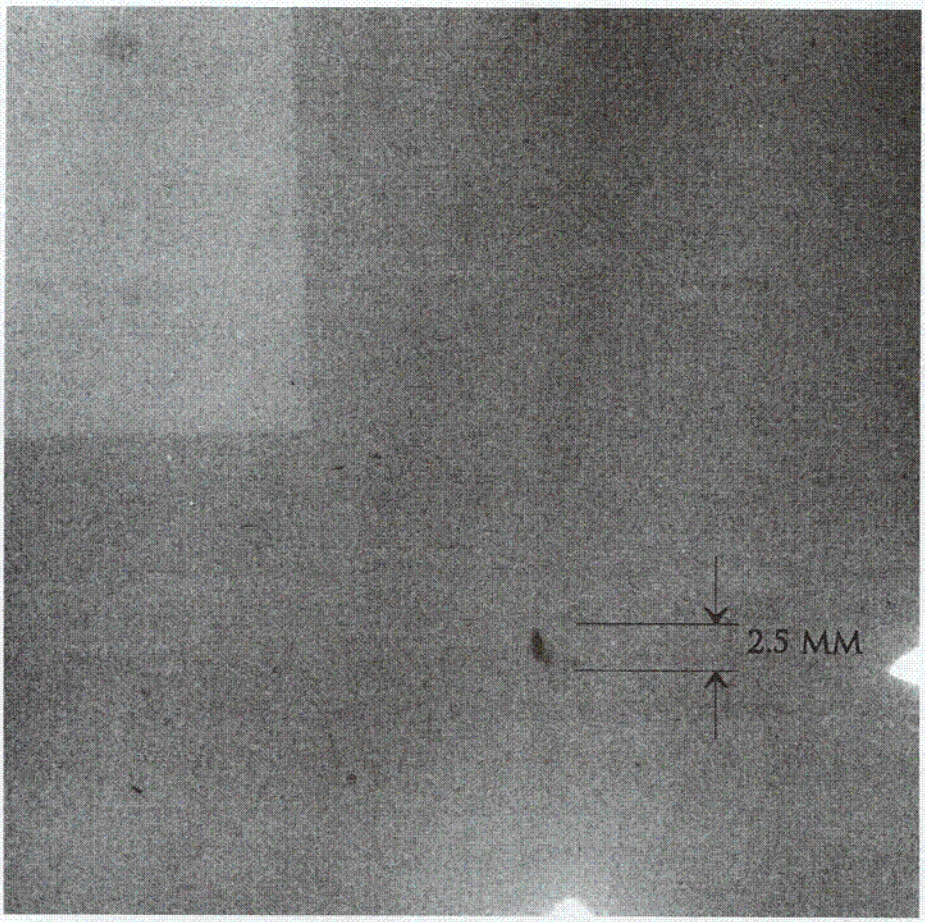

Figure 3.50 Digitized Image of Radiograph of 25-mm Plate 5-12BA-13

C30

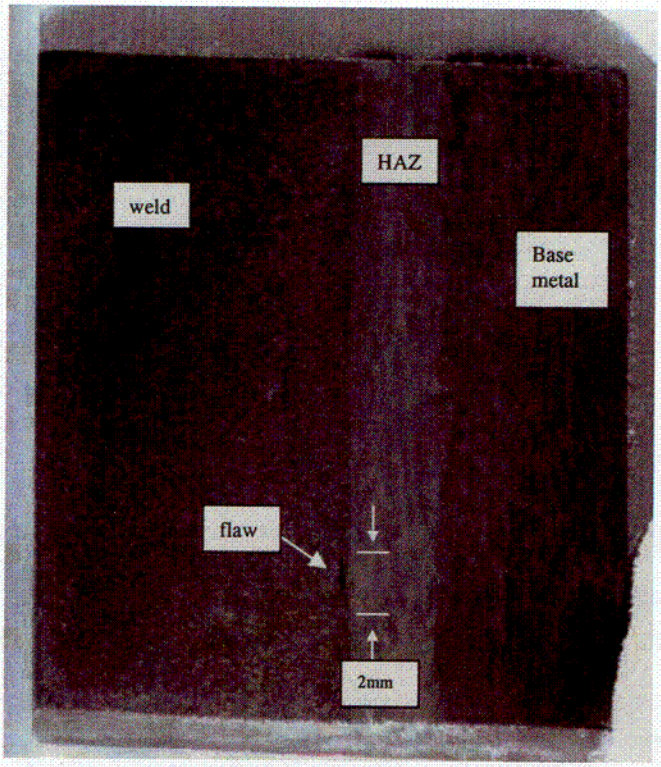

Figure 3.51 Micrograph of 25-mm Cube Showing Location of Fusion Surface Flaw

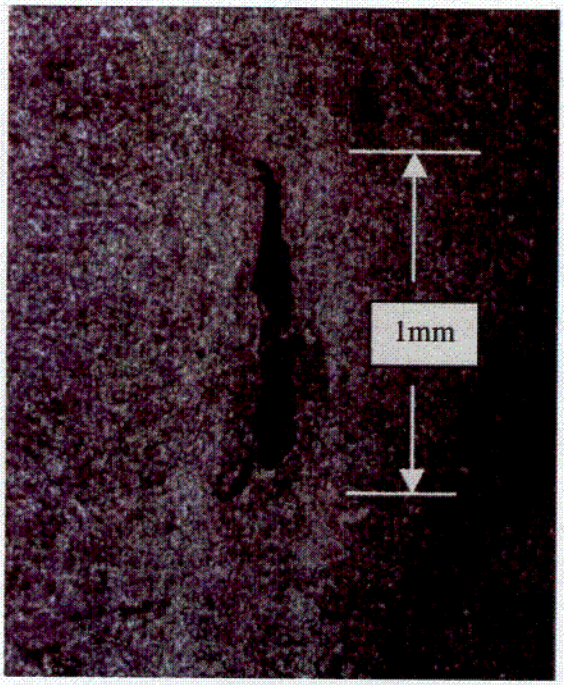

Figure 3.52 Micrograph of Fusion Surface Flaw Before Maximum Extent as Polished and Etched

C31

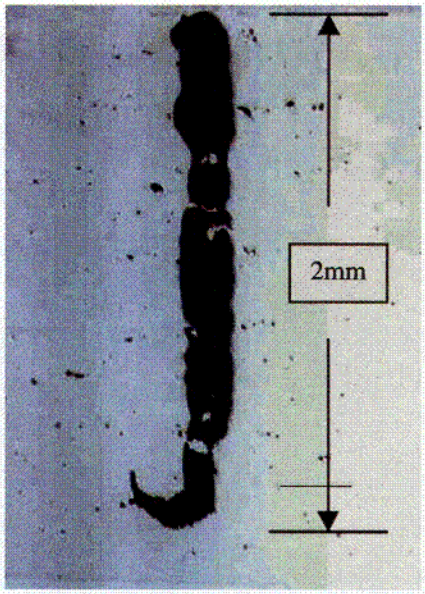

Figure 3.53 Micrograph of 2-mm Flaw at Maximum Extent as Machined

Figure 3.54 Micrograph of 25-mm Cube Showing a Portion of a Large Cluster of Small Weld Flaws. The flaws occur between the weld beads, and the alignment of the flaws follows the alignment of the weld beads.

C32

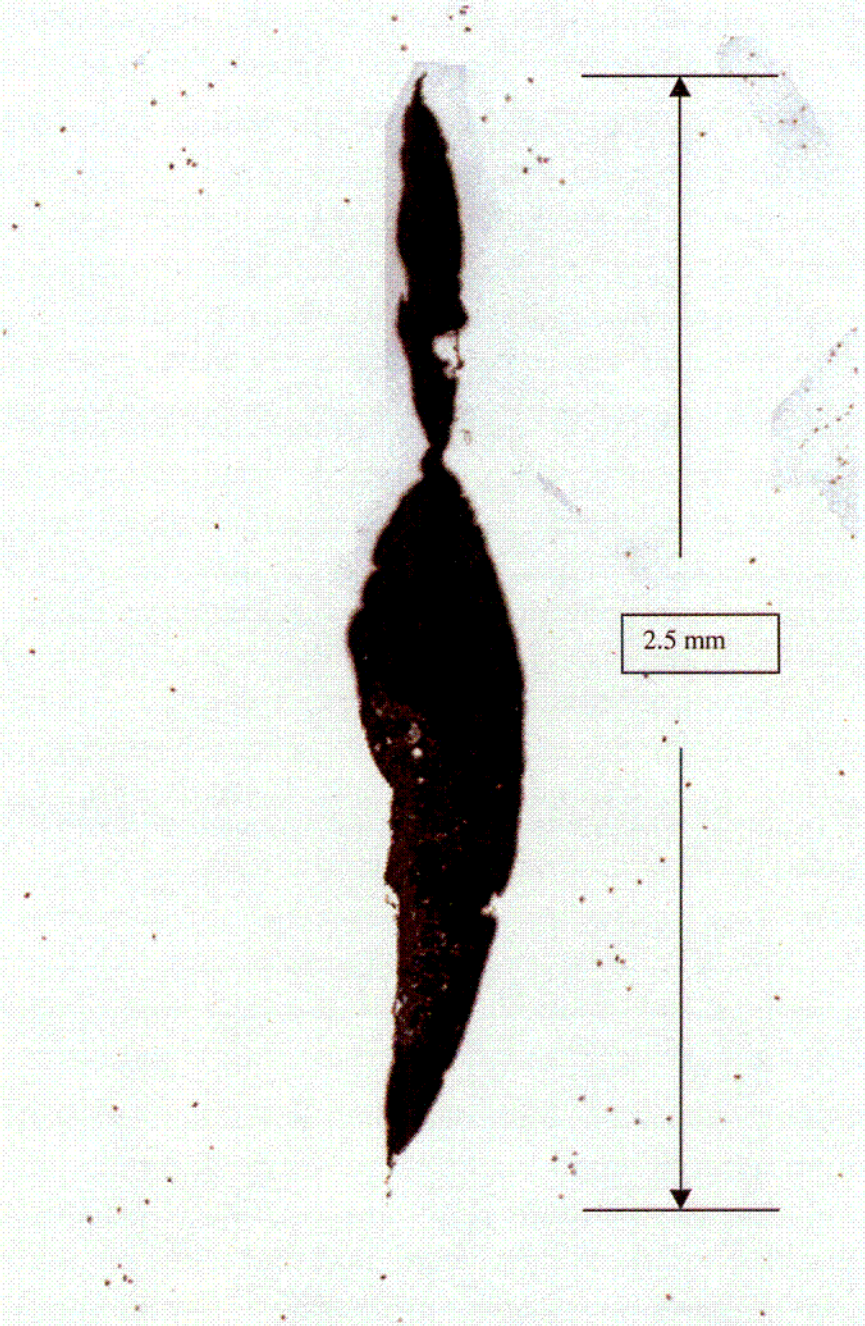

Figure 3.55 **Micrograph of a Cross-Section of One Weld Flaw from the Large Cluster. The through-wall extent of the flaw is 2.5 mm. The flawed area contains slag. Tails are visible on both flaw ends.**

C33

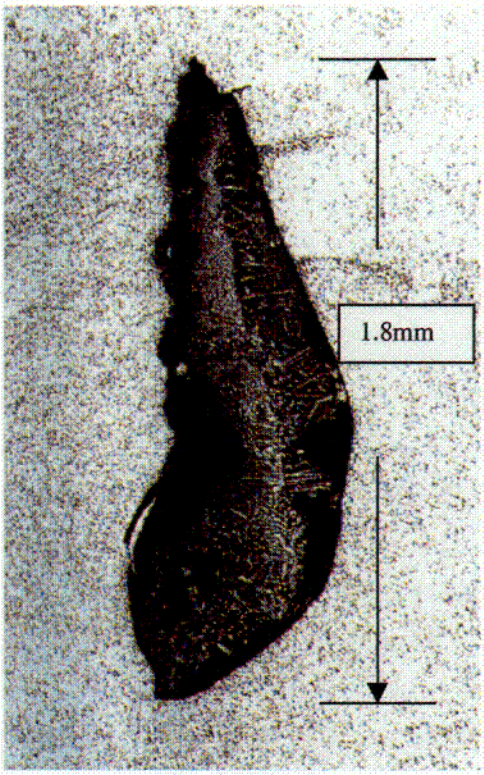

Figure 3.56 Micrograph of Flaw from the Cluster Shown in Figure 3.54. Flaw is shown to be inter-run slag.

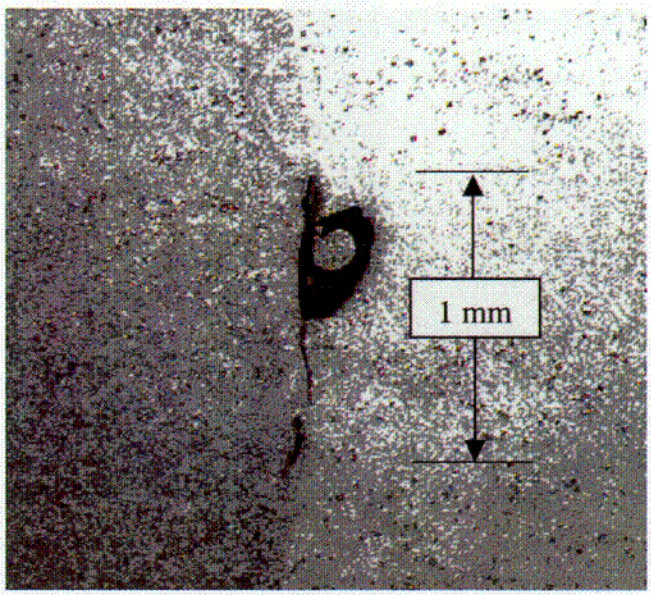

Figure 3.57 Micrograph of Small Flaw Shown in Figure 3.56. Flaw has vertical extent of 0.8 mm and planar features between the weld beads.

C34

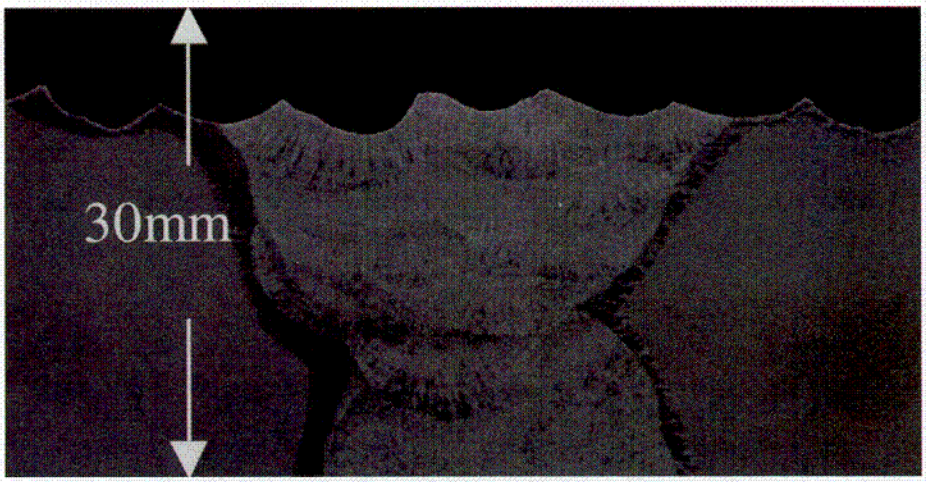

Figure 3.58 Micrograph of Typical PVRUF Weld Profile Showing Back-Gouge and Clad-to-Base Metal Interface

Figure 3.59 Photograph of 14 Near-Surface Zone 25-mm Cubes

C35

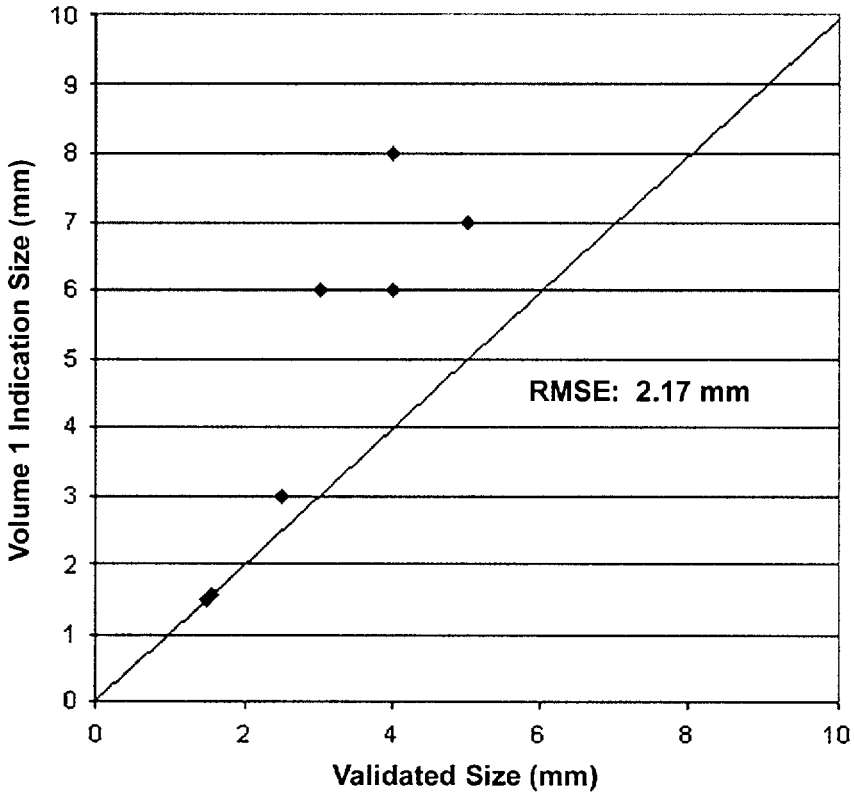

Figure 3.60 Depth Sizing Performance of SAFT-UT in the Near Surface Zone

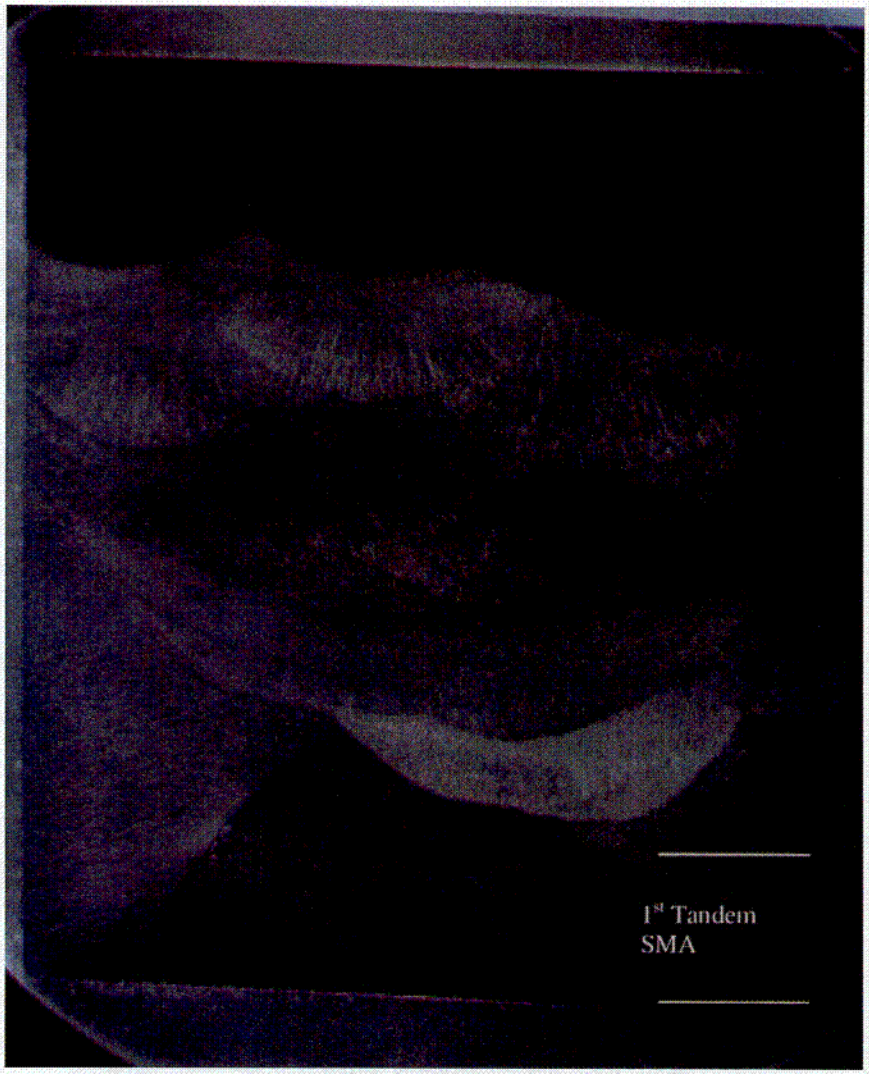

Figure 3.61 Micrograph of Cube 5-10EB1-IIbIIc Showing Shallow Back Gouge

C36

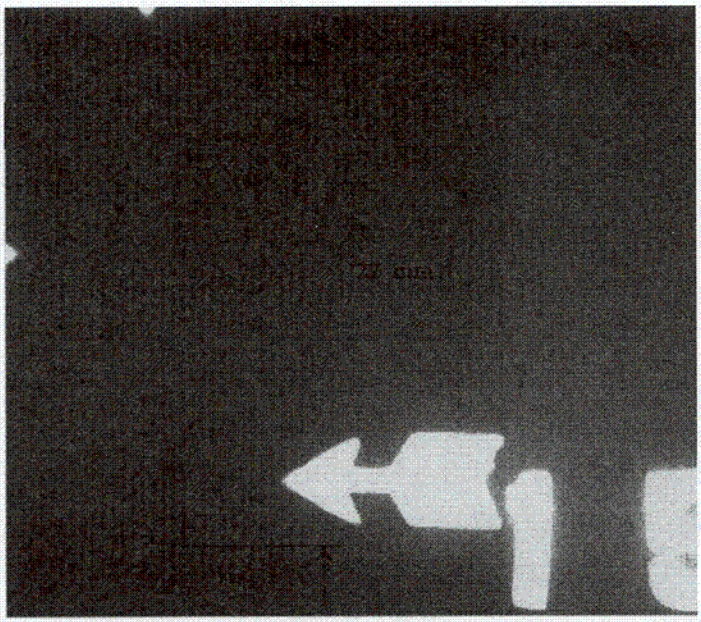

Figure 3.62 Radiograph of Cube 5-10EB1-IIbIIc

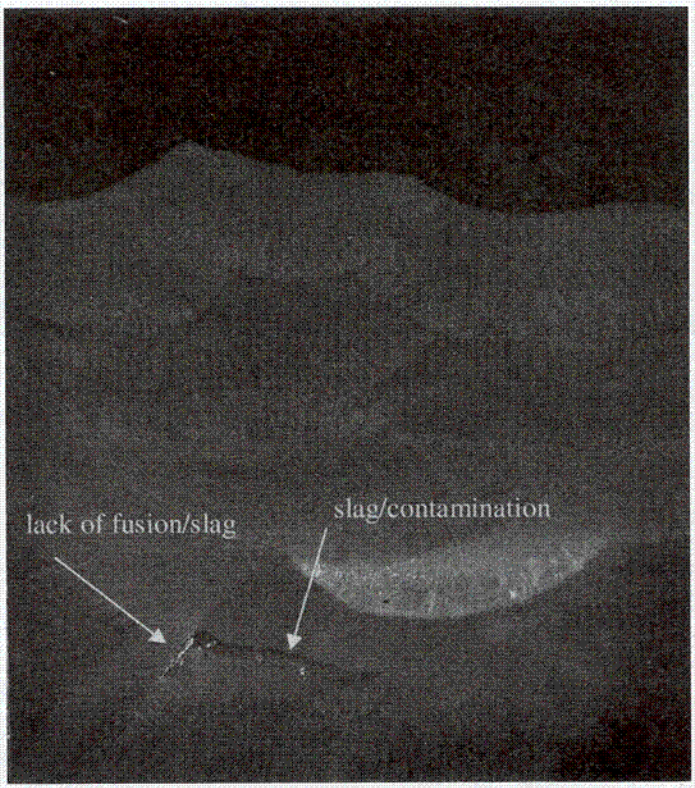

Figure 3.63 Micrograph of Cube 5-10EB1-IIbIIc Showing Complex Flaw Above First Tandem Arc Weld Passes

C37

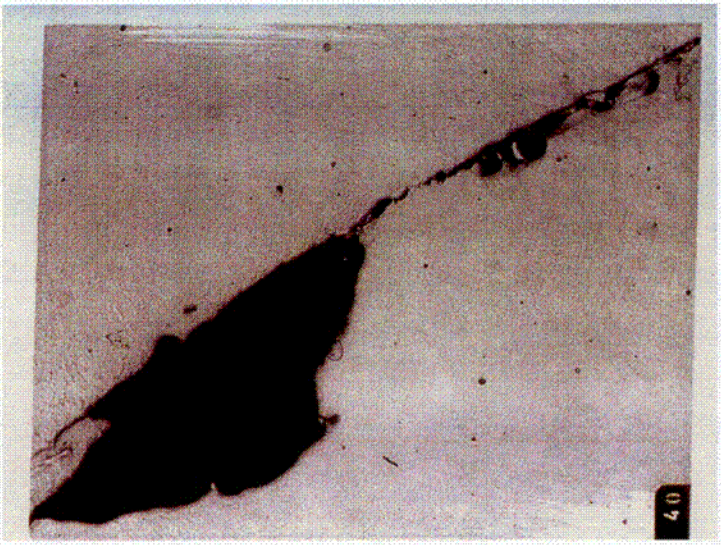

Figure 3.64 Micrograph of Lack of Side-Wall Fusion

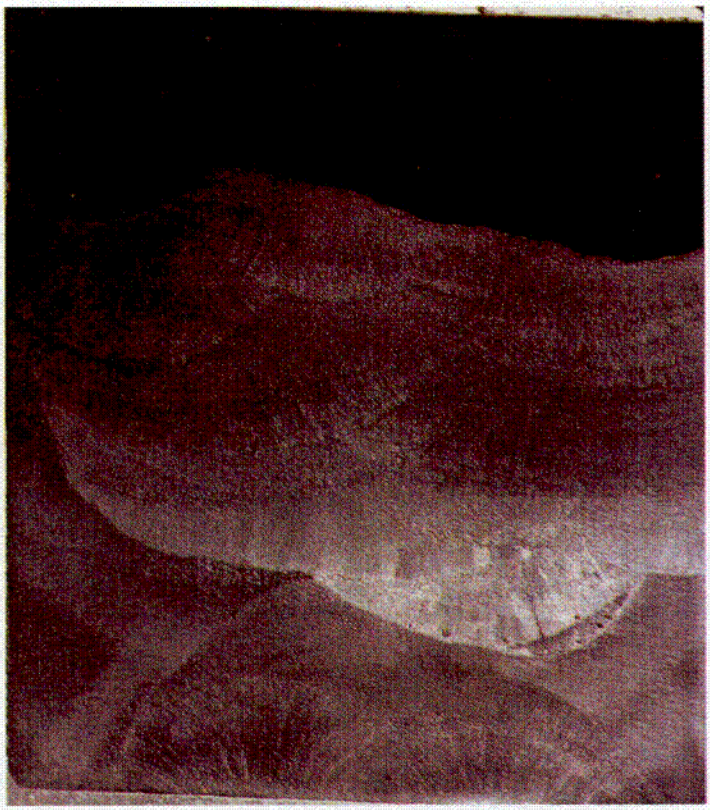

Figure 3.65 Micrograph of Cube Showing Failed Weld Bead

C38

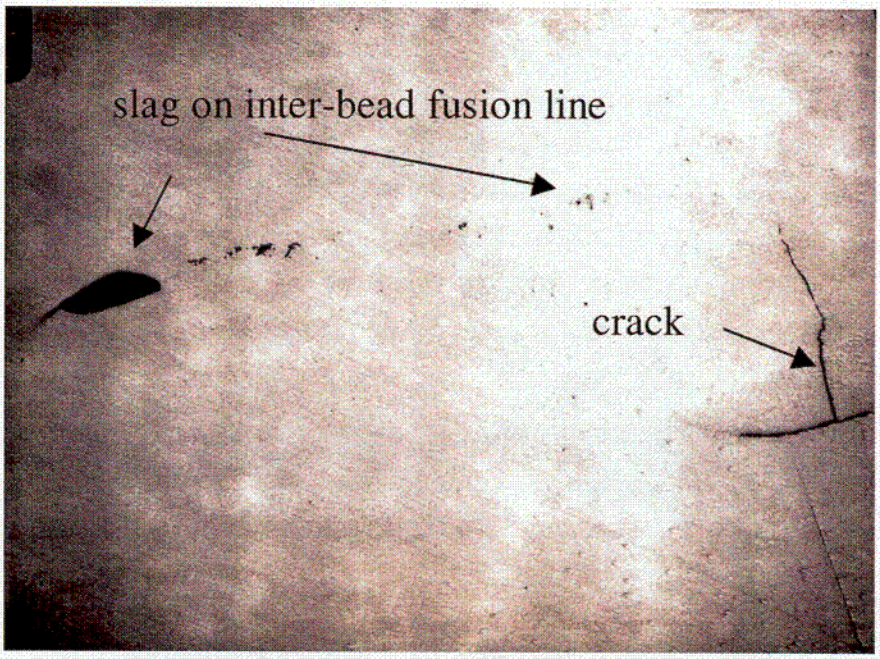

Figure 3.66 Micrograph of Cube 5-10EB1-IIbIIc Showing Flaws in the First Weld Pass of the Back-Fill

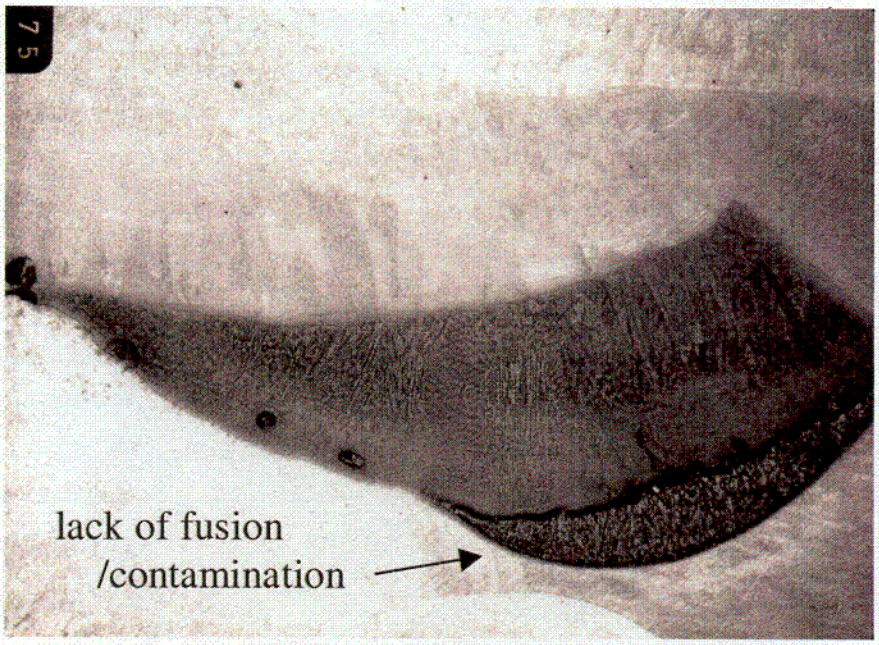

Figure 3.67 Micrograph of Cube 5-10EB1-IIbIIc Showing Contamination of the First Weld Pass of the Back-Fill

C39

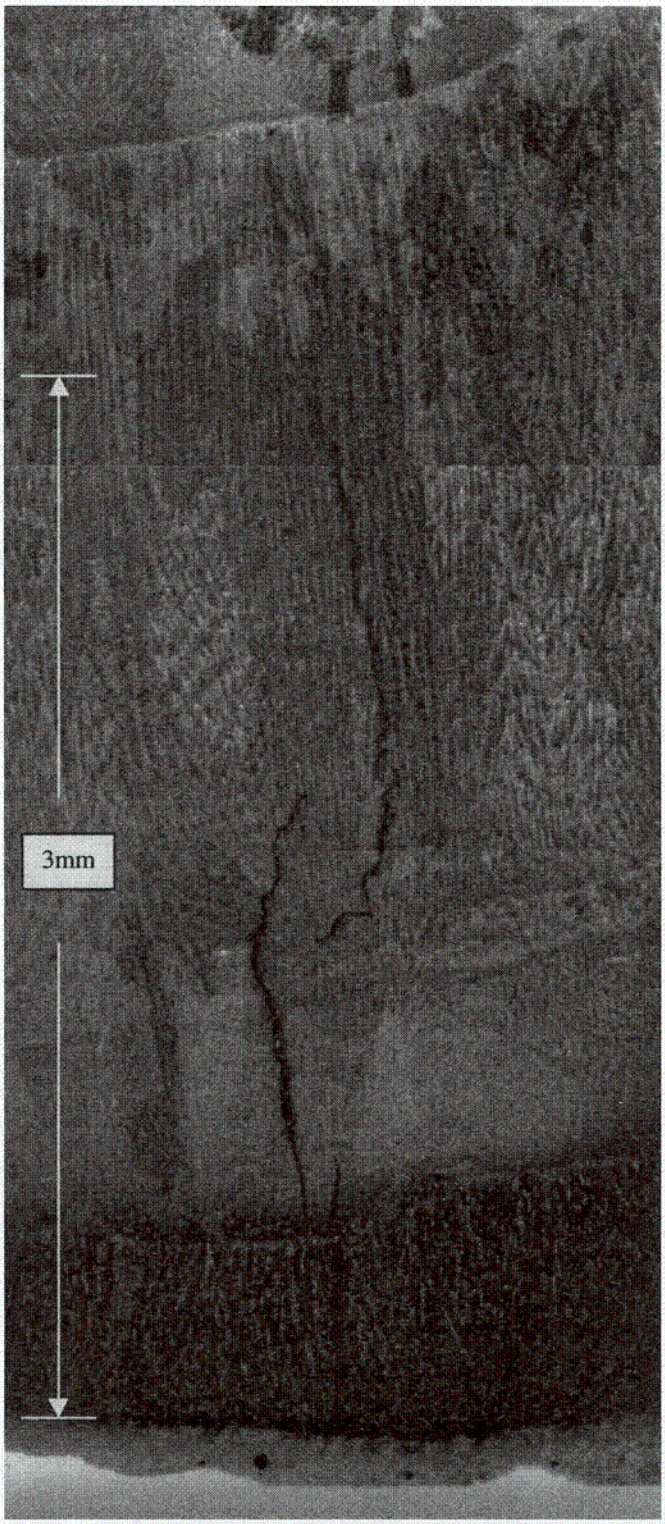

Figure 3.68 Micrograph of Crack in Flawed Weld Bead, Near Surface Zone of PVRUF

C40

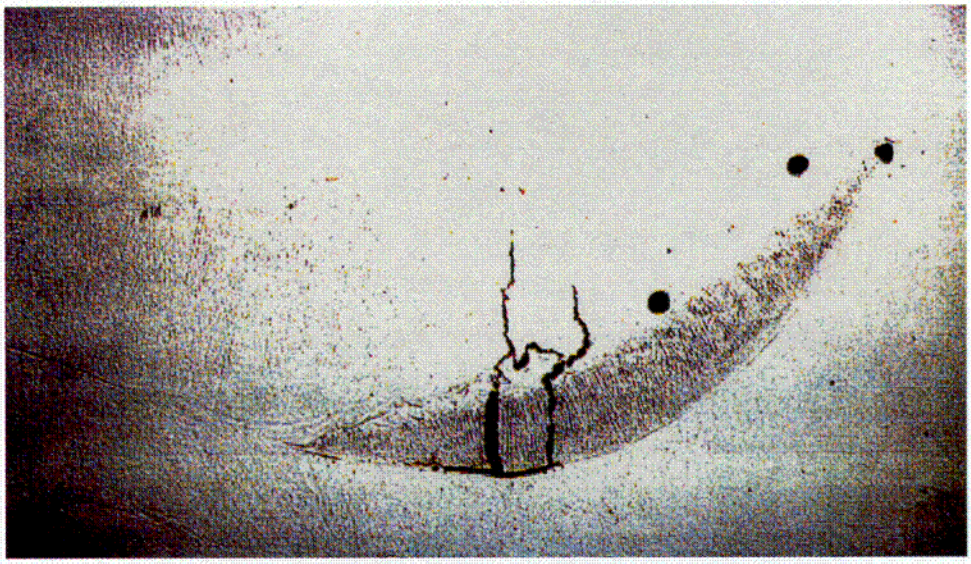

Figure 3.69 Micrograph of Cracked Weld Bead

C41

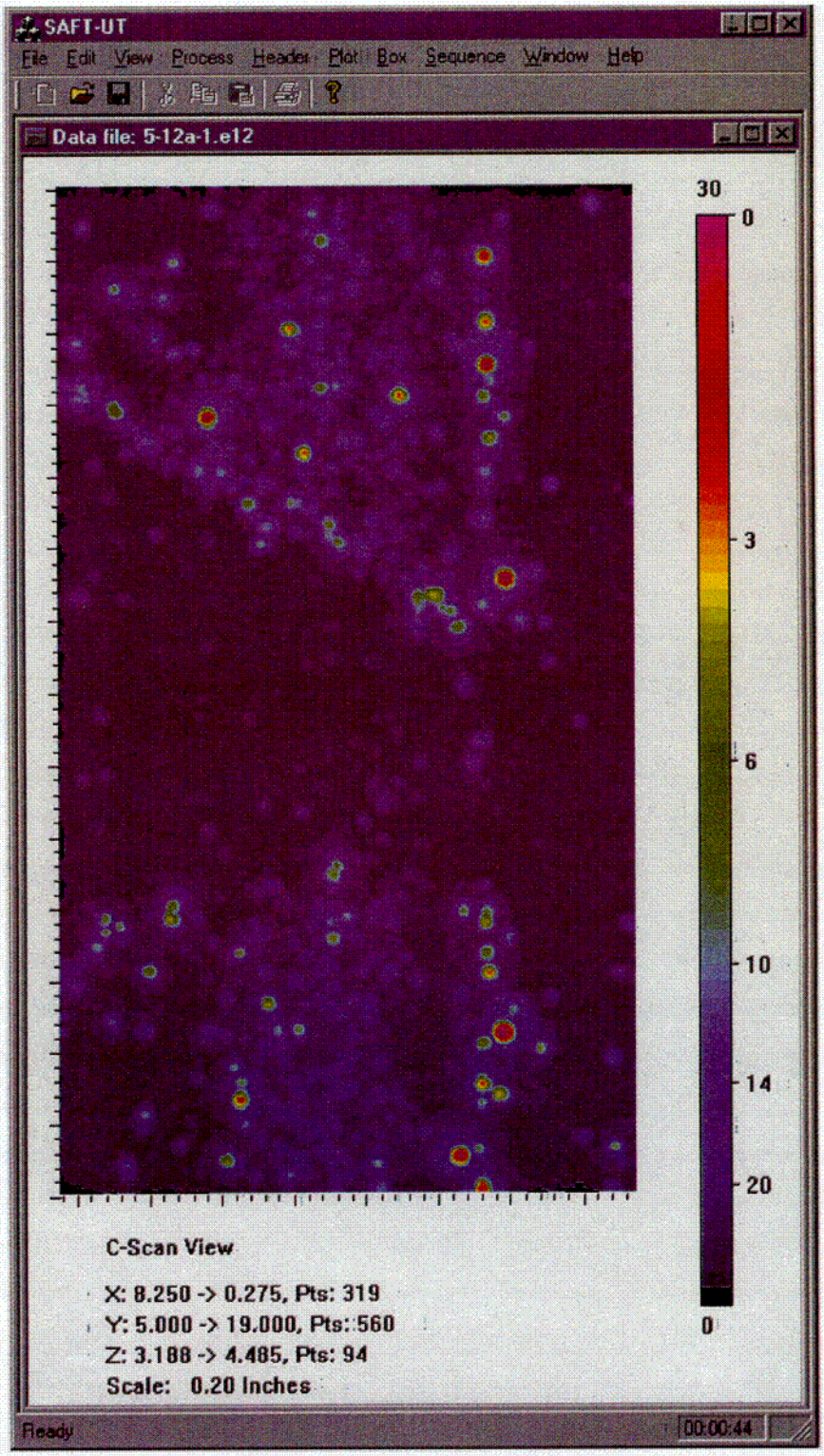

Figure 3.70 Weld-Normal UT C-scan Image of Weld Fusion Surface Showing Profile of Weld Repair's Low Acoustic Energy Signature

C42

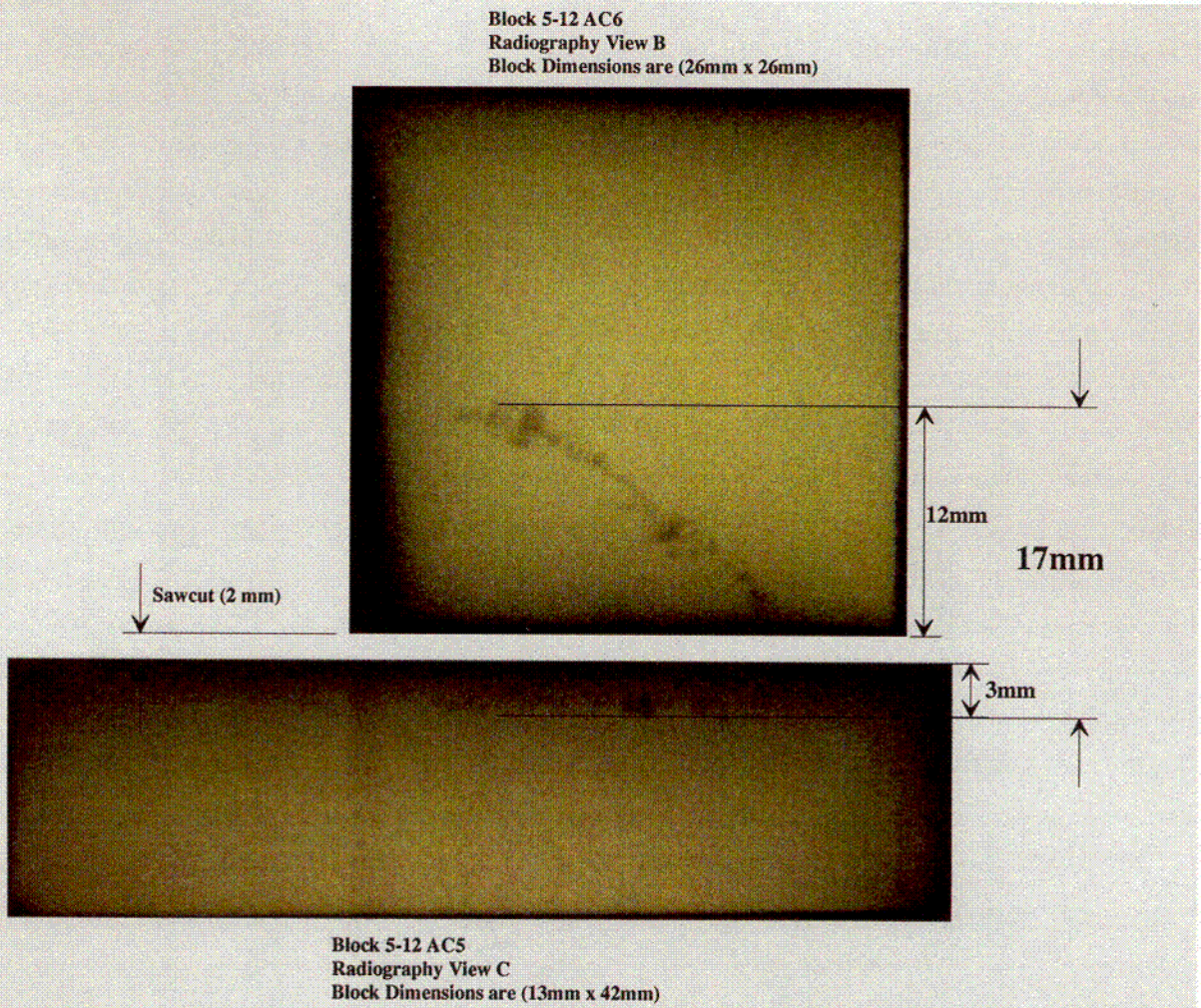

Figure 3.71 Radiographic Images of 17-mm Flaw Indication in a Repair to the Beltline Weld of the PVRUF Vessel

C43

Figure 3.72 Micrograph of a Portion of the 17-mm Flaw. The composition of the flaw is taken to be slag, porosity, and contamination.

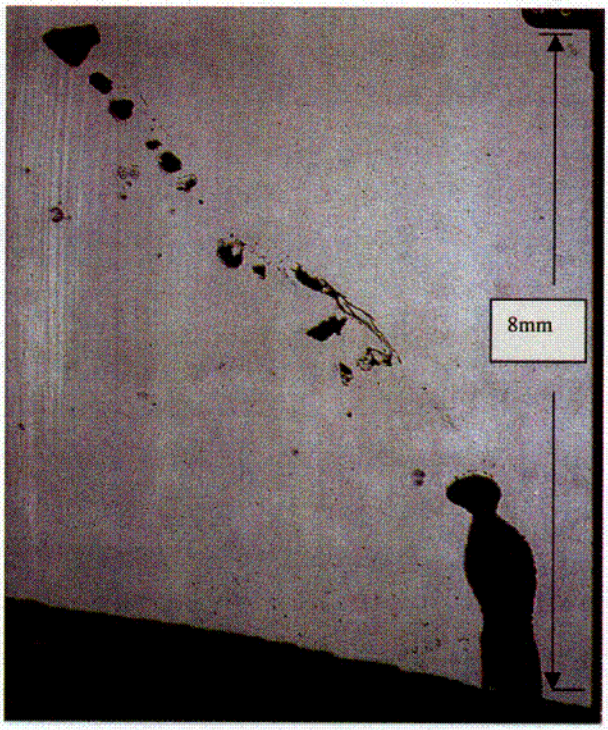

Figure 3.73 Micrograph Showing a Magnified View of a Portion of the 17-mm Flaw. A crack-like portion of the flaw is visible in this figure.

C44

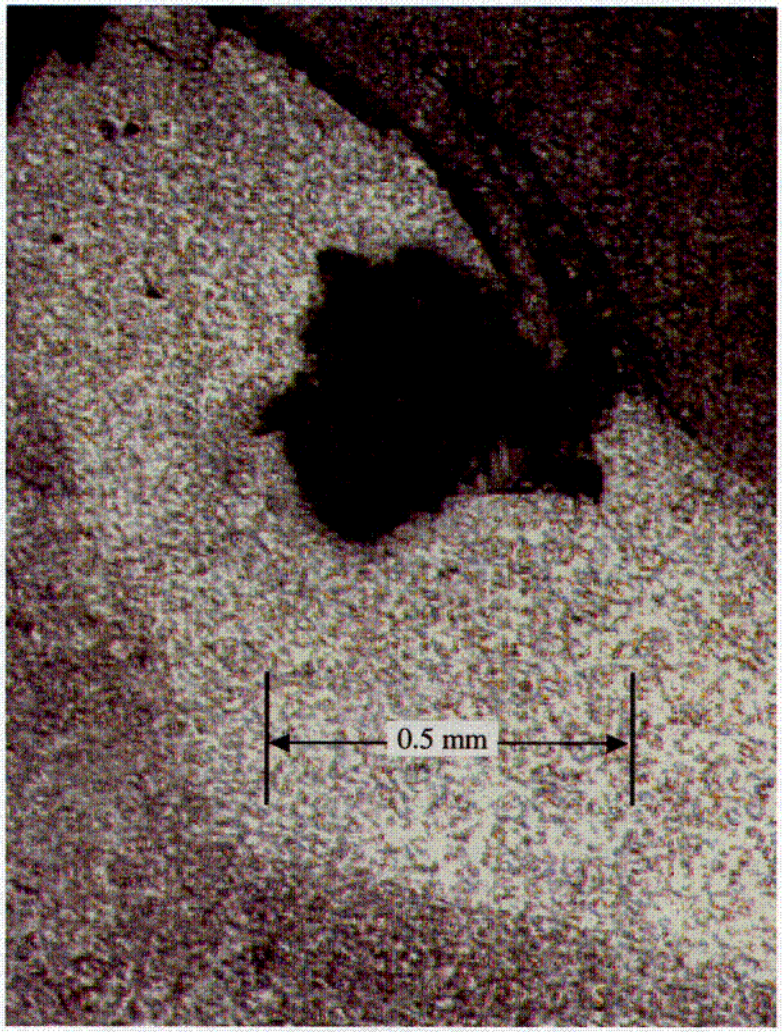

Figure 3.74 Micrograph Showing a Magnified View of the Crack-like Portion of the 17-mm Flaw. The crack originates from a small region between weld beads.

C45

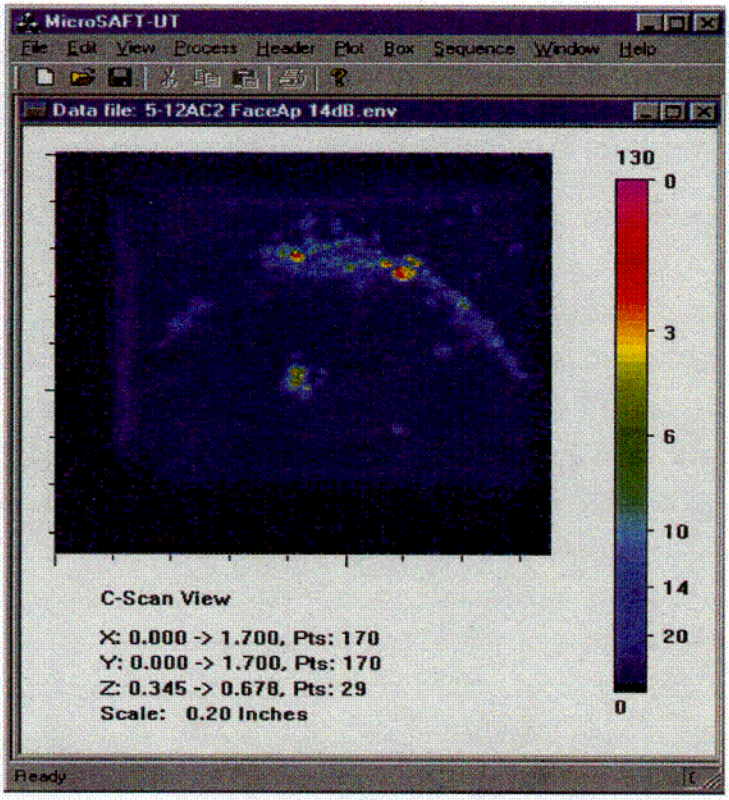

Figure 3.75 Focused Ultrasound (10-MHz Probe) Result Showing Top View of Flaw in 5-12AC2. This is a repair flaw located on the end of the repair. Vessel through-wall direction is into the page. Distance from weld center is on the abscissa. Distance along the beltline weld is on the ordinate. This image shows that the flaw is oriented principally in the axial direction.

C46

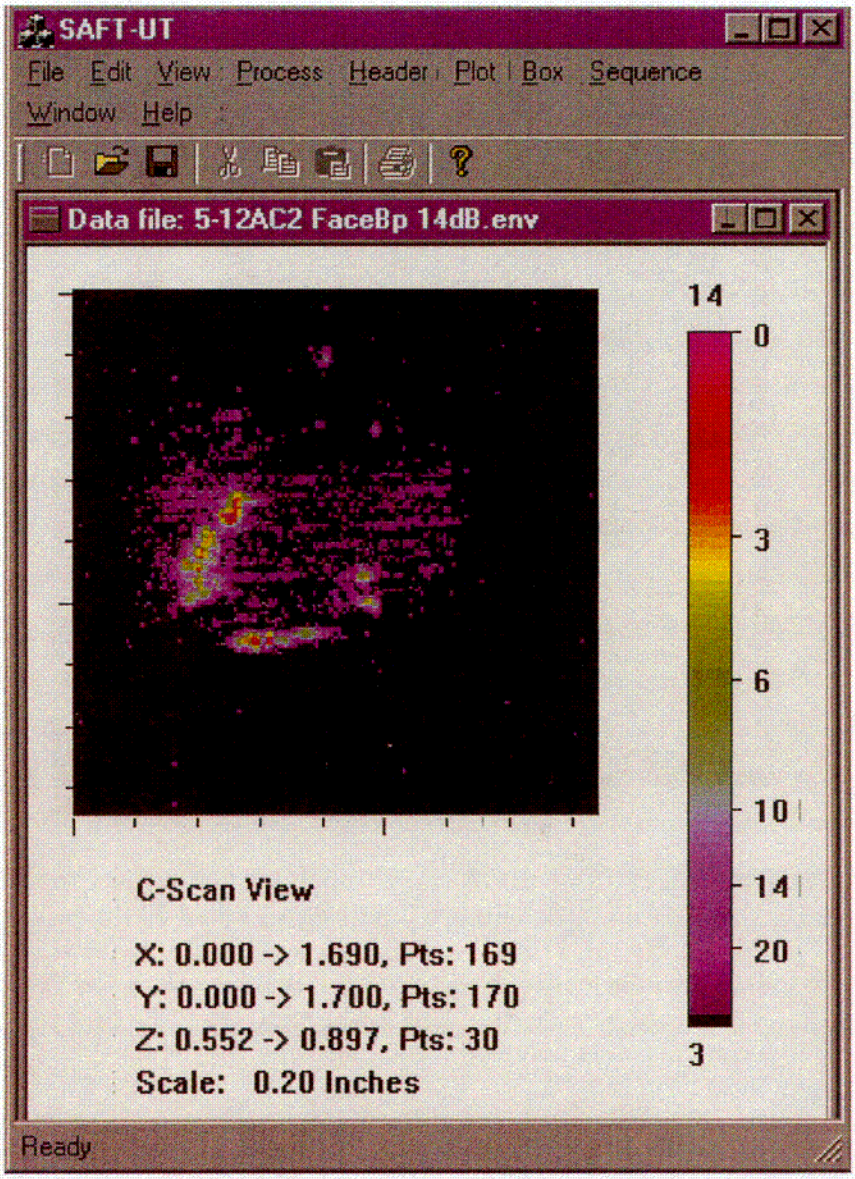

Figure 3.76 Focused Ultrasound (10-MHz probe) Result Showing Side View of Flaw in 5-12AC2. This is a repair flaw located on the end of the repair. Vessel through-wall direction is on the ordinate. Distance from weld center is into the page. Distance along the beltline weld is on the abscissa.

C47

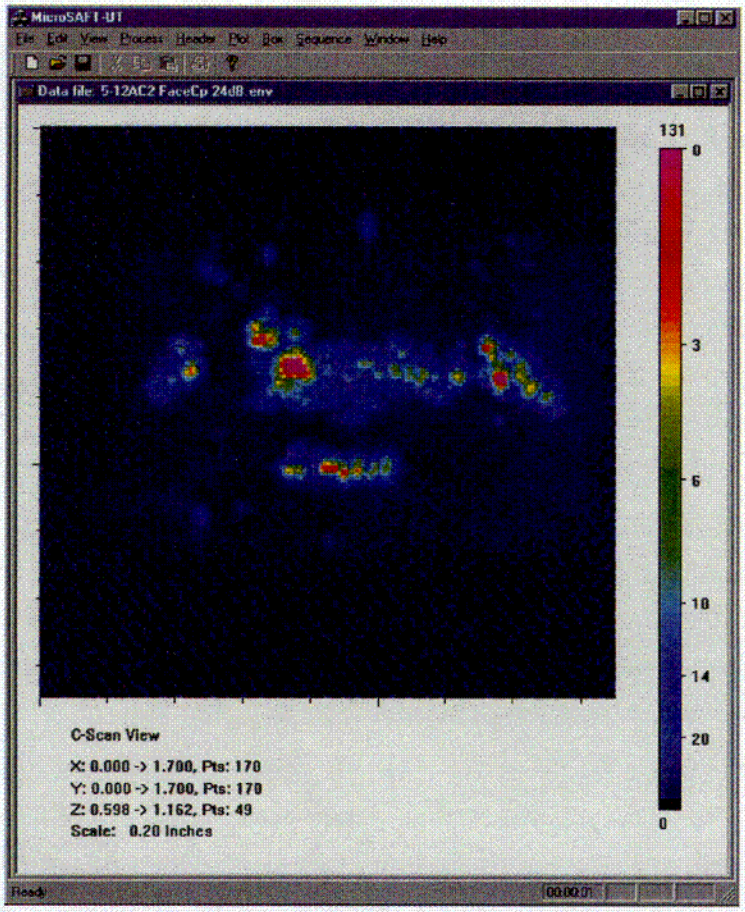

Figure 3.77 **Focused Ultrasound (10-MHz probe) Result Showing End View of Flaw in 5-12AC2. This is a repair flaw located on the end of the repair. Vessel through-wall direction is on the ordinate. Distance from weld center is on the abscissa. Distance along the beltline weld is into the page.**

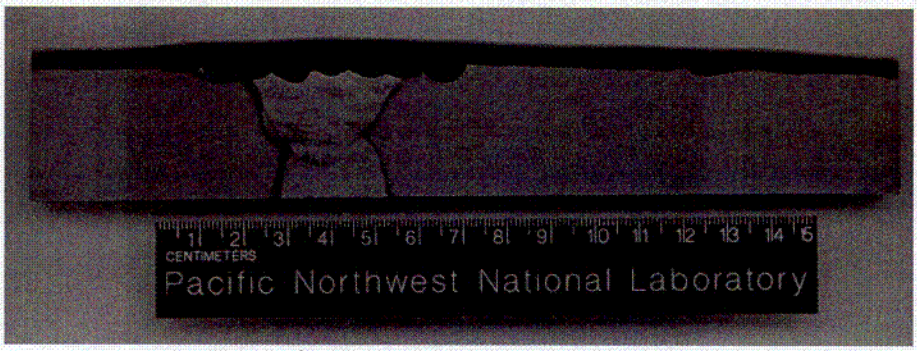

Figure 3.78 **Micrograph of Upper Portion of Weld in PVRUF Specimen 5-6Eca. A weld repair, made from inside the vessel, was reported at this location. The repair was not detected.**

C48

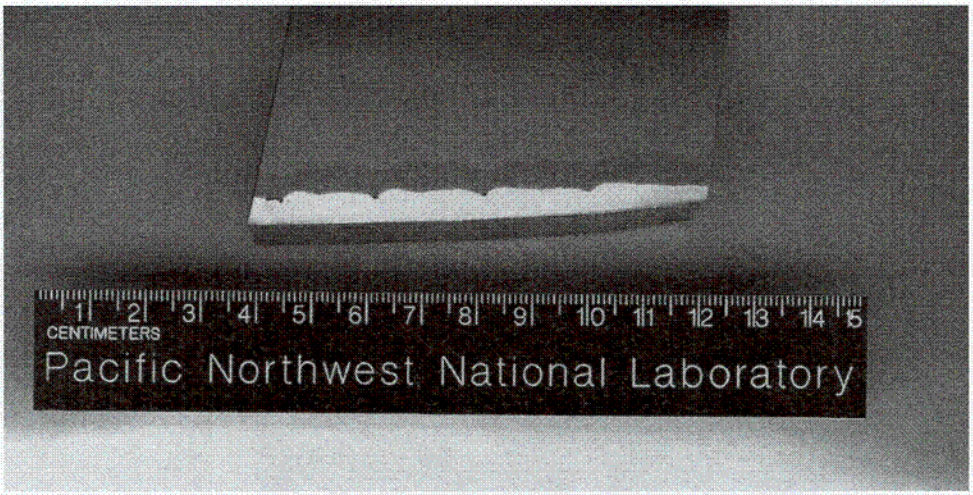

Figure 3.79 Photograph of PVRUF Specimen Showing Small Slag Inclusions at the Clad-to-Base Metal Interface.

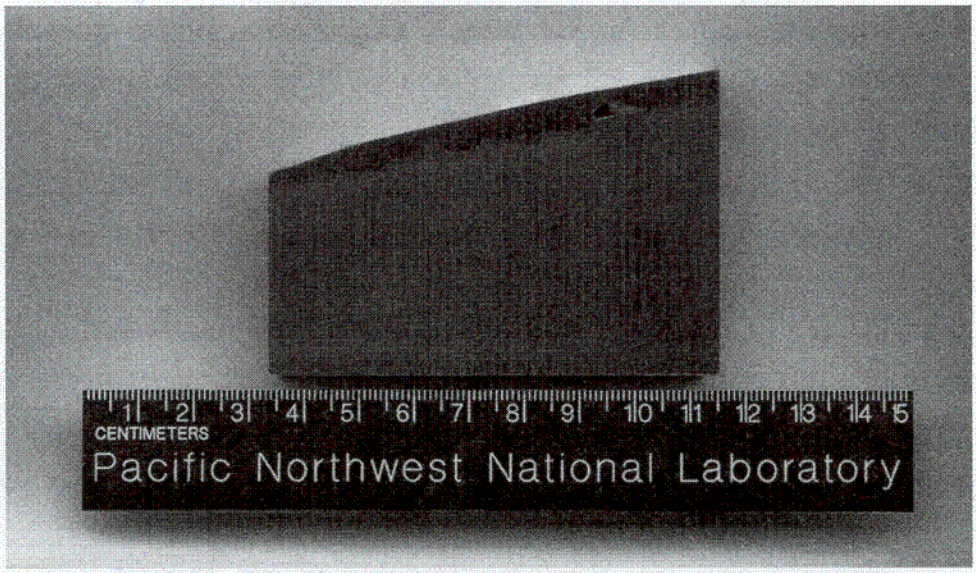

Figure 3.80 Photograph of PVRUF Specimen 4-5DBAC-Z5 as Machine Cut. The photograph shows 4-mm through-clad lack of fusion with slag.

C49

Figure 3.81 Digitized Image of Radiograph Showing of Base Metal Lamination Cluster. Vessel through-wall direction is oriented vertically in the image. Vessel elevation is oriented horizontally in the image.

C50

4 CONFIRMED FLAW FREQUENCY AND DISTRIBUTION IN PVRUF VESSEL

This chapter describes the through-wall size distribution estimated using the results of the validation research described in Chapter 3 and compares it to the Marshall distribution. The PVRUF distributions for larger flaws in weld metals used only results from the present validation effort as the source of data for these flaws. In the case of smaller flaws, it was necessary to sample the weld metal in validation testing and combine that data with the data from the prior volumetric examinations from the vessel inner surface. This approach was justified because the number and sizes of these flaws were found to be very consistent with the limited validation efforts for these flaws in the smaller size categories.

The development of distributions for base metal is the subject of future work, because the scope of the validation effort was not intended to address base metal flaws. Only two of the larger base metal flaws detected from the inner surface examinations were addressed by the current validation effort. The validation results for these flaws showed that the conservative rules used to estimate the flaw size, as expected, did not under estimate the through-wall extent of these flaws. Therefore, the data are presented below in terms of sizes of flaw indications rather than in terms of actual flaw dimensions.

The larger fabrication flaws discovered in the PVRUF vessel were complex and distributed in a volume of material, typically, along the curved boundary of a weld bead. No large voids were found—rather, combinations of small voids, inclusions, lack of fusion, and cracks. One failed weld bead was found, but, for the most part, the flaws occurred between the weld beads or between a weld bead and the base metal.

It makes sense, in light of what the data show, to characterize the flaws along the lines of the flaw types that have the potential to develop into growing cracks. These flaw types are tabulated (Chapman and Simonen 1998) as centerline cracking, heat-affected zone cracking, porosity, lack of fusion, and non-metallic inclusions. The failed weld bead is an example of centerline cracking. No cases of heat-affected zone cracking were found. Porosity where it was found was always small but was often present in the larger flaws (together with other conditions). Most of the flaws were lack of fusion (LOF) and slag inclusions.

4.1 Confirmed Flaw Frequency and Distribution in the Near Surface Zone

All Volume 1 flaw indications greater than 5 mm in through-wall size were removed from the PVRUF vessel near-surface zone. No flaws larger than 5 mm were found, but a single 25-mm cube did contain an 8-mm flawed region as described in Chapter 3.

Table 4.1 shows the validated distribution of flaws for the near-surface zone weld metal. The flaws listed in this table are characterized as *crack* and *lack of fusion*. The flaw indications are distributed across through-wall size categories with 1-mm steps. The first size category contains most of the flaw indications and includes indications less than 2.5 mm in through-wall extent. The second size category, labeled 3 mm, includes indications with through-wall size between 2.5 and 3.5 mm. Similar boundaries were used to distribute the indications in the other size categories. No flaws are shown in the 6-, 7-, and 8-mm categories because none were found.

Table 4.1 Flaws in Weld Metal of the Inner 25 mm of the PVRUF Vessel								
Jan. 2000	**<3 mm**	**3 mm**	**4 mm**	**5 mm**	**6 mm**	**7 mm**	**8 mm**	**Total ≥ 3 mm**
Crack. LOF	190	7	2	2				11

Two 5-mm flaws were validated in the weld metal of the near-surface zone. The first of these flaws was analyzed with metallography and was shown to be a failed weld bead. The second was considered volumetric in the original SAFT-UT inspections where the indication was detected in six different modalities indicating a complex flaw in cube 5-1AB14-IIbIIc. UT weld-normal confirmed a flaw size of 5 mm, and the radiography measured 1 mm. The UT shows a 5-mm flaw indication that is broken up. Because the RT did not detect the weld solidification crack and because of the complex nature of the UT responses, the 5-mm size is used in the table.

Two 4-mm flaws are shown in the validated table. The first was validated as a 4-mm fusion line slag in a micrograph of the same cube (5-10EB-IIbIIc) as the 5-mm failed weld bead. The second was validated in the radiographic testing in cube 5-7DB1-IIbIIc. The metallography of this cube showed a 1-mm lack of fusion with slag. Because the depth location of flaw changed along its length, the metallography could only show 1 mm in any one slice.

Seven 3-mm flaws are shown in the validated table. These flaws were confirmed in the weld normal UT and in the ultrasonic immersion testing of fourteen 25-mm cubes. The flaws less than 3 mm in size were confirmed in the weld-normal UT and in ultrasonic immersion testing of fourteen 25-mm cubes removed from the near surface zone.

Table 4.2 shows the size distribution of slag inclusions and lack of fusion found in the cladding and at the clad-to-base metal interface. These flaws were confirmed from the rough machine cuts through the PVRUF material. Figure 3.79 shows a photograph of the 4-mm flaw found in the cladding. Other rough machine cuts showed such flaw indications to be lack of fusion with slag. Most (90%) of these small cladding flaws were distributed along the inside diameter transition that is part of the vessel's nozzle shell course. The other 10% were distributed randomly.

Table 4.3 shows the size distribution for the base metal flaw indications that remain after the validation research. The validation of flaw indications in PVRUF included testing of only two near-surface zone base metal indications with the remaining indications listed in Table 4.3 being based on results from the volumetric examinations from the vessel inner surface. The flaw indications evaluated were planar indications #1 and #2 (Schuster et al. 1998, pp. A.36-A.37). Of the base metal indications, these were the largest. They were also interesting because they occurred under the inside diameter change of the vessel's nozzle shell course. No large base metal flaws were found. Rather, the 4-mm clad flaw shown in Figure 3.79 was found at the location of one these indications. As a consequence, the entries in Table 4.3 still are best characterized as indications.

The possible explanations for the unvalidated near surface base metal indications are

- laminations—These typically form at the vessel mid-wall but are known to occur at all depths in plate material.
- a slag inclusions at the clad-to-base metal interface where the cladding is unusually thick. Of course, these are really cladding flaws.
- under-clad cracking—This condition was not found in the validation testing.

Table 4.2 Flaws in Cladding and at the Clad-to-Base Metal Interface								
Jan. 2000	**<3 mm**	**3 mm**	**4 mm**	**5 mm**	**6 mm**	**7 mm**	**8 mm**	**Total ≥ 3 mm**
Crack. LOF	1200	3	1					4

Table 4.3 Indications in Base Metal of the Inner 25 mm of the PVRUF Vessel								
Jan. 2000	**<3 mm**	**3 mm**	**4 mm**	**5 mm**	**6 mm**	**7 mm**	**8 mm**	**Total ≥ 3 mm**
Indications	180	10	3					13

- repair to base metal—The vessel manufacturer may have performed repair welding to the inside surface of the plate material.

4.2 Confirmed Flaw Frequency in Remainder of Vessel Wall

Tables 4.4, 4.5, and 4.6 show the revised estimates of flaw frequency outside the near-surface zone. The weld and weld-repairs flaws shown in Tables 4.4 and 4.6 were confirmed to be lack of side-wall fusion and nonmetallic inclusions (slag). The base-metal flaws in Table 4.5 are characterized as a lamination and flaw indications (not validated).

The validated flaw frequency and distribution in the machine-made weld metal is given in Table 4.4. The flaws were confirmed by weld-normal UT, radiography, or metallography. The table shows 4 flaws in the size range of 7 to 8 mm (6.5 to 8.5 mm) and 19 flaws in the size range of 5 to 6 mm (4.5 to 6.5 mm). The validation research found a flaw frequency of 1400 flaws less than 5 mm in size (4.5 mm and smaller). The size distribution of these small flaws was measured by the radiographic testing of the 25-mm plates.

The radiographic testing of 33 plates showed 43 linear indications characterized as lack of side-wall fusion. The flaw rate is 1.3 flaws per linear inch of weld metal. The 33 plates were cut from the PVRUF specimens by using the weld-normal UT to position the flaw in the middle of the 25-mm plate's thickness. The weld-normal UT response for the 43 indications in the radiographic plates varied by 18 dB. These UT responses were used to detect 217 flaw indications in three PVRUF specimens. The specimens contained 122 linear inches of weld metal for a flaw rate of 1.8 flaws per inch. The small fusion-line flaws were confirmed to be slag/lack of side-wall fusion by metallographic testing as described in Chapter 3.

Few flaws were confirmed between the machine-made weld beads. A cluster of small flaws of this kind was confirmed by weld-normal testing and by metallographic analysis to be slag/lack of inter-run fusion.

Table 4.5 shows the lamination and unconfirmed base metal flaws in the PVRUF material. One base metal flaw was removed from the PVRUF material and the radiographs showed an 8-mm through-wall cluster of horizontal planar flaws.

A repair was made to the beltline weld from the vessel OD. The size of the repair was documented to be 12.0 inches (150 mm) long, 2.4 inches (300 mm) wide, and 6.5 inches (60 mm) deep. The size and frequency of repairs to the PVRUF vessel, extracted from the PVRUF construction records, are reported in Chapter 5. Table 4.6 shows seven flaws were confirmed in a repair to the beltline weld. A flaw 17 mm in through-wall extent was confirmed in the radiographic and metallographic testing. A 12-mm flaw was confirmed in the radiographic testing and ultrasonic testing. Five flaws with

Table 4.4 Flaws in Weld Metal Outside the Near-Surface of the PVRUF Vessel							
Jan. 2000	**<5 mm**	**5-6 mm**	**7-8 mm**	**9-10 mm**	**11-12 mm**	**13-14 mm**	**Total ≥ 5 mm**
LOF, slag	1400	19	4				23

Table 4.5 Indications in Base Metal Outside the Near-Surface of the PVRUF Vessel						
Jan. 2000	**<5 mm**	**5-6 mm**	**7-8 mm**	**9-10 mm**	**11-12 mm**	**Total ≥ 5 mm**
Laminations			1			1
Indications	360	10	1			11

Table 4.6 Flaws in Repairs								
Jan. 2000	**5-6 mm**	**7-8 mm**	**9-10 mm**	**11-12 mm**	**13-14 mm**	**15-16 mm**	**17-18 mm**	**Total ≥ 5 mm**
LOF	5			1			1	7

through-wall size of 5 mm were confirmed in the radiography and in the weld-normal UT.

4.3 Cumulative Flaw Rate for PVRUF and Comparison to the Marshall Distribution

Weld metal flaw rate estimates can be made from the size distribution Tables 4.1, 4.4, and 4.6 and from the amount of weld volume inspected. The flaw rate can be described by the discrete cumulative flaw rate function, which is just the sum of flaw indications greater than the size of interest divided by the volume of material inspected. The volume of material inspected in this case is the volume of weld and repair weld inspected by SAFT-UT (see Table 2.1) in the case of the PVRUF vessel. Note that PNNL inspected about 15% of the weld volume in PVRUF as reported in Volume 1.

Figure 4.1 shows the PVRUF cumulative flaw rate as calculated from the entries in Tables 4.1, 4.4, and 4.6. The data from the Marshall reports (Marshall 1976, 1982) are also shown in Figure 4.1 for comparison. Some discussion of what data the Marshall committee was considering is appropriate for this comparison.

First, the committee sought to estimate the distribution of actual crack sizes in the whole vessel, N(x) where N(x) is defined as

$$N(x) = A(x)\, B(x) \qquad (4.1)$$

A(x) is the average number of flaws per vessel per inch of depth size x after manufacture but before service as detected and sized by ultrasonic testing. B(x) describes the reliability of the ultrasonic testing which may cause N(x) to either be greater or less than A(x). This is so because perhaps the NDE found all of the flaws and there are none in the vessel after these are repaired, the ultrasonic test found only a few of them and more remain, and the repair process introduced new flaws that are difficult to detect.

A(x) was described as "defects existing after manufacture to ASME III." The committee obtained proprietary information from U.S. and U.K. sources that indicated 44 nuclear vessels contained 12 ultrasonic indications in the size

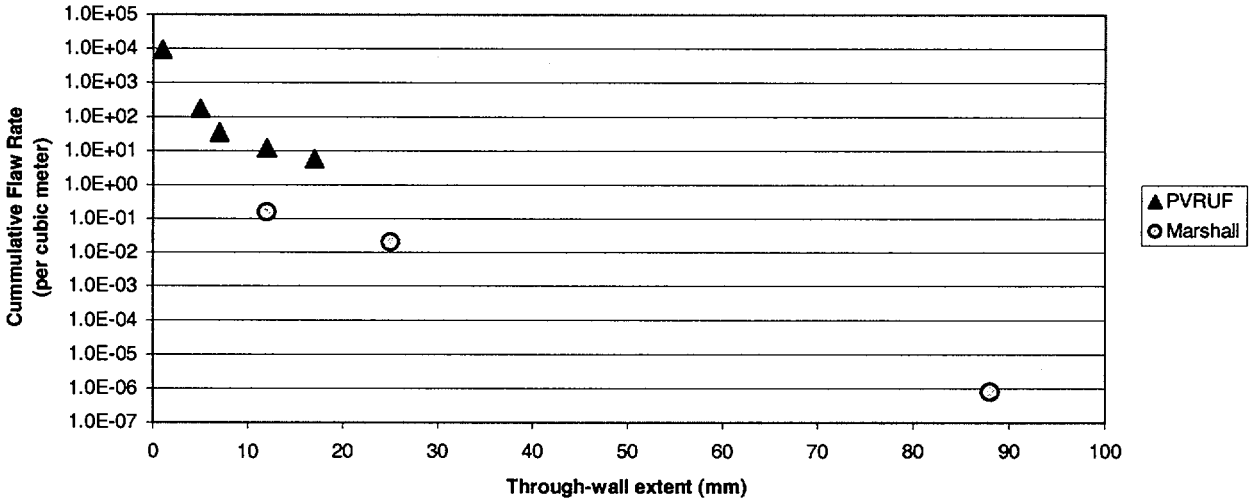

Figure 4.1. Comparison of Validated PVRUF and Marshall Cumulative Flaw Rates. This semi-log plot shows the individual data points from the PVRUF validation Tables 4.1, 4.4, and 4.6 and the Marshall data (Marshall 1976).

range of 0.5 to 1 inch (12 to 25 mm). No indications larger than 1 inch (25 mm) were reported.

Information from non-nuclear vessels was used to estimate the flaw rate for flaws greater than 1 inch in size and only for flaws greater than this amount. A known defect that caused a non-nuclear vessel to fail its pre-service test, 3.5 inches (90 mm) in through-wall size, was added to the data set after an analysis of the volume of weld metal produced by the nonnuclear industry.

The estimate for A(x) was

$$A(x) = A\exp(-\lambda x) \qquad (4.2)$$

where A was estimated to be 14.8 flaws per vessel per inch (of flaw size) (0.6 per mm) and λ was given as 4.06 per inch (0.16 per mm). The observed flaw rate is easily converted by integral calculus to the cumulative observed flaw rate:

$$\alpha(x) = 3.6\exp(-4.06x) \qquad (4.3)$$

where α is just flaws per vessel greater than size x (inches). The estimate predicts 3.6 observed flaws of all sizes per vessel.

The committee's first report estimated the "efficiency of crack detection" by ultrasonic inspection methods by means of a questionnaire sent out to several independent organizations. The estimated efficiencies were averaged over the operators and an estimate for B(x) was given as always less than unity.

$$B(x) = e + (1 - e)\exp(-ux) \qquad (4.4)$$

where e = 0.005 and u = 2.88 per inch (0.11 per mm).

Independent studies of the reliability of ultrasonic testing were undertaken. The PISC-I program performed a major effort in this area (PISC 1979). The results of the PISC-I program were used in the second Marshall report to modify B(x), and a value of unity was recommended.

An estimate of the amount of weld metal in a nuclear reactor RPV was made at 3 cubic meters. From this estimate, the value of 1.2 flaws per cubic meter (1.3 flaws per cubic yard) is derived (NRC 1987).

4.4 Flaw Rate for Small Flaws

It is important to estimate the density of flaws within the 1- to 4-mm size range. The radiographic testing results can be used for this purpose. Table 3.1 in Chapter 3 gives the through-wall size of 43 RT indications in 33 25-mm-thick plates. The beltline weld cross section is estimated to be 78-square centimeters.

Figure 4.2 shows the cumulative flaw rate for small flaws from the RT examinations along with the flaw rate from the validation tables. The RT data show size density of flaws within the 1- to 5-mm range. It is seen that the flaw rates from the RT examinations are consistent with the flaw rates from the validation tables.

4.5 Validated Flaw Length in the PVRUF Vessel

The validation research showed that long flaws were not present in the PVRUF vessel material acquired by PNNL. The larger repair flaws showed length-to-depth ratios of 19 mm to 17 mm (1.1 to 1) and 18 mm to 12 mm (1.5 to 1). The majority of the flaws in the machine-made weld metal had similar length-to-depth ratios of about 1 to 1.

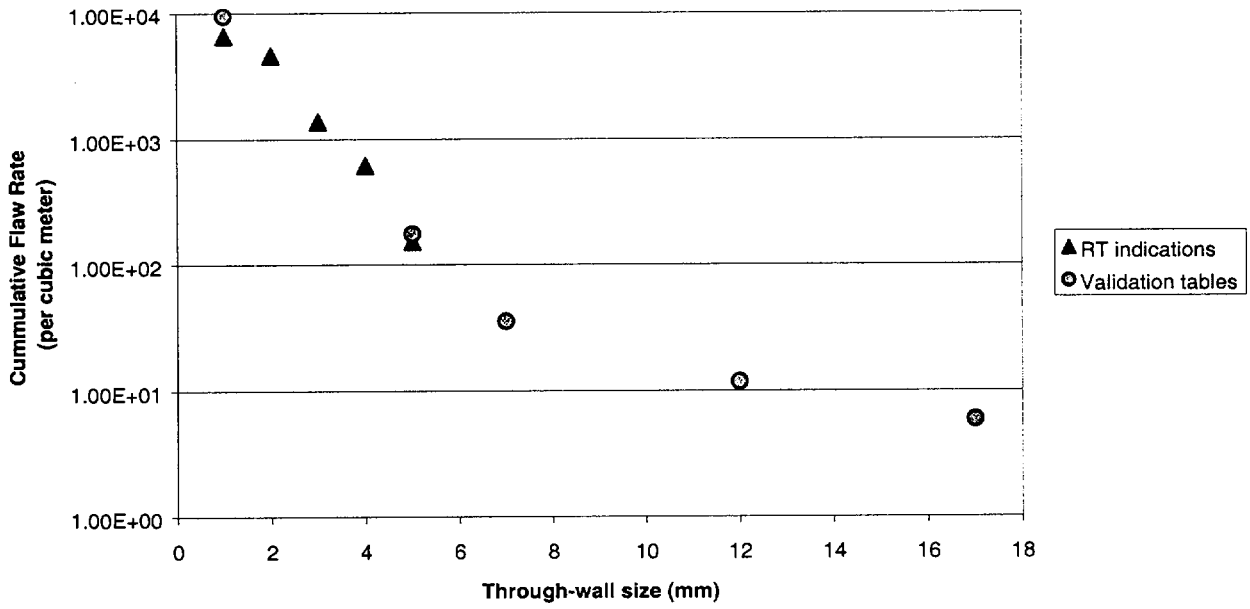

Figure 4.2. Size Distribution of Small Flaws in PVRUF Vessel as Measured by Radiographic Testing of 25-mm Thick Plate

5 SIZE AND FREQUENCY OF REPAIRS TO THE PVRUF VESSEL

The manufacturing of reactor pressure vessels involves the detection, characterization, and repair of significant flaws before the vessel is ready for service. At least four nondestructive evaluation techniques were applied at various stages during vessel fabrication to assure that significant flaws were removed before the vessel was prepared to enter service. The removal of fabrication flaws was accomplished by grinding out the flaws and filling the void with weld metal. This section of the report describes the results of PNNL's efforts to establish, from construction records, the number and size of repairs during fabrication of the PVRUF vessel.

The PVRUF vessel was manufactured using specifications in ASME Boiler and Pressure Vessel Code, Section III, Rules for Construction of Nuclear Pressure Vessels. All applicable code cases and addenda for Class A vessels that were in effect at the time of the purchase order were also applied. The PVRUF vessel was ordered in the mid-1970s. Later editions of the code may have been applied if agreed upon by the purchaser and the supplier. The vessel was completed in 1981.

For vessels like the PVRUF vessel constructed in the late 1970s, few repairs were made in contrast to what has been reported for earlier vessels. Better plate material, improved welding practices, and better interpretation of UT indications were important factors in reducing repair frequency.

Specifications were in place for the portions of the vessel that were to be inspected, the time(s) during manufacture for inspections to be conducted, the amount of vessel preparation to be conducted, and the essential variables of the test to be performed. Test and inspection records were delivered with the PVRUF vessel.

5.1 Repairs to Weld Metal

Various NDE methods were used during fabrication that might detect unacceptable conditions and initiating repair decisions. Sometimes the NDT examinations were more rigorous than the minimum ASME Code requirements in effect during this time. The following examinations were conducted using written procedures, and the result of their application is to determine the frequency of repair to the vessel:

- magnetic particle testing of all weld prep surfaces
- magnetic particle testing of back gouged area of welds
- ultrasonic testing of the shell welds before cladding
- radiographic testing of the shell welds
- dye penetrant testing of the clad surface
- magnetic particle testing of 100% of the outer vessel surface and the ID surface for two directions.

These techniques were applied to ensure that unacceptable conditions were located, evaluated, and repaired at specified time(s) during vessel construction. Repaired areas were reexamined with RT and UT.

Reportable indications were defined in the contract with the supplier. Flaw response and depth were included in the report. Radiographic evaluations were conducted using acceptance standards specified in ASME Code, Section III, paragraph NB-5320.

For an ultrasonic flaw indication to be considered for repair, the response needed to be at least 20% of reference level. For the ultrasonic discontinuities that produced a response greater than 20% and less than 50% of the reference level, evaluation was required. If these discontinuities were interpreted to be cracks or incomplete fusion, repair was required. For ultrasonic discontinuities that had amplitude greater than 50% of the reference level and length greater than 19 mm (0.75 in.), repair was required.

Figure 5.1 shows the numbering system for the welds in the PVRUF vessel assembly. This diagram is needed for the interpretation of the repair records, and this weld numbering system is used in the tables in this report.

Table 5.1 gives the size of the eight documented repairs to the circumferential welds of the PVRUF vessel. Weld 101-171 is the beltline weld and weld 101-141 is the seam between the lower shell course and the vessel bottom head. Repair #1 in the table, made from the outside of the vessel, is the one that contained the largest (17-mm) flaw confirmed in this validation study. Repairs #2 through #5 were made to the beltline weld from the inside of the vessel.

Table 5.2 gives the size of the three documented repairs made to axial welds of the PVRUF vessel. Weld 101-122B is one of the three axial welds in the upper shell course. Weld 101-124B is one of the three axial welds in the intermediate shell course. Weld 101-142B is one of three axial welds in the lower shell course.

Table 5.3 gives the size of the two repairs to the vessel closure head. Repair #1 was a repair to the flange to torus girth seam. Repair #2 was a repair to weld 101-104D, one of eight welds in the closure head torus.

Table 5.4 gives the size of the ten documented repairs to the vessel bottom head welds. Welds 101-154A-D are the four welds in the bottom head torus.

Table 5.5 gives the size of the nine documented repairs to the nozzle-to-vessel welds. Welds 107-121B and C are outlet nozzles-to-vessel welds. Welds 105-121C are inlet nozzles-to-vessel welds.

Table 5.6 gives the size of the 21 repairs to the nozzle safe ends. These are not vessel welds, and the table is given for completeness only.

5.2 Repairs to Base Metal

It is expected that a given volume of weld metal may have many more vertical planar flaws than an equal volume of base metal. It is because of the greater volume of base metal relative to weld metal that the base metal may still be important to structural integrity. The validation of flaw indications in the PVRUF vessel did not confirm vertical planar flaws in the base metal from seams, tears, cracks, etc.. It does show that the largest flaws were associated with repairs. It follows that a potential mechanism for the introduction of vertical planar flaws in the base metal regions of the PVRUF vessel is repair of the base metal plates.

It is not known how frequently base metal of RPVs was repaired. Such repairs would require a grind-out to the mid-section of the base metal plate, if the rejectable condition was mid wall, followed by welding to fill the deep grind-out region. Plate suppliers did conduct ultrasonic inspection of the plates and unacceptable discontinuities were located and evaluated. The vessel manufacturer re-inspected the plate material after forming. Both the plate supplier and the vessel manufacturer performed straight-beam and angle-beam ultrasonic inspections, as well as surface examinations.

Acceptance standards for the plate material were based on ASME Code requirements. The Code had requirements for reportable indications. The plate supplier submitted test reports on the specified indications for the entire plate.

The L-wave specifications included acceptance standards based on flaw response and loss of response from the back surface, the size of an indication was used, and a repair decision was made based on whether or not an enveloping circle that contained the flaw was greater than a specified amount, such as half the vessel thickness.

Specification for Straight-Beam Ultrasonic Examination of Steel Plates, SA435/SA435M, was used to ensure delivery of steel plate free of "gross internal discontinuities." *Specification for Ultrasonic Angle-Beam Examination of Steel Plates*, SA577/SA577M, was used for detecting internal discontinuities "not laminar in nature and of surface imperfections in the steel plates."

No repair records for the base metal plates were found in the vessel records. It is, therefore, possible that no repairs were required. Table 5.7 gives the size of the two repairs to the closure head flange mating surface, and Table 5.8 gives the sizes of the 11 repairs to the nozzle base metal.

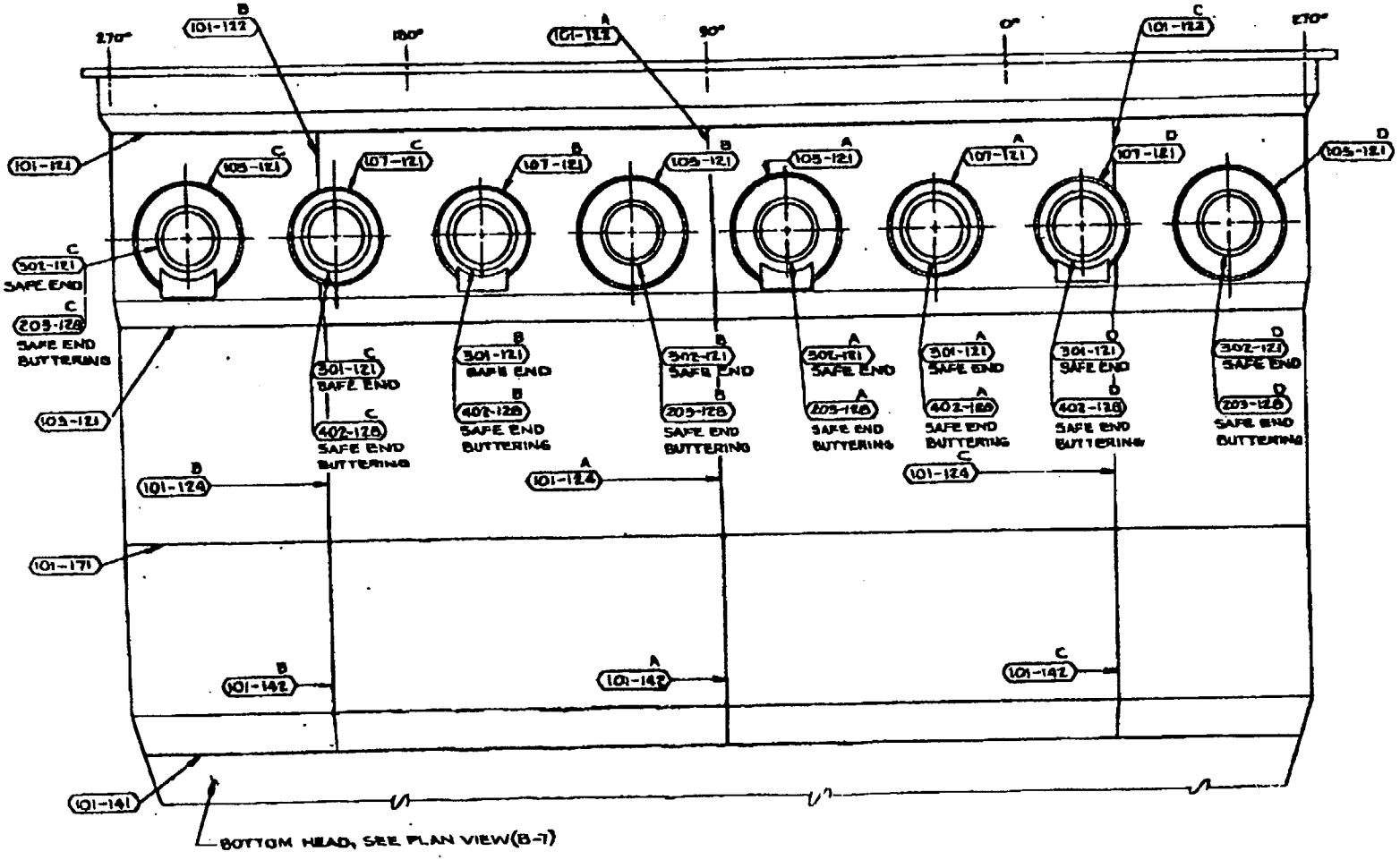

Figure 5.1 PVRUF Vessel Roll-Out Showing Weld Identification Numbers

Table 5.1 Repairs to Circumferential Welds (Girth Seams)					
Number	Weld	Repair Surface ID/OD	Excavation Length (inches)	Excavation Width (inches)	Excavation Depth (inches)
1	101-171	OD	12.0	2.4	6.5
2	101-171	ID	1.6	0.8	0.3
3	101-171	ID	7.6	1.2	0.5
4	101-171	ID	6.4	0.8	0.2
5	101-171	ID	2.5	0.4	0.2
6	101-141	OD	11.2	2.5	3.5
7	101-141	ID	13.0	4.2	3.4
8	101-141	ID	10.2	3.5	2.6

Table 5.2 Repairs to Axial Welds (Long Seams)					
Number	Weld	Repair Surface ID/OD	Excavation Length (inches)	Excavation Width (inches)	Excavation Depth (inches)
1	101-122B	OD	3.0	1.0	0.5
2	101-124B	OD	8.8	2.0	3.4
3	101-142B	ID	9.4	2.6	4.7

Table 5.3 Repairs to Closure Head					
Number	Weld	Repair Surface ID/OD	Excavation Length (inches)	Excavation Width (inches)	Excavation Depth (inches)
1	101-101	OD	56.4	?	?
2	101-104D	OD	9.0	2.4	7.1

Table 5.4 Repairs to Bottom Head					
Number	Weld	Repair Surface ID/OD	Excavation Length (inches)	Excavation Width (inches)	Excavation Depth (inches)
1	101-154A	ID	18.9	2.1	4.3
2	101-154A	ID	6.0	1.5	1.1
3	101-154A	ID	3.3	0.5	0.5
4	101-154B	ID	10.2	2.4	5.0
5	101-154C	ID	5.7	1.5	1.9
6	101-154D	ID	8.0	2.2	3.0
7	101-154D	ID	12.3	2.6	5.1
8	101-154D	ID	13.8	2.8	5.8
9	101-154D	OD	10.6	2.5	3.4
10	101-154D	OD	6.2	1.8	1.0

Table 5.5 Repairs to Nozzle-to-Vessel Welds					
Number	Weld	Repair Surface ID/OD	Excavation Length (inches)	Excavation Width (inches)	Excavation Depth (inches)
1	107-121B	OD	5.4	2.5	0.6
2	107-121B	OD	7.2	4.4	1.7
3	107-121B	ID	5.5	1.4	1.2
4	107-121C	OD	8.8	3.2	2.1
5	105-121C	OD	11.3	3.5	3.8
6	105-121C	OD	11.8	5.4	1.6
7	105-121C	OD	13.0	6.4	2.3
8	105-121C	ID	2.5	0.8	0.8
9	105-121C	ID	4.3	1.7	1.4

Table 5.6 Repairs to Safe Ends					
Number	Weld	Repair Surface ID/OD	Excavation Length (inches)	Excavation Width (inches)	Excavation Depth (inches)
1	301-121B	OD	6.4	1.2	2.4
2	301-121B	OD	4.2	1.4	1.7
3	301-121B	OD	8.1	1.0	1.1
4	301-121B	OD	4.5	1.6	1.1
5	301-121B	ID	4.3	0.9	0.6
6	301-121B	ID	3.6	1.0	1.1
7	301-121B	ID	4.7	1.0	0.4
8	301-121C	ID	3.5	0.9	0.7
9	301-121D	OD	4.2	1.0	1.5
10	301-121D	OD	4.9	1.3	1.2
11	301-121D	OD	4.2	0.9	1.1
12	301-121D	OD	4.9	1.2	1.1
13	301-121D	OD	5.7	1.3	1.6
14	301-121D	ID	3.3	0.6	0.3
15	301-121D	ID	3.2	0.7	0.4
16	302-121B	OD	5.4	1.5	1.7
17	302-121B	OD	4.0	1.0	0.8
18	302-121B	OD	6.5	1.1	1.4
19	302-121C	OD	6.7	0.9	1.7
20	302-121C	ID	4.3	0.4	0.3
21	302-121C	ID	3.5	0.5	0.3

Table 5.7 Repairs to Mating Surface 203-106 and 204-106 (closure head flange)			
Number	Excavation Length (inches)	Excavation Width (inches)	Excavation Depth (inches)
1	9.7	1.1	1.3
2	8.9	0.8	1.1
3	20.2	1.0	1.2
4	46.6	0.8	1.2
5	22.0	0.9	1.2

Table 5.8 Repairs to Nozzle Base Metal				
Number	Nozzle	Excavation Length (inches)	Excavation Width (inches)	Excavation Depth (inches)
1	107-121C	1.6	0.5	0.2
2	107-121C	1.4	0.7	0.2
3	107-121C	2.0	1.3	0.2
4	107-121C	4.5	0.5	0.1
5	107-121C	2.1	0.4	0.1
6	107-121C	1.1	0.9	0.2
7	107-121C	6.0	0.4	0.1
8	107-121C	1.4	0.4	0.1
9	107-121B	6.1	0.5	0.2
10	107-121A	1.1	0.3	0.2
11	107-121A	1.1	0.3	0.2

6 CONCLUSIONS

The results of the flaw-validation research led to a number of significant conclusions. A comparison with the Marshall committee data is useful to place into perspective what was learned from the PVRUF vessel and what remains. The validated flaws are mostly small, less than 4 mm in through-wall extent, as originally estimated from prior volumetric examinations. The fusion surface, between the weld and the base metal, contains an elevated concentration of vertical planar discontinuities. The largest flaws, greater than 8 mm in through-wall extent, were all associated with a repair to the beltline weld. These larger flaws were complex, a combination of cracks, lack of fusion, slag, and porosity.

A comparison of the PVRUF data with the Marshall committee data was possible. The Marshall data does not extend very well to flaws less than 12 mm in size. This conclusion is warranted because the ultrasonic testing procedures used at the time were not sensitive to smaller flaws. The overlapping size range between the two data sets shows the importance of repair flaws in the 12- to 17-mm range. For nuclear vessels, little is known about flaws greater than 25 mm in through-wall size and a welding model for repair welds may be useful.

PVRUF flaws greater than 8 mm in through-wall size are associated with repairs. The largest confirmed flaw in the machine-made weld metal is shown to be 7 mm. A repair to the beltline weld contained a 17-mm and a 12-mm flaw. These repair flaws were found on the fusion surface of the repair with the base metal.

The larger flaws were found to be complex. Metallographic analysis of PVRUF flaw specimens shows that the fabrication flaws are composed of a mixture of cracks, lack of fusion, contamination, and porosity. It follows from this that significant fabrication flaws can have an ultrasonic straight-beam response during in-service inspection.

The PVRUF examinations show that flaws can repeat on the next weld pass. The examinations also show that the interior of the structural weld remote from the fusion line was mostly free of small flaws. One interesting cluster of small flaws was found. This cluster was characterized during validation as separate small flaws and did not contribute to the larger size categories of interest to structural integrity assessment. The cluster did show that on four consecutive weld passes, a flaw was generated between the beads in the same portion of the vessel, creating a cluster of vertically oriented small flaws. This phenomenon is of known interest to the modeling of welding flaws (Chapman and Simonen 1998).

The weld fusion surfaces contain an elevated concentration of vertical planar discontinuities. The SAFT-UT inspections of the PVRUF structural welds showed that most of the detectable indications were located on the fusion surface of the weld with the base metal. Weld-normal ultrasonic testing of weld specimens removed from the vessel confirmed that most of the structural weld flaws are small and located on the fusion surface. Radiographic testing shows that 75% of these fusion surface flaws are linear indications, and metallographic testing showed lack of fusion with slag. The remaining 25% are taken to be inclusions and porosity.

The flaws are mostly small, as originally estimated. The 2400 flaws that were tabulated in the smallest size category (Schuster et al. 1998, 1999) were confirmed to be small. Portions of the beltline weld, sectioned for radiographic testing, confirmed the presence and character of the small welding flaws. A radiographic size of 1.8 mm was estimated for this part of the distribution.

The Volume 1 flaw indications are confirmed to be fabrication flaws. The majority of the flaws can be divided into two groups. In the largest group were the flaws at the clad-to-base metal interface of little or no significance to structural integrity. The sectioning of PVRUF cladded material confirms lack of fusion, slag, and voids at the clad-to-base metal interface. The second largest group were the flaws on the fusion surface of the structural weld with the base metal. Radiographic testing and metallography confirm lack of fusion with slag for the majority of these flaws.

Vertically oriented echoes are not always an indication of a large flaw. In ultrasonic testing of embedded flaws, sometimes responses are received from the top and bottom (tip-diffracted signals) and not from the face of the flaw. Because of the elevated concentration of small flaws on the weld fusion surfaces and because small flaws can repeat on the next weld pass, vertically oriented ultrasonic signals are not specific to the upper and lower tips of a large flaw, but can be signals from two smaller flaws.

The intended scope of the flaw-validation effort did not specifically include flaws in base metal. However, two of the larger flaw indications in base metal were examined. In both cases the indications were found to have little or no significance to structural integrity. Unlike the flaws in weld metal, the validation efforts have not validated a size distribution for base metal flaws. Future research will specifically address base metal flaws in the PVRUF vessel.

The studies of PVRUF flaws were designed to characterize the flaws in the vessel. As such, evaluations of the significance of these flaws to structural integrity were outside the scope of the PNNL effort. The present characterizations of flaws in terms of through-wall dimensions are believed to be consistent with accepted industry practices used to evaluate flaws by use of conservative fracture mechanics approaches. It should nevertheless be noted that the flaws in the PVRUF vessel, although crack-like in nature, were not ideal planar cracks as conservatively assumed in fracture mechanics calculations. Treatment of the PVRUF flaws in such a manner would tend to over estimate the structural significance of the observed flaws. In many cases the crack-like flaws did not have highly sharpened crack tips. In other cases (in particular for the largest flaws associated with repairs to welds), the flaws had complex morphologies consisting of only partially linked lack-of-fusions, porosity, slag, and other sources of contamination. Modeling such flaws as planar cracks for purposes of structural integrity evaluation is conservative, but is a common practice in fracture mechanics evaluations made necessary by limitations of the current state-of-knowledge in the fracture mechanics field.

7 RECOMMENDATIONS

PNNL's recommendations address the use of additional validation methods, the analysis of vessel construction records for fabrication information, continued non-destructive evaluation for surface-connected flaws, future measurements of density and distribution of flaws in base metal, and improvements to the performance of the SAFT-UT system.

The combined use of weld-normal ultrasonic testing, radiographic testing of 25-mm-thick plates, and the metallographic testing of 25-mm cubes has been effective at showing the characteristics of fabrication flaws in weld metal. Radiographic computed tomography (CT) should be added to the Laboratory's methodology. PNNL is investigating the use of CT on a 25-mm cube containing a 12-mm repair flaw. Preliminary results indicate that CT will show the 3-dimensional shape of the complex flaw.

The density and distribution of surface-connected flaws is important for the assessment of vessel structural integrity. The presence of repairs may be a principal determinant of this distribution. Repairs should be studied further. The inner surface region of the base metal should be studied further because it is large in volume compared to the volume of the structural welds.

The density and distribution of vertical-planar flaws in base metal is not well known. The inner third of the base metal is relevant to concerns for surface-connected flaws. Mechanisms for introducing vertical-planar flaws in base metal regions include repairs, seam, laps, and under-clad cracking. Additional examinations of base metal (plate and forging materials) are recommended.

Improvements and new functionality have been added to the SAFT-UT field data acquisition system and this trend should continue. Improvements to inspection speed, dynamic range, and ultrasonic electronics have made this work possible and promising.

8 REFERENCES

American Society of Mechanical Engineers. 1998. "Section XI Rules for Inservice Inspection of Nuclear Power Plant Components." In *ASME Boiler and Pressure Vessel Code*. American Society of Mechanical Engineers, New York.

American Welding Society, Inc. (AWS). 1984. *Standard Welding Terms and Definitions*, ANSI/AWS A3.0-85. American Welding Society, Inc., Miami, Florida.

Booth, D. L. 1989. *Material Documentation Report for the Weld Material Removed from the Consumers Power (Midland) Reactor Vessel (620-0012-51)*. The Babcock and Wilcox Company, Nuclear Power Division, Lynchburg, Virginia.

Busse, L. J, H. D. Collins, and S. R. Doctor. 1984. *Review and Discussion of the Development of Synthetic Aperture Focusing Technique for Ultrasonic Testing, SAFT-UT*. NUREG/CR-3625, PNL-4957. U.S. Nuclear Regulatory Commission, Washington, D.C.

Chapman, O. J. V., and F. A. Simonen. 1998. *RR-PRODIGAL - A Model for Estimating the Probabilities of Defects in Reactor Pressure Vessel Welds*. NUREG/CR-5505, PNNL-11898. U.S. Nuclear Regulatory Commission, Washington, D.C.

Doctor, S. R., G. J. Schuster, L. D. Reid, and T. E. Hall. 1996. *Real-Time 3-D SAFT-UT Evaluation and Validation*. NUREG/CR-6344, PNL-10571. U.S. Nuclear Regulatory Commission, Washington, D.C.

Doctor, S. R., G. J. Schuster, and F. A. Simonen. 1999. "NDE's Role in Reactor Pressure Vessel Assessments," *Transactions of 15th Int'l Conf. on Structural Mechanics in Reactor Technology*, Vol. 1, pp. I-53 to I-71, Seoul, South Korea.

Marshall, W. 1976. "An Assessment of the Integrity of PWR Pressure Vessels, Summary Report." Report of a study group under the Chairmanship of Dr. Walter Marshall, CBE FRS, UKAEA, London.

Marshall, W. 1982. "An Assessment of the Integrity of PWR Pressure Vessels, Summary Report." Second report of a study group under the Chairmanship of Dr. Walter Marshall, CBE FRS, UKAEA, London.

Nichols, R. W., and S. Crutzen 1988. *Ultrasonic Inspection of Heavy Section Steel Components, The PISC II Final Report*. Elsevier Science Publishing Co., Inc., New York.

Pennel, W. E. 1989. *Mission Survey for the Pressure Vessel Research Users' Facility (PVRUF)*. NUREG/CR-5350, Oak Ridge National Laboratory, Oak Ridge, Tennessee.

Plate Inspection Steering Committee Report No. 1, "A Description of the PISC Project." May 1979, issued as an European Commission of the European Communities Report, September 1979.

Schuster, G. J., S. R. Doctor, and F. A. Pardini. 1997. "Validation of Reactor Pressure Vessel Fabrication Flaws," *Proceedings of NDE Damage Assessment Workshop*, October 6-7, 1997, Electric Power Research Institute, La Jolla, California.

Schuster, G. J., S. R. Doctor, and P. G. Heasler. 1998. *Characterization of Flaws in U.S. Reactor Pressure Vessels: Density and Distribution of Flaw Indication in PVRUF*. NUREG/CR-6471, Vol. 1, PNNL-11143. U.S. Nuclear Regulatory Commission, Washington, D.C.

Schuster, G. J., S. R. Doctor, S.L. Crawford, and A.F. Pardini. 1999. *Characterization of Flaws in U.S. Reactor Pressure Vessels: Density and Distribution of Flaw Indication in the Shoreham Vessel.* NUREG/CR-6471, Vol. 3, PNNL-11143A. U.S. Nuclear Regulatory Commission, Washington, D.C.

U.S. Nuclear Regulatory Commission (NRC). 1987. *Format and Content of Plant-Specific Pressurized Thermal Shock Safety Analysis Reports For Pressurized Water Reactors.* Regulatory Guide 1.154. U.S. Nuclear Regulatory Commission, Washington, D.C.

NRC FORM 335 (2-89) NRCM 1102, 3201, 3202

U.S. NUCLEAR REGULATORY COMMISSION

BIBLIOGRAPHIC DATA SHEET

(See instructions on the reverse)

1. REPORT NUMBER
(Assigned by NRC, Add Vol., Supp., Rev., and Addendum Numbers, if any.)

NUREG/CR-6471, Vol. 2
PNNL-11143B

2. TITLE AND SUBTITLE

Characterization of Flaws in U.S. Reactor Pressure Vessels

Validation of Flaw Density and Distribution in the Weld Metall of the PVRUF Vessel

3. DATE REPORT PUBLISHED

MONTH	YEAR
August	2000

4. FIN OR GRANT NUMBER

W6275

5. AUTHOR(S)

G.J. Schuste, S.R. Doctor, A.F. Pardini, S.L. Crawford

6. TYPE OF REPORT

Technical

7. PERIOD COVERED *(Inclusive Dates)*

8. PERFORMING ORGANIZATION - NAME AND ADDRESS *(If NRC, provide Division, Office or Region, U.S. Nuclear Regulatory Commission, and mailing address; if contractor, provide name and mailing address.)*

Pacific Northwest National Laboratory
Richland, WA 99352

9. SPONSORING ORGANIZATION - NAME AND ADDRESS *(If NRC, type "Same as above"; if contractor, provide NRC Division, Office or Region, U.S. Nuclear Regulatory Commission, and mailing address.)*

Division of Engineering Technology
Office of Nuclear Regulatory Research
U.S. Nuclear Regulatory Commission
Washington, DC 20555-0001

10. SUPPLEMENTARY NOTES

D.A. Jackson, NRC Project Manager

11. ABSTRACT *(200 words or less)*

Characterization of Flaws in U.S. Reactor Pressure Vessels is a multi-volume report. Volume 2, this document, contains the results of a destructive analysis for fabrication flaws in weld metal removed from the Pressure Vessel Research User Facility (PVRUF) vessel. Confirmed flaw rates are estimated, and a comparison is made to the Marshall distribution. The first volume of this multi-volume report gives the density and distribution of flaw indications recorded from the volumetric ultrasonic inspections of the vessel made through the cladding. Volume 3 reports the distribution of flaw indications in material removed from a BWR vessel, the Shoreham vessel.

This volume provides a description of research methods developed at Pacific Northwest National Laboratory for confirming flaw rates in weld metal. The data, acquired during the research, are shown with the estimates of flaw density as a function of through-wall size. Because the largest flaws were found in repair weld metal, the report contains the size and number of repairs to the PVRUF vessel.

12. KEY WORDS/DESCRIPTORS *(List words or phrases that will assist researchers in locating the report.)*

Ultrasonic Testing, Inservice Inspection, Nondestructive Testing, Nondestructive Examination, Nondestructive Evaluation, Reactor Pressure Vessels, Fabrication Flaw

13. AVAILABILITY STATEMENT

unlimited

14. SECURITY CLASSIFICATION

(This Page)
unclassified

(This Report)
unclassified

15. NUMBER OF PAGES

16. PRICE

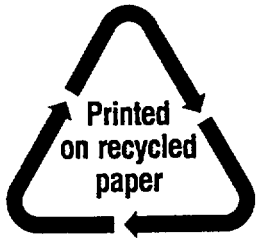

Federal Recycling Program

ISBN 0-16-050490-2

UNITED STATES
NUCLEAR REGULATORY COMMISSION
WASHINGTON, D.C. 20555-0001